

GUNMA UNIVERSITY

**Study of NO_x removal
characteristics under dielectric
barrier discharge field**

by

TRAN QUANG VINH

Under the guidance of

Professor MASATAKA ARAI, Ph.D.Eng.

A thesis submitted in partial fulfillment for the
degree of Doctor of Philosophy

in the

Department of Mechanical System Engineering

July 2012

Declaration of Authorship

I, TRAN QUANG VINH, declare that this thesis titled, ‘STUDY OF NO_x REMOVAL CHARACTERISTICS UNDER DIELECTRIC BARRIER DISCHARGE FIELD’ and the work presented in it are my own. I confirm that:

- This work was done wholly or mainly while in candidature for a research degree at Gunma University.
- Where any part of this thesis has previously been submitted for a degree or any other qualification at this University or any other institution, this has been clearly stated.
- Where I have consulted the published work of others, this is always clearly attributed.
- Where I have quoted from the work of others, the source is always given. With the exception of such quotations, this thesis is entirely my own work.
- I have acknowledged all main sources of help.
- Where the thesis is based on work done by myself jointly with others, I have made clear exactly what was done by others and what I have contributed myself.

Signed:

Date:

“Everything should be made as simple as possible, but not simpler.”

Albert Einstein

Abstract

Removal nitrogen oxides (NO_x) from diesel engine exhaust gas has become an essential issue because of increasingly stringent emission legislation. NO_x removal using non-thermal plasma has been studied widely and has shown its potentiality. In recent years, there has been an increasing interest in simultaneously removing NO_x and particulate matter (PM) from diesel engine exhaust. The objective of this research is to investigate experimentally de NO_x characteristics under barrier discharge field with a diesel particulate filter (DPF) worked as dielectric barrier layer. The combination between a dielectric barrier discharge reactor and a DPF was also considered as a novel suggestion to the diesel engine emission elimination. In this study, the wire-to-cylinder discharge reactors were used. The cylinder had inner diameter of 36mm and total length of 180mm. The DPF was a cordierite wall-flow lab-scaled one with volume of 31.6cm^3 . The reactor was supplied by 50Hz alternative high voltage source in range from 5kV to 15kV. The simulated exhaust gas mixture of NO, NO_2 , O_2 , and N_2 at different fractions were employed in NO_x removal characteristic experiments. The sampled gas taken from reactor's outlet was analyzed by an FT-IR exhaust gas analyzer, Horiba Co.,Ltd., MEXA-4000FT. The effects of PM on de NO_x process under discharge field were studied by using DPF loaded with PM. Comparing experimental results in cases of gas mixture without oxygen and the one with oxygen at various gas flow rates, it showed that oxygen played a key role in the NO oxidation process that was dominant in latter case. Moreover, as oxygen fraction increases, the NO oxidation process run faster and this lead to lowering the necessary energy density to reduce NO concentration to zero. In PM effect analysis, PM enhanced NO_x removal characteristics under dielectric barrier discharge field with gas mixture containing oxygen. However, this effect deteriorated with elapsed time. The most significant NO_x removal performance was observed when PM was "Fresh". In actual PDF system, loaded DPF was oxidized under forced regeneration process or continuous PM oxidation process during operation. Conversely, new "Fresh PM" was always supplied from engine and then deposited over the old PM where its surface has already lost the effective role of NO_x removal. As a result, there are many possibilities of NO_x removal by PM in actual operating engine.

Acknowledgements

Special thanks to my supervisor, Professor Dr. Masataka Arai, for his great guidance and support. Without his support this study could not have been done properly.

The author gratefully acknowledges the research support of Dr. Tomohiko Furuhata, Dr. Masahiro Saito, Dr. Yoshio Zama and Mr. Goro Ogiwara during my study. My great appreciation also goes to other members of our experimental group, MSc. Shuya Watanabe and Mr. Daisuke Kawabata for their help in setting up and collecting data of this work.

The author would like to forward gratitude to Japanese Ministry of Education, Culture, Sports, Science and Technology (MEXT) for providing the financial support.

I would like to thank Hanoi University of Science and Technology (HUST), School of Transportation Engineering, Department of Internal Combustion Engine for permission to pursue Ph.D. degree. Special thanks are due to Professor Dr. Pham Minh Tuan, Dr. Le Anh Tuan and my colleagues in HUST for their support and encourage during my study.

Finally, I also would like to thank to my beloved wife, Nguyen Thi Hanh, and my little daughters, Khanh Van and Thuy Mai, for their patience and moral support . . .

Contents

Declaration of Authorship	i
Abstract	iii
Acknowledgements	iv
List of Figures	viii
Abbreviations	x
Symbols	xii
1 NO_x treatment using non-thermal plasma	1
1.1 NO _x problem and deNO _x method	1
1.1.1 NO _x problem	1
1.1.2 NO _x treatment	3
1.2 NO _x removal by non-thermal plasma	5
1.2.1 Non-thermal plasma	5
1.2.2 NO _x removal using corona discharge	8
1.2.3 NO _x removal using dielectric barrier discharge	13
1.3 Emissions and aftertreatment system of internal combustion engine	16
1.3.1 NO _x and other harmful emission from internal combustion engine	16
1.3.2 Aftertreatment system of internal combustion engine	18
1.3.3 NO _x and PM treatment by non-thermal plasma	21
1.3.4 NO _x and HC treatment system by non-thermal plasma	23
1.4 Purpose of this research study	24
1.4.1 Laboratory scale experiment	24
1.4.2 Objective of this study	28
1.4.3 Outline of the thesis	29
2 Experimental apparatus and method	30

2.1	Methodology	30
2.1.1	Dielectric barrier discharge applicable for deNO _x reactor	30
2.1.2	Plasma reactor with DPF	33
2.2	Apparatus and procedure	35
2.2.1	Experimental setup	35
2.2.2	Test gas	42
2.2.3	PM	43
2.2.4	Experimental parameter and data analysis	48
2.2.5	Experimental condition and procedure	49
2.3	Basic performance of the reactor	49
2.3.1	Spark discharge limit and maximum safety voltage	49
2.3.2	Electric currents of pre-reactor and main reactor	50
2.3.3	Current-voltage characteristics	51
2.3.4	Power factor and discharge power	52
2.4	Summary	53
3	Effects of oxygen on NO_x removal characteristics	54
3.1	Fundamental NO removal reaction	54
3.2	NO _x removal in NO + N ₂ mixture	56
3.2.1	NO _x removal characteristics and less effective area	56
3.2.2	DeNO _x efficiency and minimum energy density	58
3.3	NO _x removal in NO + N ₂ + O ₂ mixture	60
3.3.1	NO and NO ₂ removal characteristics	60
3.3.2	Effect of gas flow rate	62
3.3.3	DeNO _x efficiency and minimum energy density	63
3.3.4	Effect of oxygen fraction	64
3.4	Explanation using reaction scheme	67
3.5	Role of residence time	69
3.6	Summary	70
4	Effects of particulate matter on NO_x removal characteristics	71
4.1	Purpose and experimental setup to investigate PM effect on NO _x removal	71
4.2	Experimental results with PM loaded DPF	73
4.2.1	Simulated exhaust gas without oxygen	73
4.2.2	Simulated exhaust gas with oxygen	75
4.2.3	PM loading mass and NO _x removal characteristics	78
4.3	PM aging	79
4.3.1	PM aging effect	79
4.3.2	Experimental results in cases of DPF with “Fresh PM”	80
4.3.3	Experimental results in cases of DPF with “Aged PM”	81
4.4	NO _x adsorption effect by PM	83
4.5	Summary	86
5	NO_x removal performance in transient test	87

5.1	Purpose of various transient tests	87
5.2	“Fresh PM” pre-treatment effect on NO _x removal	88
5.2.1	NO _x removal characteristics in four hours running mode	88
5.2.2	“Fresh PM” oxidation effect on NO _x removal	91
5.3	“Aged PM” treatment effect on NO _x removal	92
5.3.1	NO _x removal characteristics in six hours running mode	92
5.3.2	Difference between “Fresh PM” and “Aged PM”	95
5.4	N radical pre-treatment	96
5.5	Engine application	97
5.6	Summary	98
6	Conclusions	99
	Bibliography	101

List of Figures

1.1	Role of radicals in NO _x reduction	8
1.2	Experimental setup by Vinogradov et al.	9
1.3	Relative positive-negative corona cleanness behavior	9
1.4	Effect of residence time on cleanness and corona power	10
1.5	NO _x removal with hybrid corona discharge-catalyst reactor	11
1.6	NO destruction with pulsed corona discharge reactor	12
1.7	Cleanness behavior using pulsed corona discharge reactor	12
1.8	DBD wire-to-cylinder reactor layout	14
1.9	NO _x conversion vs. energy density in DBD reactor	15
1.10	Operating principle of the lean NO _x reduction system	18
1.11	DBD reactor configuration to remove NO _x , HC and PM	21
1.12	PM, HC and NO _x removal efficiencies as a function of peak voltage	22
1.13	Schematic of the DBD reactor	23
1.14	Effect of HCs on NO and NO _x removal efficiencies	23
2.1	The necessity for deNO _x reactor	30
2.2	Dielectric discharge NTP reactors	31
2.3	Dielectric barrier discharge reactor with DPF	35
2.4	Picture of DBD reactor with DPF	36
2.5	Diesel particulate filter	37
2.6	Photo of test DPF	37
2.7	Schematic diagram of experimental apparatus	38
2.8	Picture of experimental apparatus	38
2.9	High voltage electric circuit of the reactor	39
2.10	Principle of the FTIR analyzer	40
2.11	The operating principle of the PM composition analyzer	41
2.12	The operating principle of TSI SMPS-3034	42
2.13	PM generator	44
2.14	Composition of different PM samples	45
2.15	PM particle size distribution	46
2.16	PM sampling chart	47
2.17	Model of electrode with PM inside DPF	48
2.18	Discharge and displacement currents	50
2.19	Current-voltage characteristics of the reactor	52
2.20	Phase angle of the reactor	53

3.1	NO _x removal in N ₂ + NO mixture ($Q=1\text{L}/\text{min}$)	55
3.2	NO _x removal in NO+N ₂ mixture ($Q=2\text{L}/\text{min}$)	57
3.3	NO _x removal in NO + N ₂ mixture ($Q=1\text{L}/\text{min}$)	58
3.4	NO _x removal in NO+N ₂ mixture ($Q=0.5\text{L}/\text{min}$)	58
3.5	DeNO _x efficiency in N ₂ + NO mixture	59
3.6	NO _x removal in N ₂ + NO + O ₂ mixture (O ₂ =10% and $Q=2\text{L}/\text{min}$) .	60
3.7	NO _x removal in N ₂ + NO + O ₂ mixture (O ₂ =10% and $Q=1\text{L}/\text{min}$) .	62
3.8	NO _x removal in N ₂ + NO + O ₂ mixture (O ₂ =10% and $Q=0.5\text{L}/\text{min}$)	63
3.9	DeNO _x efficiency in N ₂ + NO + O ₂ mixture	64
3.10	NO _x removal in N ₂ + NO + O ₂ mixture (O ₂ =15% and $Q=0.5\text{L}/\text{min}$)	65
3.11	NO _x removal in N ₂ + NO + O ₂ mixture (O ₂ =20% and $Q=0.5\text{L}/\text{min}$)	66
3.12	Effect of oxygen on NO _x removal at $Q=0.5\text{L}/\text{min}$	67
3.13	Effect of residence time on NO _x removal efficiency	70
4.1	SOF fraction in PM and NO _x removal	72
4.2	Sulfate fraction in PM and NO _x removal	72
4.3	NO _x removal in N ₂ + NO mixture (PM=100mg and $Q=1\text{L}/\text{min}$) . .	73
4.4	NO _x removal in N ₂ + NO mixture (with and without PM, $Q=1\text{L}/\text{min}$)	75
4.5	NO _x removal in N ₂ +NO+O ₂ mixture (PM=100mg, O ₂ =1%, and $Q=1\text{L}/\text{min}$)	76
4.6	NO _x removal in N ₂ +NO+O ₂ mixture (PM=100mg, O ₂ =5%, and $Q=1\text{L}/\text{min}$)	77
4.7	NO _x removal in N ₂ +NO+O ₂ mixture (PM=100mg, $Q=1\text{L}/\text{min}$, and O ₂ =10% and 15%)	77
4.8	NO _x reduction at different PM mass loaded on DPF (O ₂ =10%) . .	78
4.9	Effect of “Aged PM” on NO _x treatment	80
4.10	NO _x reduction at different O ₂ fractions and “Fresh PM”	81
4.11	NO _x reduction at “Aged PM” after 4 running hours	82
4.12	NO _x adsorption following energy at PM=0mg	83
4.13	NO _x adsorption following energy at PM=100mg	84
5.1	NO _x removal performance in 4 hours mode (Test 4-(1))	89
5.2	NO _x removal performance in 4 hours mode (Test 4-(2))	89
5.3	NO _x removal performance in 4 hours mode (Test 4-(3))	90
5.4	NO _x removal performance in 4 hours mode in summary	91
5.5	NO _x removal performance in 6 hours mode (Test 6-(1))	93
5.6	NO _x removal performance in 6 hours mode (Test 6-(2))	94
5.7	NO _x removal performance in 6 hours mode (Test 6-(3))	94
5.8	NO _x removal performance in 6 hours mode in summary	95
5.9	Illustration of adsorbed N radical and O radical on PM	96
5.10	Application of DBD reactor to diesel exhaust aftertreatment system	97

Abbreviations

AC	A lternative C urrent
CO	C arbon monoxide
CO₂	C arbon dioxide
CRT	C ontinuously R egeneration T rap
CPC	C ondensation P article C ounter
DBD	D ielectric B arrier D ischarge
DC	D irect C urrent
DMA	D ifferential M obility A nalyzer
DPF	D iesel P articulate F ilter
EGR	E xhaust G as R ecirculation
EU	E uropean U ion
FTIR	F ourier T ransform I nfra- R ed
GC-MC	G as C hromatography- M ass S pectrometry
HC	H ydrocarbon
HCCI	H omogeneous C harge C ompression I gnition
HDV	H eavy D uty V ehicle
HFAC	H igh F requency A lternative C urrent
HV	H igh V oltage
Kr	K rypton
LDV	L ight D uty V ehicle
LEV	L ow E mission V ehicle
LNT	L ean N O _x T rap
MEXA	M otor E Xhaust gas A nalyzer
MFC	M ass F low C ontroller

NAC	NO_x Adsorber Catalyst
NDIR	Non-Dispersive Infra-Red
NMHC	Non-Methane HydroCarbons
NMOG	Non-Methane Organic Gases
NO	Nitric oxide
NO₂	Nitrogen dioxide
N₂O	Nitrous oxide
NO_x	Nitrogen Oxides
NO_x-SR	NO_x Storage Reduction
NSCR	Non Selective Catalytic Reduction
NTP	Non-Thermal Plasma
PAN	PeroxyAcetylNitrate
PGM	Platinum Group Metal
PM	Particulate Matter
PN	Particulate Number
Pd	Palladium
Pt	Platinum
RF	Radio Frequency
Rh	Rhodium
RMS	Root-Mean-Square
SCR	Selective Catalytic Reduction
SED	Specific Energy Density
SMPS	Scanning Mobility Particle Sizer
SOF	Soluble Organic Fraction
SULEV	Super Ultra Low Emission Vehicle
TWC	Three-Way Catalyst
ULEV	Ultra Low Emission Vehicle
UV	Ultra-Violet
VOC	Volatile Organic Compound

Symbols

a	distance	mm
d	diameter	mm
D	distance	mm
E	energy density	J/L
f	frequency	Hz (kHz)
I	current	A (mA, μ A)
L	length	mm
L_f	flame height	mm
M_f	fuel consumption rate	mg/s
Q	flow rate	L/min
t	running time	h (min)
V	applied voltage	V (kV)
$h\nu$	photon energy	
τ	residence time	sec (ns)
ϵ	dielectric constant	
φ	phase angle between voltage and current	$^\circ$

Dedicated to my loving father, Tran Thin...

Chapter 1

NO_x treatment using non-thermal plasma

1.1 NO_x problem and deNO_x method

1.1.1 NO_x problem

(1) Air pollution and its harmful effect

Nitrogen oxides (NO_x), together with CO, sulphur oxides and volatile organic compounds (VOC) are primary chemicals of the air pollution. Main oxides of nitrogen in the atmosphere are nitric oxide (NO), nitrogen dioxide (NO₂) and nitrous oxide (N₂O).[1] NO_x commonly stands for NO and NO₂. But in sometimes, it means a sum of NO, NO₂, and N₂O.

NO_x adversely affects the environment and human health by causing ground-level ozone formation, water quality deterioration, global warming, production of toxic reaction products, and inhalable fine particles that lead to visibility degradation and pose a respiratory hazard. NO₂ plays a major role in the chemical reactions which generate ground-level ozone and photochemical smog. Photochemical smog is a type of air pollution produced when sunlight acts upon motor vehicle exhaust gases to form harmful substances such as ozone, aldehydes and peroxyacetylnitrate (PAN). These formation mechanisms are described as follows.

Firstly, nitrogen dioxide is excited by sunlight to form nitric oxide and atomic oxygen with the following photochemical reaction:

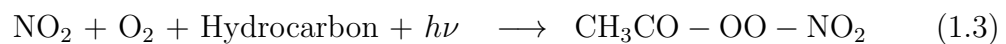


Then oxygen atom reacts with oxygen molecules in the air to form ozone:



Finally, ozone and atomic oxygen react with hydrocarbons to form many kinds of aldehydes and peroxyacetylnitrate (PAN).

When volatile organic compounds (VOC) such as hydrocarbons react in the atmosphere to form oxygenated products such as aldehydes, the oxygen in these molecules allows NO to form NO₂, without breaking down ozone, thus ozone accumulates. In the presence of sunlight, PAN (CH₃CO – OO – NO₂), is formed from nitrogen dioxide, oxygen, and hydrocarbons :



Additionally, nitrogen dioxide reacts with water to form a mixture of nitrous acid and nitric acid. These acids cause to the acid rain.



Nitrous oxide, N₂O, occurs in less quantities than NO and NO₂, but it becomes a strong greenhouse gas which absorbs long wavelength infrared light related with heat radiation from the Earth. Thereby it contributes to global warming.

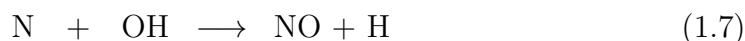
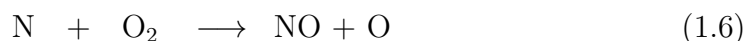
(2) NO_x formation mechanism and its emission source

NO_x from combustion is primarily in the form of NO. The principal source of NO is the oxidation of atmospheric nitrogen. It is generally accepted that there are three mechanisms for NO formation.[2] They are:

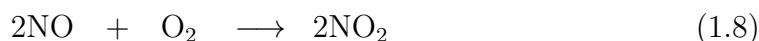
- 1- Thermal NO - Thermal NO is formed by the combination of oxygen and nitrogen under high temperature condition, such as combustion flame. Then, the concentration of “thermal NO_x” is controlled by the nitrogen and oxygen concentrations and the temperature of combustion gas. Combustion at temperatures below 760°C forms very low concentrations of thermal NO.
- 2- Fuel NO - Fuel that contains nitrogen creates “fuel NO” that results from oxidation of already-ionized nitrogen contained in the fuel.
- 3- Prompt NO - Prompt NO is formed from molecular nitrogen in the air combining with fuel in fuel-rich combustion reaction zone.

Thermal NO is produced under lean to stoichiometric mixture and high temperature combustion conditions. The well-known expanded Zeldovich mechanism

explaining the NO formation is given as below.[3]



NO₂ is usually formed from NO through following slow oxidation:



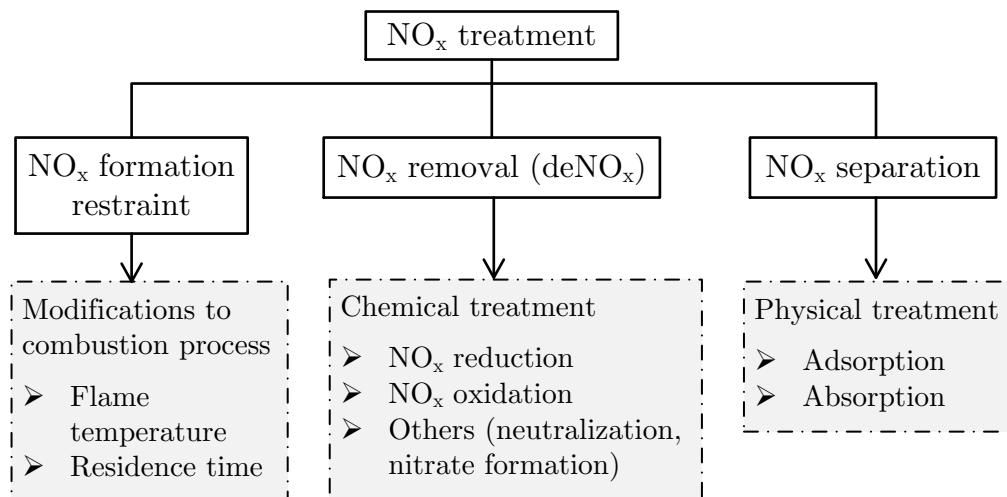
Emission sources of NO_x are automobiles, boilers and incinerators, as well as other high-temperature industrial operations such as metallurgical furnaces, blast furnaces, plasma furnaces, and kilns. Other sources include nitric acid plants and industrial processes involving nitric acid operation. As calculated, primary sources of NO_x emissions include motor vehicles (55%) and industrial, commercial, and residential processes (45%).[4] Removal of nitrogen oxides from combustion emission has been studied for many years. There are two strategies of NO_x control: (1) combustion modifications to suppress the formation of NO_x, and (2) aftertreatment approach to reduce nitrogen oxides to molecular nitrogen. The brief description of them will be expressed in the next section.

1.1.2 NO_x treatment

(1) Classification of NO_x treatment

NO_x treatment methods have been used up to now can be summarized and classified as in Table 1.1.

TABLE 1.1 Classification of NO_x treatment



NO_x formation control includes modifications to combustion process in order to restrain the formation of NO_x. NO_x removal and NO_x separation belong to the aftertreatment approach mentioned above. NO_x separation uses physical treatment methods such as NO_x adsorption and absorption. In another manner, NO_x removal (or deNO_x) mainly employs chemical treatment methods. They are NO_x reduction technique, NO_x oxidation technique, and other NO_x destruction techniques (i.e. neutralization, nitrate formation, etc.). The main component contributed to NO_x removal, NO removal, can be classified as NO reduction (to return to N₂) and NO oxidation (to form NO₂). The oxidation process can be briefly described as follows: N₂ → N₂O → NO → NO₂ → N₂O₅. The reduction process can be described by following scheme: N₂O₅ → NO₂ → NO → N₂O → N₂.

(2) Restraint of NO_x formation

As discussed above, NO is formed under lean to stoichiometric mixture and high temperature combustion conditions. Thus to control or suppress the formation of NO_x, decreasing the oxygen fraction at the peak temperature and shortening of residence time in the combustion zone are needed. Flame temperature may be reduced by: (1) using fuel rich mixture to limit the amount of oxygen available; (2) using fuel lean mixture to limit temperature by diluting energy input; (3) injecting cooled oxygen-depleted flue gas into the combustion air to dilute energy; (4) injecting cooled flue gas with added fuel; or (5) injecting water or steam. Reduce of residence time in high combustion temperature zone can be done by ignition or injection timing control in internal combustion engines.[2]

(3) Adsorption and absorption of NO_x

Adsorption is the binding of atoms, ions, or molecules of gas, liquid, or particles to the surface of a solid or a liquid (adsorbent). This process forms a molecular or atomic film. NO_x adsorption uses adsorbent to store NO_x under lean conditions and release and catalytically reduce the stored NO_x under rich conditions. NO and NO₂ are acidic oxides and can be trapped on basic oxides. Below is the chemical reaction represents the adsorption of NO.



where M is a basic metal.

Absorption is a process in which a substance diffuses into a liquid or a solid to form a solution. For NO_x absorption, absorbents used usually are water and solutions of nitric acid (HNO₃), sodium hydroxide (NaOH), sodium sulfite (Na₂SO₃),

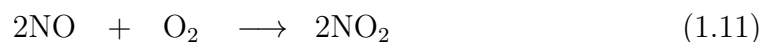
ferrous sulfate (FeSO₄), etc.

(4) NO_x removal

Chemical reduction of NO_x is achieved by providing a chemically reducing substance to remove oxygen from nitrogen oxides. The reducing agents of NO_x include PM, HC, N radical, photon, etc. Examples include selective catalytic reduction (SCR) which uses ammonia, selective non-catalytic reduction (SNCR) which use ammonia or urea. Current commercial system involves the injection of ammonia or urea into the exhaust gas stream to chemically reduce NO_x usually in the presence of a catalyst. However, the loss of expensive catalyst is a big problem encountered. The scheme of NO reduction is as follows.



The technique of oxidation of NO_x intentionally raises the valence of the nitrogen ion to allow water to absorb it (i.e., it is based on the greater solubility of NO_x at higher valence). This is accomplished either injecting hydrogen peroxide or injecting ozone into the gas flow. An example of this technique is NO_x-SR. It catalytic oxidizes NO to NO₂ that is more soluble in caustic solutions.[5] Non-thermal plasma, when used without a reducing agent, can be used to oxidize NO. The oxidation of NO can be express in below reaction.



The other techniques of NO_x removal use chemical agents (i.e. ammonia, hydrated lime, etc.) to neutralize nitric acid (HNO₃) which formed from NO_x at previous medium process.

1.2 NO_x removal by non-thermal plasma

1.2.1 Non-thermal plasma

(1) Plasma

Plasma is an ionized gas with free electrons, a distinct fourth state of matter. “Ionized” means that at least one electron is not bound to an atom or molecule, converting the atoms or molecules into positively charged ions. Ionized gas is usually called plasma when it is electrically neutral (i.e., electron density is balanced by that of positive ions). It contains a significant number of the electrically charged particles that can affect its electrical properties and behavior.[6]

Based on the relative temperature of free electrons, ions and neutrals, plasma is classified as thermal plasma and non-thermal plasma. Thermal plasma has

electrons and heavy particles at the same temperature, and they are in thermal equilibrium status. Non-thermal plasma, on the other hand, has the ions and neutrals of cold temperature (normally room temperature) state, whereas electrons are much “hotter”.

(2) Electric discharge

Non-thermal plasma is generated by applying a sufficiently strong electric field to ensure discharge of electrons. Electric discharge creates a quasi neutral medium containing neutrals, ions, radicals, electrons and UV photons. Due to light mass of electrons, they are usually first to receive the energy from an electric field and get high temperatures while the heavier ions remain relatively cold through energy exchange by collisions with background gaseous species. Ionic atoms and molecules have high energy and ability to lower activation barriers of chemical reactions.

Another feature of plasma ions results in the so-called ion or plasma catalysis, which is particularly essential in exhaust gas treatment. Atoms and radicals contribute to numerous plasma-stimulated oxidation processes. Finally, plasma-generated photons play a key role in a wide range of applications. Plasma light source to UV sterilization of water is an example of it.

(3) Non-thermal plasma

In the last two decades, the possibility of NO_x reduction from exhaust gases (deNO_x process) by means of non-thermal plasma (NTP) has been intensively studied.[7–19] The classification of NTP is rather complex and depends on multiple characteristics, such as:

- Type of discharge: DC or pulsed corona discharge, surface discharge, dielectric barrier discharge, ferro-electric packed bed discharge,...
- Type of power supply: AC, DC, pulse, microwave, radio frequency (RF),...
- Other characteristics: Electrode configuration, voltage level, polarity, gas composition,...

An increasing area of recent interest is the use of NTP at low-reaction temperature to eliminate NO_x from both of stationary and mobile sources. According to the research work by Sher [20], pulsed electrical field with dielectric barrier or corona discharges, was typically used to generate NTP. NTP oxidizes NO to NO₂ and N₂O₅, and also it generates O atoms or OH radicals which oxidize the hydrocarbons into aldehydes. NTP has the main function of activating NO_x and HC. It

provides a lower temperature pathway for their oxidation conversion. Low temperature treatment is quite important for exhaust emissions from vehicle where most part of engine out exhaust was low temperature. As for diesel engine, the mean temperature of the exhaust is below 200°C for over 70% of the operating cycles. As a consequence, there is an increasingly high relevant interest for application of NTP for treatment of diesel emissions.[21–23]

(4) Formation of N radical and ozone

The physical mechanism of N radical formation under non-thermal plasma was suggested by Vandenbroucke et al.[24]. N₂ molecules are firstly attacked by free electrons of which temperatures ranging typically from 10,000K to 250,000K (1–20eV).



The excited gas molecules from N₂^{*} above reaction lose their excess energy by emitting photons or heat.



Following this excitation, other processes like ionization, dissociation and electron attachment also occur. Through these reaction channels, unstable reactive species like ions and free radicals are formed.



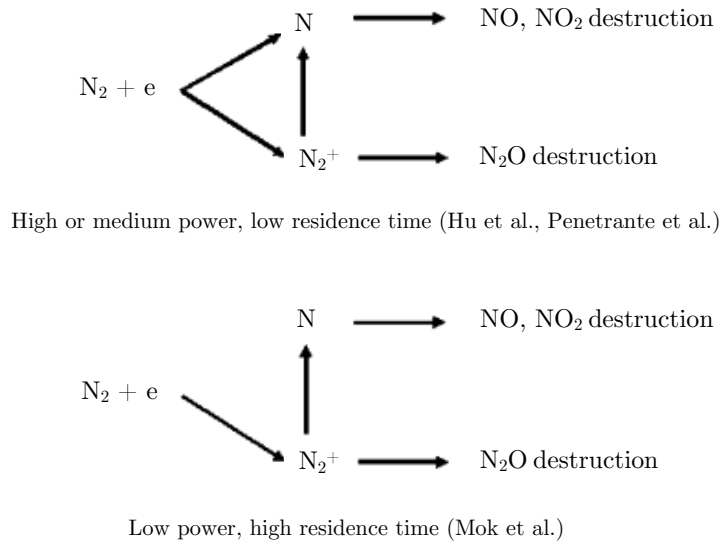
The destruction role of the radical and ionic species in the decomposition of nitrogen oxides is summarized in Fig.1.1.[7, 25, 26]

N₂O decomposes to form nitrogen and oxygen. The mechanism of this process involves N₂⁺ ions produced by primary ionization of nitrogen, charge transfer reaction to form N₂O⁺, and electron-impact dissociation. The extent of destruction is limited by the conversion of N₂⁺ ions to N radicals.

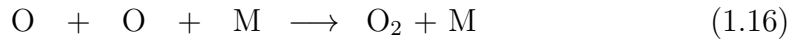
The formation of ozone from oxygen and from air under plasma was described in a report by Kogelschatz [27]. Similarly to the formation of N radical above, at first O radicals are formed from electron impact on O₂ molecules. Ozone is then formed in a three-body reaction involving O and O₂:



M is a third collision partner. O₃^{*} stands for a transient excited state. The time scale for ozone formation in atmospheric pressure oxygen is a few microseconds.

FIGURE 1.1 Role of radicals and ions in NO_x reduction [26]

Side reactions, also using O atoms, compete with ozone formation.[28–32]



These side reactions pose an upper limit on the atoms concentration tolerable in the discharge field.

1.2.2 NO_x removal using corona discharge

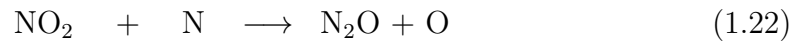
(1) Radical formation and NO_x destruction

Corona discharge is the simplest type of plasma generator. A feature of the corona discharge, which differs to the other discharges, is that there is no dielectric involved. Corona discharges are transient discharges generated by strongly inhomogeneous electric fields. The most common types are pin-to-plate [33], wire-to-cylinder [15, 34], and wire-to-plane [35]. The discharge can be supplied by a constant voltage (DC corona), or an alternating voltage (AC corona or a pulsed corona). Generally, the electric field in corona reactors is about 50kV/cm.[1, 36]

The destruction of NO and NO_2 involves N radicals. These radicals may arise from direct electron-impact dissociation of nitrogen or the electron-assisted conversion of N_2^+ ions (Fig.1.1). N radical reacts with nitrogen oxide to form molecular nitrogen and oxygen atoms according to the following reaction.[37–39]



The destruction of NO_2 with N radicals is relating to the following reaction chain.[7, 40]



(2) Corona discharge and NO_x destruction

Vinogradov et al.[35] used a multi-needle-to-plate reactor consisting of Perspex rectangular box (Fig.1.2). Test gas was an exhaust gas from a diesel engine. Flow rate of test gas was 8L/min. Electrode length was in the range from 45mm to 150mm. Distance between needle and flat electrode was 14mm–50mm and distance between the rows of needle was 5mm–20mm.

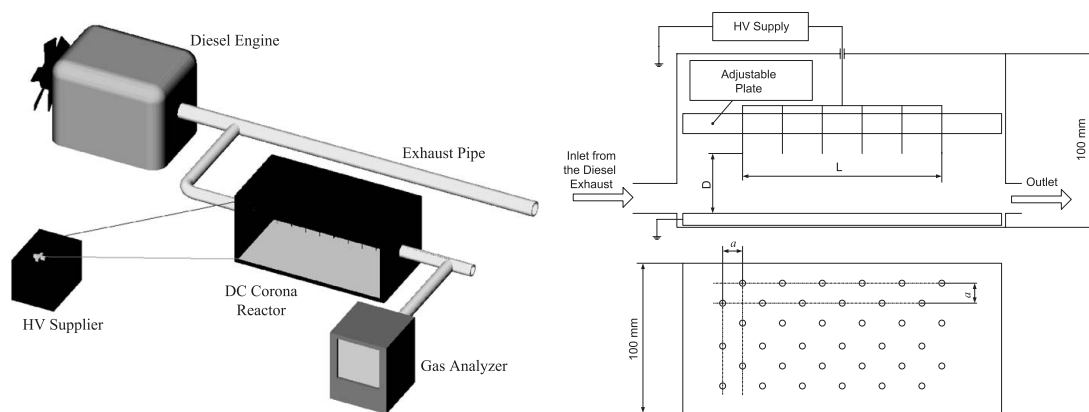


FIGURE 1.2 Experimental setup by Vinogradov et al.[35]

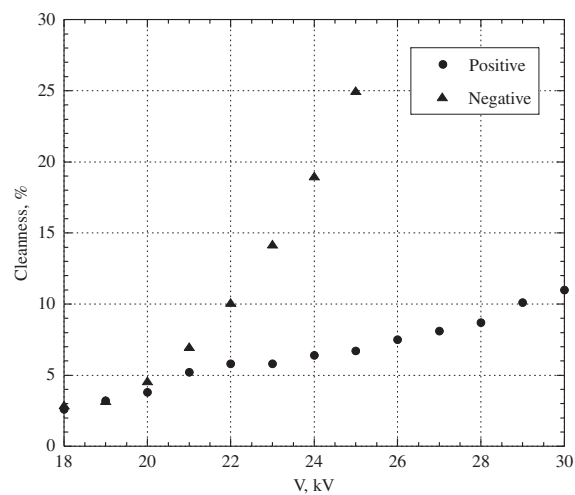


FIGURE 1.3 Relative positive-negative corona cleanliness behavior [35]

Experimental results in Fig.1.3 shows that the negative corona discharge has much higher NO_x cleanness comparing to the positive one. However, the relative positive-negative corona cleanness behavior is basically independent of geometrical parameters of the reactor as well as of the engine load.

Kozlov and Solovyov [41] also pointed out that in atmospheric air condition, the limit current of the negative corona configuration was higher than in the positive corona reactor. However, Fujii et al.[42] concluded that positive corona reactor showed better removal rate of NO_x than negative one. Another work by Dors et al.[43] also supported Fujii's conclusion.

(3) Residence time and discharge energy

The residence time is defined as the volume of the reactor divided by the flow rate of exhaust gas. H. Lin et al. [33] used a needle-to-cylinder corona discharge reactor to investigate the influence of the residence time on NO_x efficiency from wet flue gas. They suggested that the longer the residence time is, the higher the $deNO_x$ efficiency will be.

The experimental result in Fig.1.4 expresses the NO_x cleanness [35] depending on residence time at various reactor's dimensions. From the test results, they

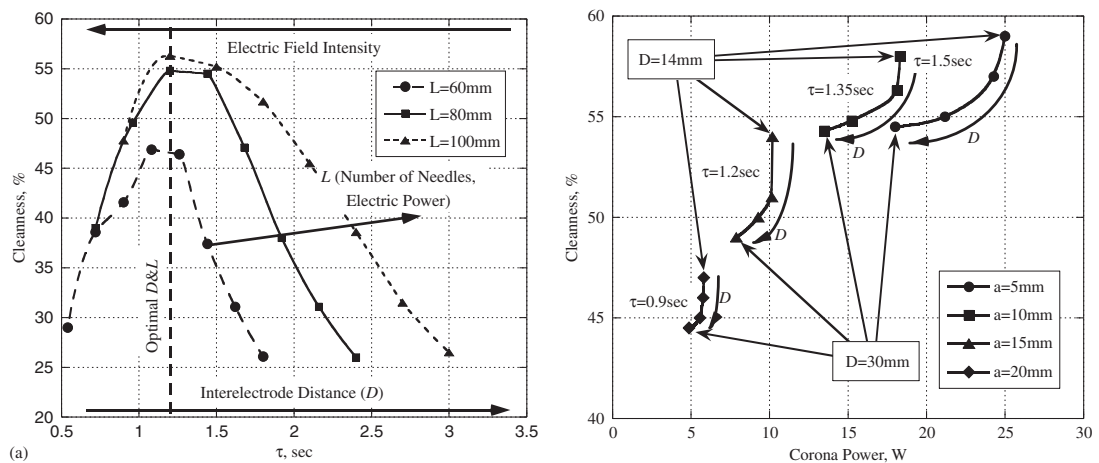


FIGURE 1.4 Effect of residence time on cleanness and corona power [35]

concluded that the increase of residence time positively affects both the cleanness and the energy efficiency until the moment at which discharge radicals outnumber pollutant molecules. Once the residence time is sufficient for all the gas molecules to interact with radicals, the cleanness growth rate reduced. And further improvement of cleanness is much slower.

(4) Corona discharge-catalyst reactor

Dors and Mizeraczyk [44] studied NO_x removal in a hybrid system consisted of a DC streamer corona discharge with a catalyst operating at ambient temperature in the presence of NH_3 (see Fig.1.5). The positive DC corona discharge was generated between a hollow needle (out diameter of 2mm) electrode and flat brass mesh (spacing of 40mm) electrode. The catalyst was a layer of V_2O_5 and TiO_2 deposited on Al_2O_3 globules.

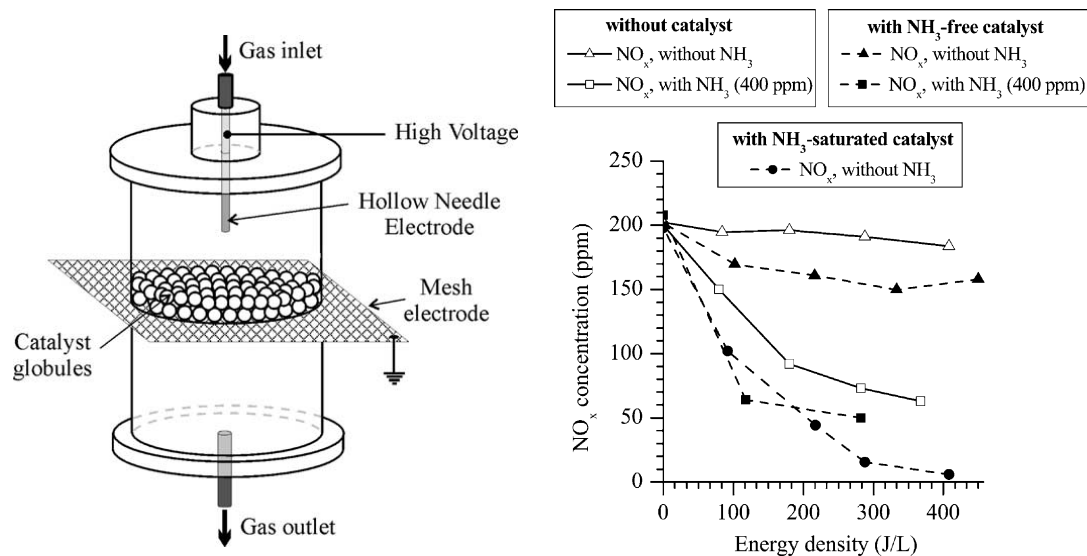
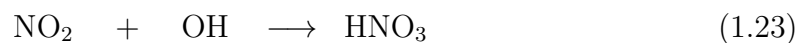


FIGURE 1.5 NO_x removal with hybrid corona discharge-catalyst reactor [44]

The results showed that the catalyst increased significantly NO_x removal (maximum 96% at 400J/L) when the catalyst was saturated with NH_3 . Comparing to the case of without catalyst and gaseous NH_3 supply, the removal efficiency of NO was not higher than 25% (at 400J/L). With the presence of NH_3 , the corona discharge produced solid particles of NH_4NO_3 which depositing on the catalyst surface shortened the active life of the catalyst. The mechanism was explained by following reactions:



(5) Pulsed corona discharge and NO_x destruction

In corona discharge, as electron streamers are able to reach the opposite electrode, a spark discharge formed then results in local overheating and non-uniformity

plasma that is unacceptable for applications. The solution to increase corona voltage and power without spark formation is using pulsed corona discharge.[45]

Decomposition of nitrogen oxides in a pulsed corona discharge were studied experimentally by X. Hu et al.[25]. As seen in Fig.1.6, for NO in N_2 , the exper-

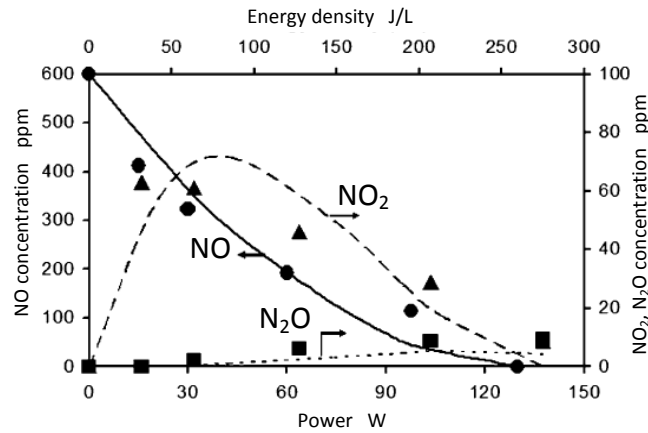


FIGURE 1.6 Model calculation and tested results of NO destruction with pulsed corona discharge reactor in NO + N_2 mixture [25]

imental data show that complete removal of NO can be reached. NO_2 reached a maximum at an medium input power and then was continuously destroyed as power increased. A small amount of N_2O was formed and its concentration increased at higher power levels.

To investigate the NO_x treatment from diesel engine exhaust, Vinogradov et al.[46] used the pulsed corona discharge cylinder-to-cylinder reactor (see Fig.1.7). The experimental results showed that cleanness does not depend on initial NO_x

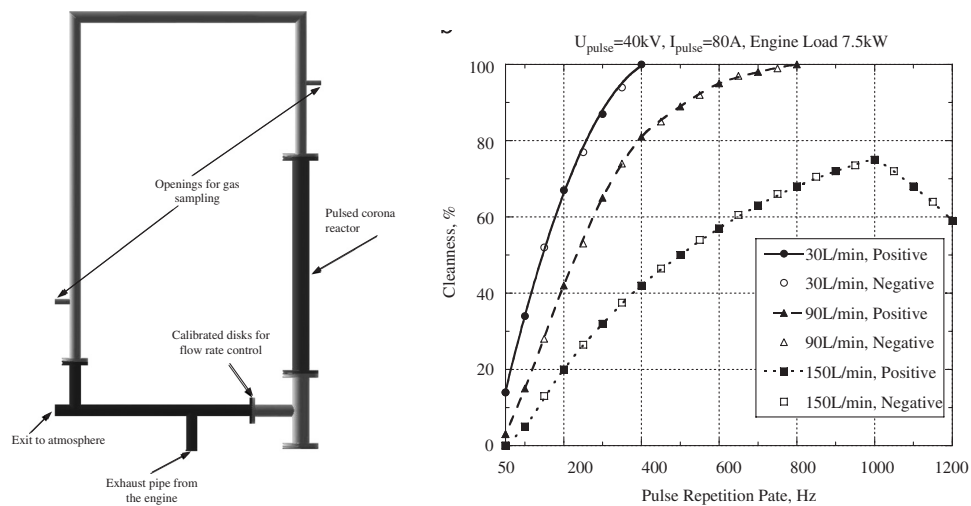


FIGURE 1.7 Cleanness behavior using pulsed corona discharge reactor [46]

concentration, within 10% accuracy. Therefore, it was concluded that the number density of the pollutant was much lower than that of the radicals produced by the discharge.

(6) DeNO_x characteristics in corona discharge

There are some conclusions that could be made from preceding research works concerning NO_x removal using corona discharge reactor.

- 1- The negative polarity produced larger amount of radicals (i.e., higher total current) despite the lower average mobility of the negative ions. The higher cleanness of the negative polarity stems from three reasons: the higher total current, the plasma region extension, and the presence of OH ions.
- 2- It is concluded that direct decomposition of NO_x through corona-assisted-dissociation reactions plays the dominant role in deNO_x process.
- 3- The NO removal efficiency of the corona discharge reactor is improved when combining with a catalyst at the same amount of energy density.
- 4- Pulsed corona discharge is effective to restrict spark discharge.

1.2.3 NO_x removal using dielectric barrier discharge

(1) Dielectric barrier discharge and its reactor

Dielectric barrier discharges (DBD) is the case in which a dielectric material is placed on the electrode surfaces. Similar to corona discharges, small-scale electron streamers are formed. In the DBD mode of operation, the threshold electric field is relatively low and low-energy electrons are formed. DBD reactors can be also configured as concentric cylinders or as arrays of alternating positive and negative dielectric-coated electrodes. The parallel-plate architecture, however, features the most simple and cost-effective design.[27]

DBD can be operated in AC mode or in pulsed mode. The most common discharge configurations are the planar electrode configuration and the coaxial configuration.[37] As for the effect of discharge configuration on current and performance of DBD reactor, Kuroda et al.[29] showed that discharge current of the electrode with punched holes was higher than of the plane electrode. The collective efficiency obtained with punched electrode was also higher than that with the plane electrode.

Dielectric packed-bed reactors are used as well for investigations of plasma-chemical reactions in plasma.[47] In this configuration, the discharge gap is

filled with dielectric pellets: glass beads, $BaTiO_3$, and Al_2O_3 being some of the most usual. When the high voltage is applied, the pellets are polarized and an intense electric field is formed at the contact points between pellets. Because the pellets are packed close together, the electric field in the micro-discharges can be significantly enhanced, thus, potentially increasing the production of chemically active species.

(2) NO_x removal by dielectric barrier discharge

Santillan et al.[48] used a DBD wire-cylinder reactor (Fig.1.8) for NO_x treatment contained in a gas mixture ($N_2 : O_2 : CO_2 : H_2O : C_3H_6 : NO$) simulating the vehicle exhaust gas. They also numerically simulated the DBD wire-cylinder reactor to explain the chemical reactions in the reactor.

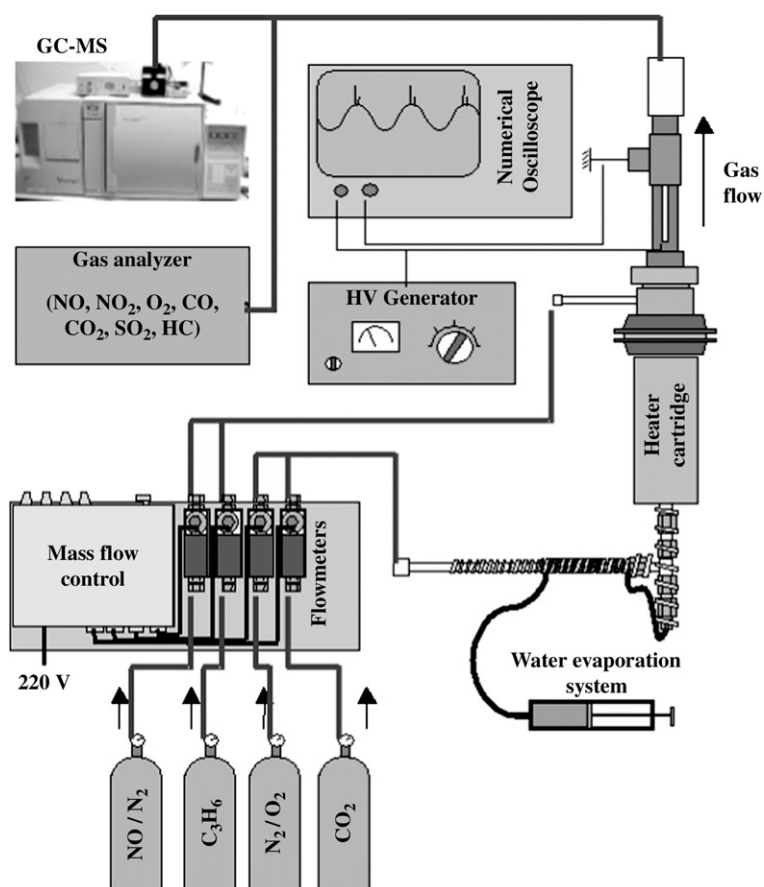


FIGURE 1.8 DBD wire-to-cylinder reactor layout [48]

The reactor was fed with a gas mixture slightly above atmospheric pressure. The mass flow of each gas, excluding water vapour, was controlled by a mass flowmeter. A pre-mixture containing 10% O_2 , 10% CO_2 and N_2 left was introduced into a chamber. In order to convert non-soluble compounds into soluble ones, water

was added using a manual injector and was vaporized through use of a heating resistance. The preheated mixture was then enriched with NO (250–1000ppm) and C_3H_6 (1000–2000ppm) and fed into the plasma reactor. The maximal total gas flow used was about 13L/min. Gas temperature was measured by a probe placed 30mm after the discharge zone.

The experimental results of NO conversion in the plasma reactor at initial concentrations of 250, 500, 1000ppm are showed in Fig.1.9. Mass balance in NO_x

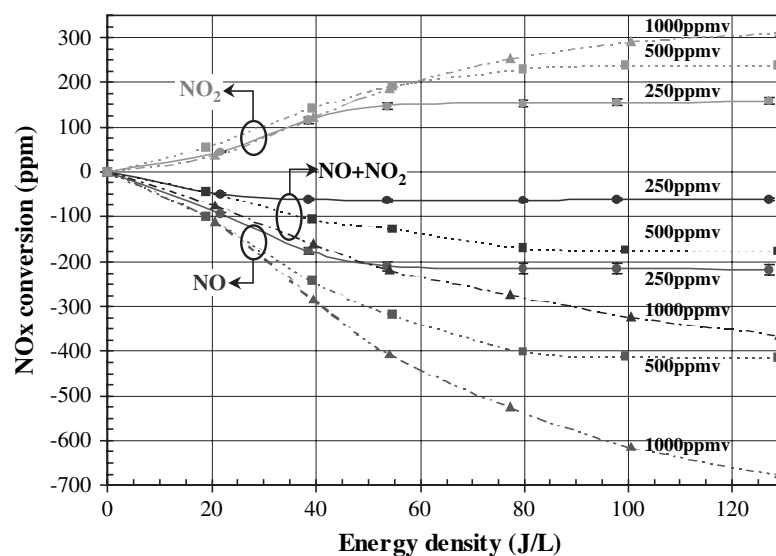


FIGURE 1.9 NO_x conversion vs. energy density in DBD reactor at various initial concentrations [48]

shows that an increase in energy density increases NO oxidation. Therefore, NO transformation is a direct function of the voltage applied. Furthermore, an increase in NO concentration requires a greater energy input. For example, to transform 70% of the NO supplied, energy densities of 40, 55 and 125J/L were, respectively, required for NO initial concentrations of 250, 500 and 1000ppm. The decrease in NO is linked to an increase in NO_2 through the oxidation process. The oxidizing vector can be produced by the $O_2(O + O)$, $CO_2(CO + O)$ or $H_2O(OH + O)$ in the gas mixture. Santillan et al.[48] commented that the global mass of NO_x is not balanced ($NO + NO_2 = 0$). This can be due to NO_x being trapped in $C_3H_6 = (R - NO_x)$ or water (HNO_3), or else to some adsorption on the outlet tubes.

(3) Merit and demerit of dielectric barrier discharge for NO_x treatment

Comparing to corona discharge, the flexibility of DBD configurations with respect to geometrical shape, operating medium and operating parameters is remarkable.[27]

Additionally, electrodes in BDB reactor are covered by dielectric layer preventing them from erosion by reactive emissions such as combustion gas. Conversely, the energy density inside DBD reactor is lower than that of corona discharge reactor.

There is a technical problem that requires optimization is the necessary energy to maintain the plasma (typically, 20–60J/L). Besides that, the application of optimized conditions in small laboratory experiments into the large installations (i.e. vehicles) is not clear and need more investigations.

1.3 Emissions and aftertreatment system of internal combustion engine

1.3.1 NO_x and other harmful emission from internal combustion engine

(1) Emissions from gasoline engine

The major pollutants in gasoline engine exhaust are nitrogen oxides (NO_x, mostly NO), carbon monoxide (CO), and hydrocarbons (HC). The main product of combustion, carbon dioxide (CO₂), is although non-toxic but contributes to the greenhouse effect. The relative emission amounts depend on engine design and operating conditions but are order of: NO_x, 500–1000ppm; CO, 1–2%; HC, 1000–3000ppm (as C₁).[3]

NO emissions in gasoline engine depend on fuel/air ratio, the burned gas fraction, and spark timing. The key factors for emission control are temperature and oxygen concentration during combustion process and early part of the expansion stroke. CO emissions from internal combustion engines are controlled primarily by the fuel/air ratio. Since gasoline engines often operate close to stoichiometric at part load and fuel rich at full load, CO emissions are significant and must be controlled. HCs are consequence of incomplete combustion of the hydrocarbon fuel. The level of unburned HC in the exhaust is generally specified in terms of the total HC concentration expressed in ppm C₁. While total HC emission is a useful measure of combustion inefficiency, it is not necessarily a significant index of pollutant emissions.

(2) Emissions from diesel engine

In diesel engine exhaust, concentrations of NO_x are comparable to those from gasoline engine. The critical difference in NO_x formation mechanism is that injection

of fuel occurs just before combustion starts, and that non-uniform distributions temperature and fuel exist during combustion.

The primary combustion mechanism in a diesel engine is the diffusion process, that is controlled by the rate at which fuel and air are mixed. This is preceded by the so called premixed process in which a small number of fuel-air nuclei combust spontaneously at a rate controlled by reaction kinetics. As fuel is injected into the charge air, it entrains air and diffuses, giving a widely varying equivalence ratio. At the core of the spray there is liquid fuel in droplet form; at the other extreme is a region with an equivalence ratio of less than one. NO_x formation occurs predominantly in the lean flame region during the premixed combustion phase and particulate matter is formed mainly in the fuel rich regions during the diffusion burning period. Actions to reduce NO_x formation, such as reducing the proportion of premixed combustion, will therefore have the effect of increasing the diffusion burning phase. Hence, it results the tendency to increase particulate formation and vice versa. This phenomenon is known as the NO_x-PM trade-off.[20]

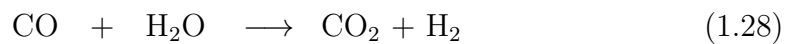
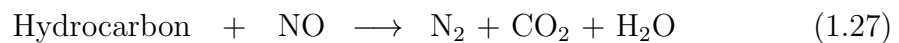
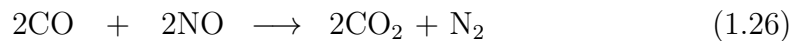
Diesel engines emit particulate matter (PM) which consist primarily of soot with some additional absorbed hydrocarbon material. Most particulate material results from incomplete combustion of fuel HCs. Further particulate matter is added by sulphur dioxide (SO₂) and sulphates, which bind with water on the carbon nuclei. These particles can make up as much as 20% of the total PM produced. Another source of particulates is lubricating oil. PM from the lubricating oil can make up as much as 40% of the total. The PM emission rates are typically 0.2–0.6g/km for light duty diesel vehicles. In larger DI engines, PM emission rates are 0.5–1.5g/brake kWh.[3]

Diesel engines are not a significant source of carbon monoxide because they always operate on the lean side of stoichiometric. Diesel hydrocarbon emissions are significant though exhaust concentrations are much lower than typical gasoline engine levels. The hydrocarbons in the exhaust may also condense to form white smoke during engine starting and warm-up. There are two major causes of HC emissions in diesel engines under normal operating conditions: (1) fuel mixed to leaner than lean combustion limit during the ignition delay period; (2) undermixing of fuel which leaves from the fuel injector nozzle with low velocity.

1.3.2 Aftertreatment system of internal combustion engine

(1) Three-way catalyst

Three-way catalyst (TWC), or non-selective catalytic reduction (NSCR) catalyst, is used at or close to stoichiometric operating conditions of engine for simultaneous conversion of NO_x , CO, and hydrocarbon. There are many reaction pathways in a three-way catalyst system. The most important reactions can be summarized as follows.[49]



Typical TWC is a monolithic type in which the exhaust gas passes through a honeycomb ceramic block, maximizing the exposed surface area. The ceramic block is covered with a thin coating of support material such as platinum (Pt), palladium (Pd), or rhodium (Rh), and mounted in a stainless steel container.[50] Other support materials used recently are alumina, ceria (CeO_2), zirconia (ZrO_2), etc. Generally, TWC can efficiently convert about 80% of NO , CO, and HC at a narrow range of air/fuel ratio near stoichiometric point. And it just works in the temperature range of 350°C – 600°C .

(2) Lean NO_x reduction system

The operating principle of lean NO_x reduction system is expressed in Fig.1.10.

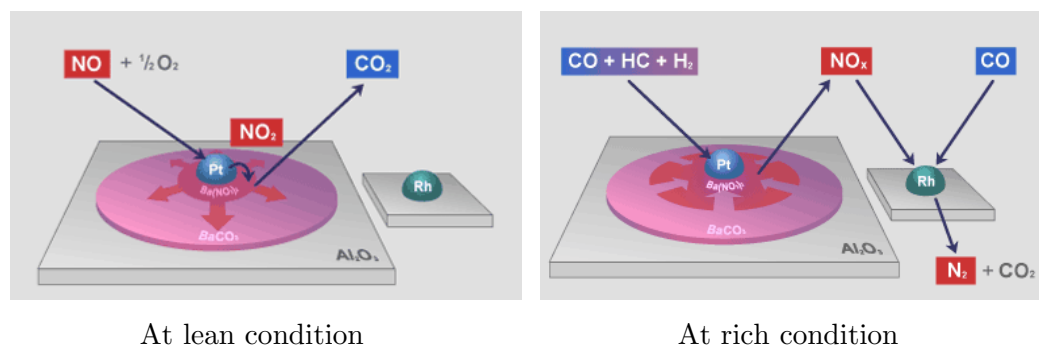


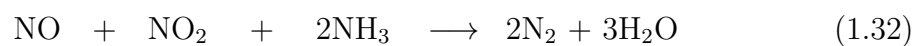
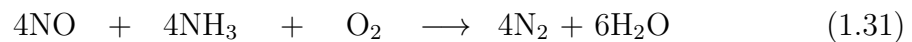
FIGURE 1.10 Operating principle of the lean NO_x reduction system [Matthey]

Lean NO_x reduction system, also known as NO_x storage reduction (NO_x-SR) or NO_x adsorber catalyst (NAC), was used for partial lean burn gasoline engines and for diesel engines. The adsorbers, which are incorporated into the catalyst washcoat, chemically capture nitrogen oxides during lean engine operation. After the adsorber capacity is saturated, the system is regenerated. And released NO_x is catalytically reduced during a period of rich engine operation.[1, 51, 52]

(3) Urea selective catalytic reduction

Selective catalytic reduction (SCR) technology has been used successfully for more than two decades to reduce NO_x emissions from power stations, marine vessels and stationary diesel engines. Also it has been used for heavy duty vehicles. According to a report [53] by Bosteels and Searles (2002), SCR for heavy duty vehicles reduces NO_x emissions by around 80%, HC emissions by around 90% and PM emissions by around 40% in the EU test cycles, with normal diesel fuel (less than 350ppm sulfur).

Ammonia (NH₃) has proven to be the reducing agent with the greatest selectivity. However, for safety reasons, liquid urea is often used as reducing agent in the vehicles. Urea is chemically stable under the ambient condition and rapidly hydrolyses to produce ammonia in the exhaust stream.[54] The reaction mechanism of NO_x with ammonia is expressed as below.[1, 55]



(4) Diesel particulate filter system

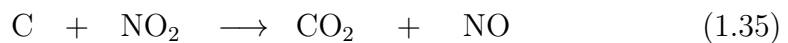
Diesel particulate filter is used to trap particulate matter (soot) from diesel exhaust emissions. It has a cellular structure with individual channel that has open and plugged ends at opposite side. Exhaust gases enter the open end, flow through the pores of the cell walls, and exit the filter through the adjacent channel (so called wall-flow type). Soot particles are collected on the channel walls. The most popular filter materials are cordierite Mg₂Al₄Si₅O₁₈, aluminum titanate TiAl₂O₅, and silicon carbide (SiC). Conventional DPF has a diameter from 190mm to 305mm and a length of 178mm–280mm.[56, 57] Collection efficiencies of these various filters range from 30% to over 90%, but most DPFs achieve over 99% when expressed as numbers of ultra fine particles.[53]

Since the wall flow filter would steadily become plugged with particulate material in a short time, it is necessary to “regenerate” the filtration properties by burning off the collected PM. Some remarkable methods are:

- 1- Reburning in high temperature (more than 600°C) with oxygen rich condition:



- 2- Putting a platinum group metal (PGM)-based oxidation catalyst in front of the DPF to generate the NO_2 .^[58] This is also called continuously regenerating trap (CRT). PM is removed following below scheme:



This reaction occurs at temperature over 250°C which can be seen in most diesel exhausts.

- 3- Using very small amount of fuel-borne catalyst, such as ceria for the PM removal reaction:



This reaction requires temperatures of around 400°C.

- 4- Electrical heating of the DPF either on or off the vehicle.

(5) Role of PM for catalyst and adsorption material

It has been reported that PM takes part in reaction converting NO_2 to NO and NO_x to N_2 .^[59, 60] Additionally, the fundamental unit of PM, the soot agglomerates, are spherules with the diameters of 10–15nm. The surface of these spherules can adhere hydrocarbons material, soluble organic fraction (SOF), and inorganic material. In case of existence of gaseous oxidant such as oxygen, CO_2 , NO_2 , these oxidants first move to the surface and be adsorbed to form surface intermediates, which then rearrange, desorb and escape into the gas phase. The PM surface may be the wall of a pore deep inside, so that diffusion of oxidant and oxidized products to the bulk gas phase occurs.^[59]

(6) New approach of aftertreatment system

Although there is a wide range of emissions control technique as showed above, it still demands more new approaches to meet tight emission legislations. In recent years, some new aftertreatment systems have been introduced. They include plasma technique, hydrocarbon adsorber, electrically heated catalyst system,

combined emission control systems (i.e. DPF and SCR, diesel oxidation catalyst (DOC) for HC and PM oxidation), etc. Among them, plasma approach has been introduced as a new promising aftertreatment technology.

1.3.3 NO_x and PM treatment by non-thermal plasma

For simultaneous removal of NO_x and PM from stationary diesel engine exhaust, Mok et al.[26] used a DBD reactor consisting of ceramic tubes and steel rods. In another work, Grundmann et al.[61] used a coaxial DBD reactor to study the soot treatment by DBD and ozone. DBD reduced the activation energy of the reaction which decomposed soot to form CO.[12, 16, 26, 47, 61–64]

Song et al.[65] used a DBD in coaxial configuration to study the effect of NTP on the reduction in NO_x , HC and PM including carbon soot and soluble organic fraction (SOF). A schematic layout and the DBD reactor configuration is shown in Fig.1.11. The system mainly consists of an exhaust gas supply, DBD

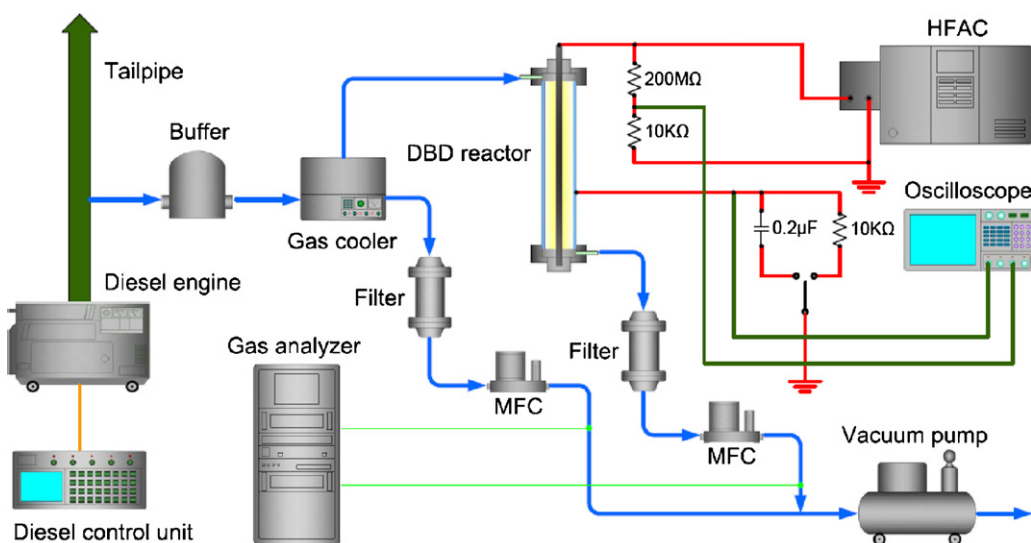


FIGURE 1.11 DBD reactor configuration to remove NO_x , HC and PM [65]

reactor, high frequency AC power supply (HFAC: 0–14kV, 10–27kHz), indicating and analytical systems. Exhaust gas was produced by an diesel engine and sampled partially from the tailpipe by vacuum pump, which was set at the end of the line. The engine featured a 17.5:1 compression ratio, one cylinder, direct injection, air cooler, cylinder displacement of 296mL and rated power of 2.4kW at 3000rpm. The flow rate passing through the reactor was kept constant at 5L/min for all experimental runs. Two concentric quartz tubes were used for dielectric barrier layers with wall thickness of 1mm. The outer and inner one had the outside

diameters of 18mm and 8mm, respectively. The high voltage electrode was placed on the axis center of quartz tubes using a stainless steel rod of 6mm diameter, and connected to HFAC.

The experimental data of PM, HC, and NO_x abatement efficiencies are illustrated in Fig.1.12. The test conditions were: applied frequency of 15.5kHz, initial PM=73.67 μ g/L, HC=107.6ppm, and NO_x =476.3ppm. For the PM removal, it can be seen that in the range of 6kV–8.5kV removal efficiency is proportional to peak voltage. At the value of 8.5kV the removal efficiency approaches to the maximum of 82%. Two reasons may be attributed to the saturation of removal efficiency. First, as shown in Fig.1.12, there exists a systematic increase in the reactor temperature with increasing specific energy density and more energy is converted into heat, resulting in the energy utilization efficiency for the DBD system decreasing. Second, the high temperatures condition would induce segmental active species such as ozone, which benefit the removal reaction.

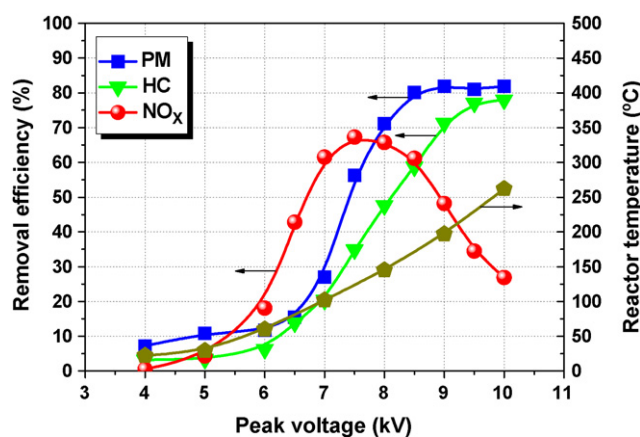


FIGURE 1.12 Results of PM, HC and NO_x removal efficiencies as a function of peak voltage [65]

As for the removal of HC, Fig.1.12 illustrates the similar trend to that of PM. Namely, the removal efficiency for HC increases with the peak voltage from 4kV to 10kV (34–730J/L) and the maximum of HC removal efficiency is around 78% at 10kV. In addition, when the peak voltage exceeds 9kV, the curve of removal efficiency for HC versus peak voltage also becomes smoother because of the two reasons mentioned above. The trend of NO_x removal efficiency is distinguished from that of PM and HC. In the range of 4kV–7.5kV (34J/L–178J/L), a significant increase of NO_x removal efficiency from 0.5% to 67.3% is observed.

1.3.4 NO_x and HC treatment system by non-thermal plasma

The role of hydrocarbon as an additive in NO_x abatement process was investigated by Ravi et al.[66]. The plasma reactor layout is showed on Fig.1.13. A cylindrical glass tube (inner diameter: 25.8mm; outer diameter: 30.2mm) was used as the dielectric material and a copper rod (diameter: 9mm) was used as the discharging electrode. An aluminium foil wrapped over the glass tube acted as the ground electrode. The space between the glass tube and the discharging electrode was filled with glass beads of 5mm diameter. Gas mixture consisted of $NO=300$ ppm, $O_2=10\%$,and N_2 remaining. The hydrocarbon additives were acetylene, ethylene and n-hexane. These additives were injected into the gas stream in equal concentrations of 750ppm. Gas flow rate was kept at 2L/min.

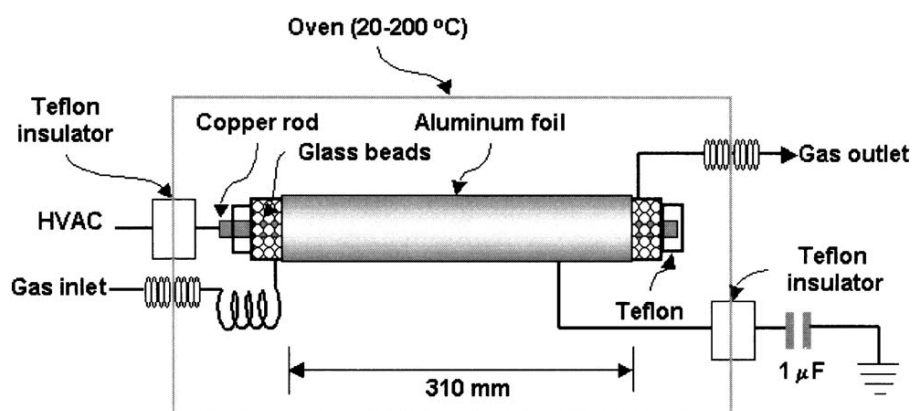


FIGURE 1.13 Schematic of the DBD reactor by Ravi et al.[66]

Effect of hydrocarbons on NO and NO_x removal efficiencies at various energy densities at room temperature is expressed on Fig.1.14. There was no NO_x removal

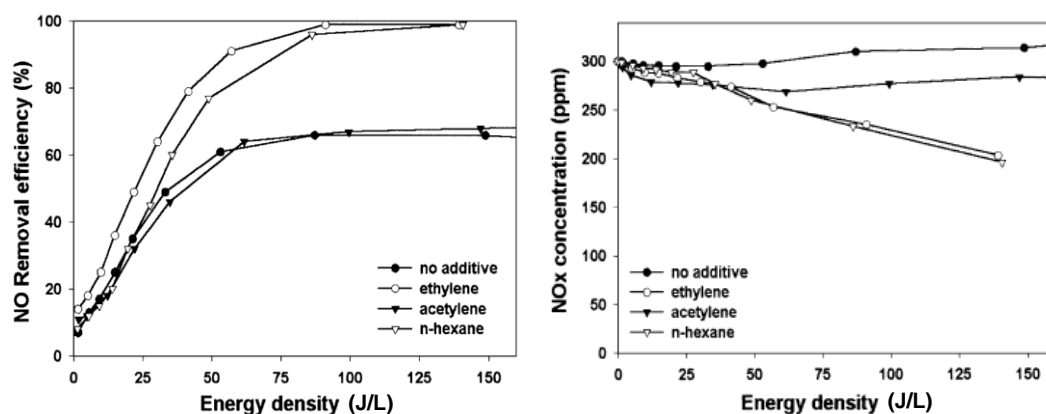
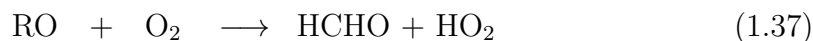


FIGURE 1.14 Effect of HCs on NO and NO_x removal efficiencies [66]

without additive whereas it was negligible in the presence of acetylene. In the presence of ethylene and n-hexane, the NO_x removal efficiencies obtained in this experimental condition were 32% and 35%, respectively. Briefly, the NO_x removal was insignificant in all these cases.

From these results, Ravi et al. concluded that the presence of both ethylene and n-hexane enhanced the oxidation of NO to NO₂ significantly, whereas the addition of acetylene was found to be no better than that without any additive. At an energy density of 50J/L, the NO removal efficiency was as high as 80% with ethylene and 75% with n-hexane, while acetylene and no additive case showed only 60% removal.

The mechanism of NO removal in presence of hydrocarbons was explained as follows. The important radicals for the oxidation of NO are alkyl (R), alkoxy (RO) and acyl (RCO) radicals, which are generated when hydrocarbons react with O, OH, O₃, etc. Initially, alkoxy (CH₃O, C₂H₅O, etc.) and alkyl radicals (such as CH₃, C₂H₅, etc.) react with oxygen to liberate active species



NO is oxidized with HO₂ or RO₂ through the following reactions.



1.4 Purpose of this research study

1.4.1 Laboratory scale experiment

(1) Current problem for vehicle emission treatment

Since the legislations concerning exhaust emission from vehicles are continuously tightened, NO_x aftertreatment systems have become increasingly important. Regarding current emission legislations, Table 1.2 illustrates the emission standards for diesel passenger cars in Japan, EU, and US (California). In the Table 1.3 is the standards for the gasoline cars in the same places.[1, Dieselnets] Compliance with these strict emission regulations has led to the implementation of at least one or some combined aftertreatment systems. To clear the limit of PM emissions at 5mg/km, the DPF has to be installed in the exhaust system and becomes mandatory for Euro 5. On the other hand, to reach the NO_x emission limit of 180mg/km, it is necessary to modify the EGR system in a way to minimize the

TABLE 1.2 Emission standards for diesel cars in Japan, EU, and US

Country	Standard	Date	CO	HC	HC+NO _x	NO _x	PM	PN	
			g/km						#/km
Japan	Emission Standards for Diesel Passenger Cars								
	Vehicle Weight								
	< 1250 kg	2002	0.63	0.12		0.28	0.052		
		2005	0.63	0.024		0.14	0.013		
		2009	0.63	0.024		0.08	0.005		
	> 1250 kg	2002	0.63	0.12		0.3	0.056		
	2005	0.63	0.024		0.15	0.014			
	2009	0.63	0.024		0.08	0.005			
EU	Emission Standards for Diesel Passenger Cars								
	Euro 4	2005.01	0.5		0.3	0.25	0.025		
	Euro 5a	2009.09	0.5		0.23	0.18	0.005		
	Euro 5b	2011.09	0.5		0.23	0.18	0.005	6E+11	
Euro 6	2014.09	0.5		0.17	0.08	0.005	6E+11		
US California	LEV II Emission Standards for Passenger Cars and LDVs < 8500 lbs; 50,000 miles/5 years								
			NMOG	CO	NO _x	PM	HCHO		
		2004-2010	g/mile						
	LEV		0.075	3.4	0.05		0.015		
	ULEV		0.04	1.7	0.05		0.008		
	SULEV								

Note: PN - Particle Number NMOG - non-methane organic gases HCHO - formaldehyde

TABLE 1.3 Emission standards for gasoline cars in Japan, EU, and US

Country	Standard	Date	CO	HC	NO _x	PM	PN		
			g/km						#/km
Japan	Emission Standards for Gasoline Light Duty Vehicles								
		2003	0.67	0.08	0.08				
		2010	1.15	0.05	0.05	0.005			
EU	Emission Standards for Gasoline Passenger Cars								
	Euro 4	2005.01	1	0.1	0.08				
	Euro 5	2009.09	1	0.1	0.06	0.005			
	Euro 6	2014.09	1	0.1	0.06	0.005	6E+12		
US California	LEV II Emission Standards for Passenger Cars and LDVs; 50,000 miles/5 years								
			NMOG	CO	NO _x	PM	HCHO		
		2004-2010	g/mile						
	LEV		0.075	3.4	0.05		0.015		
	ULEV		0.04	1.7	0.05		0.008		
	SULEV								

Note: PN - Particle Number NMOG - non-methane organic gases HCHO - formaldehyde

engine-out NO_x emissions. However, increase of EGR ratio will lower combustion temperature that may result in increases of unburnt hydrocarbon concentration, CO, and PM.

As for exhaust gas from gasoline engines, the most well-known system is the three-way catalysts (TWC). However, it is not efficient enough for NO_x treatment under lean-burn conditions. As for Urea-SCR or NH₃-SCR, first main obstacle is requirement of pure ammonia for its operation. Ammonia is an irritating and toxic gas so it should be released in the exhaust line at level of under 10ppm. There is another point concerning the installation this large system into vehicle. Besides that, an urea tank volume and its availability are also problems.

The application of lean NO_x reduction system, or lean NO_x trap (LNT), has four major issues. Firstly, due to its operating principle that mentioned above, the engine must create rich conditions in the exhaust line so it makes fuel over-consumption. Secondly, there are HC penalties and more methane emissions which pass through catalyst without any conversion. It reduces significantly the efficiency of LNT regeneration.[5] The next difficulty is that this system is particularly sensitive to sulfur. Because sulfur and more specifically SO₂ take the place of NO₂ on the material surface causing a decrease in the number of available sites dedicated to NO_x adsorption.[1] Finally, similar to three-way catalyst (TWC), LNT uses noble metals (typically are Pt, Pd, and Rh). Thus they are high cost NO_x aftertreatment systems.

(2) Practical system and model system for research work

As discussed above, the severity of emission standards leads to some PM and NO_x aftertreatment systems become mandatory in legislation context. Thus it implies a cost and generates a complex implementation. Furthermore, PM and NO_x aftertreatment systems have an impact on the engine operation and fuel penalties.[67] Therefore it is necessary either to find some auxiliary systems to decrease this impact or to find some brand new deNO_x aftertreatment systems.

To find a suitable auxiliary system, it requires more investigations to understand the mutual affect when combining this system with the main one. Due to difficulties in application of aftertreatment techniques in real systems as mentioned before, the model system (or lab-scale size system) is a good solution. The cost is significantly reduced while characteristics of system is reliable. These advantages of using model system for research purposes are also true in case of finding a new system. Additionally, due to the difficulties of observing and controlling

treatment processes in the real system, it is better to use the simplified system to understand the physical and chemical reaction mechanisms in the system. For all of those reasons, in this study, the simplified model of dielectric barrier discharge reactor was proposed to investigate NO_x removal characteristics.

(3) Practical exhaust gas and simulated exhaust gas

There are also some difficulties in controlling and sampling of the practical exhaust gas. Firstly, it is very hard to keep the engine operating stable during a long test time. In addition, engine is a complicated system so there are many parameters that influence in emission composition. Typically, diesel engine exhaust gas contains 50ppm-2500ppm of NO, 20ppm-400ppm of HC, 5ppm-600ppm of CO, and 8%-12.6% of O₂. Both of those make the experimental results become unreliable. Finally, the cost to run engine should be concerned.

Alternatively, the simulated exhaust gas was chosen in order to avoid the complexity of using the practical one. This method becomes more significant for adjustment of gas composition in small amounts and in short intervals, where it is impossible in the real system. In the literatures, the NO concentration in the simulated gas was adjusted in a concentration from 50ppm to 500ppm.

(4) Combined system with DPF

Using non-thermal plasma to remove NO_x has showed potentiality. The advantage of this aspect is the low temperature elimination of NO_x that is quite important for vehicle emission exhaust where most of emission testing cycles occurs at low temperature. In addition, as mentioned in previous section, PM and NO_x aftertreatment systems now become mandatory in legislation context due to very strict emission standards. Hence, the combined system of an dielectric barrier discharge reactor and a DPF was proposed.

In the literatures, most researches concerning NO_x and PM emission elimination using non-thermal plasma was conducted by employing either a DBD reactor alone or a plasma-assisted catalysis working under high temperature condition (over 150°C).[26, 61, 68] Although there have been evidences that non-thermal plasma decomposes diesel particulate matter but its mechanism is still not clear. Moreover, the experimental data are rather controversial, and there is no general agreement about PM reduction under discharge field. Therefore, it is necessary to investigate extensively the effect of PM on NO_x removal process and its mechanism.

1.4.2 Objective of this study

The aim of this study is first to examine and validate the NO_x removal behavior under barrier discharge field. The NO_x treatment following applied voltage, energy density, and running time is investigated experimentally. The simplified model for laboratory experiments consists of a wire-to-cylinder DBD reactor combined with a diesel particulate filter (DPF).

(1) NO_x removal efficiency

The effect of oxygen on NO_x abatement process at different gas flow rates is considered. Experiments of various oxygen fraction at constant gas flow rate are carried out. By this way, the mechanism and efficiency of NO_x removal process are studied. The results are also referred to previous works in the literatures.

(2) PM effect on NO_x removal

This study focuses on extensively investigating the effects of particulate matter (PM) on NO_x removal in DBD reactor. Firstly, the experiments in cases of DPF without and with PM are done. In the next step, different PM mass are loaded on DPF. The effect of PM depending on test running time is investigated. The chemical reaction mechanisms in these processes are also discussed.

(3) “Fresh PM” and “Aged PM”

Through this study, two new definitions of “Fresh PM” and “Aged PM” are proposed to explain the significant effect of PM on NO_x removal process. The tests with “Fresh PM” and “Aged PM” in the same conditions of gas composition and flow rate are done. These results are compared to that of the case of DPF without PM to see the differences.

(4) Adsorption effect of PM

The experiments in transient mode of four hours and six hours with pre-treatment in DBD are carried out. At pre-treatment stage, different gas compositions and energy densities are applied. From the test results, the NO_x adsorption effect of PM can be identified. By conducting this study, basic knowledge of NO_x treatment using non-thermal plasma can be understood. Moreover, this work may help in establishing more effective catalyst applied for the real diesel engines.

1.4.3 Outline of the thesis

Chapter 1

This chapter gives an overview of NO_x problem and deNO_x methods have been used up to now. The reviews of previous research works in the literature relating to NO_x removal by non-thermal plasma are also available. Finally, objectives of this study are given.

Chapter 2

The methodology and experimental apparatus are described in this chapter. Related contents include test procedure, gas composition. PM sampling, experimental parameters, and data analysis are showed. Further basic performances of the proposed reactor are introduced here.

Chapter 3

In this chapter, the experimental results of NO_x reduction by N radical and regarding the effects of oxygen on NO_x removal characteristics are given. In addition to the test results, the reaction mechanism and some discussions are made.

Chapter 4

This chapter shows the experimental results regarding the effects of particulate matter (PM) on NO_x removal behavior. The definitions of “Fresh PM” and “Aged PM” are described. The test results, chemical mechanism and related discussions are given.

Chapter 5

The experimental results of NO_x removal performance in transient tests are showed. Detailed description of each kind of tests (four hours mode and six hours mode) are available. Through test results, N radical adsorption, NO_x adsorption effect of “Fresh PM” and “Aged PM” are identified and discussed.

Chapter 6

This chapter summarizes the conclusions that are made through this study.

Chapter 2

Experimental apparatus and method

2.1 Methodology

2.1.1 Dielectric barrier discharge applicable for deNO_x reactor

(1) Demand for deNO_x plasma reactor

The harmful effects of nitrogen oxides (NO_x) being known for many years, regulations in NO_x emissions have been progressively introduced in most of the countries worldwide. Therefore, it requires an reactor to convert them to N₂ (see Fig.2.1). Among deNO_x aftertreatment techniques, the plasma reactor has been introduced as a new promising approach.[36]

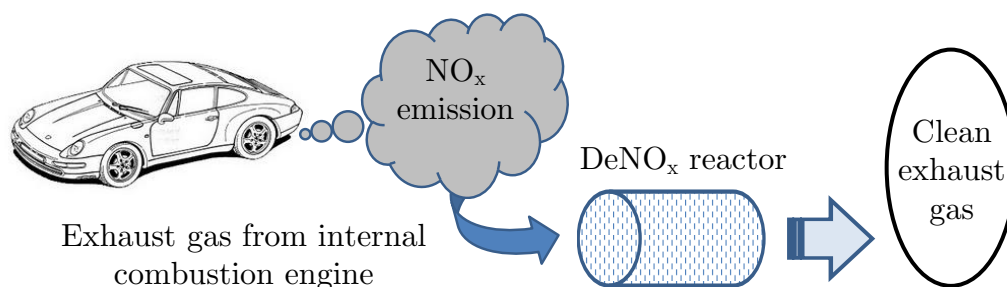


FIGURE 2.1 The necessity for deNO_x reactor

From that point of view, the plasma reactor should meet following demands. Firstly, it is applicable to practical system. Secondly, it is also applicable for engine

aftertreatment system. These demands cover the capability of transferring from lab-scale size model to a big one in the real system. It should not be complex. This leads to the third requirement, a compact design of the reactor. Additionally, the cost should be concerned.

For the conventional NTP reactors that are employed in laboratory experiments, there are some common types of dielectric discharge NTP reactor as shown in Fig.2.2.[24] Brief descriptions of each type are given and technical verdict for deNO_x reactor are performed in this research work.

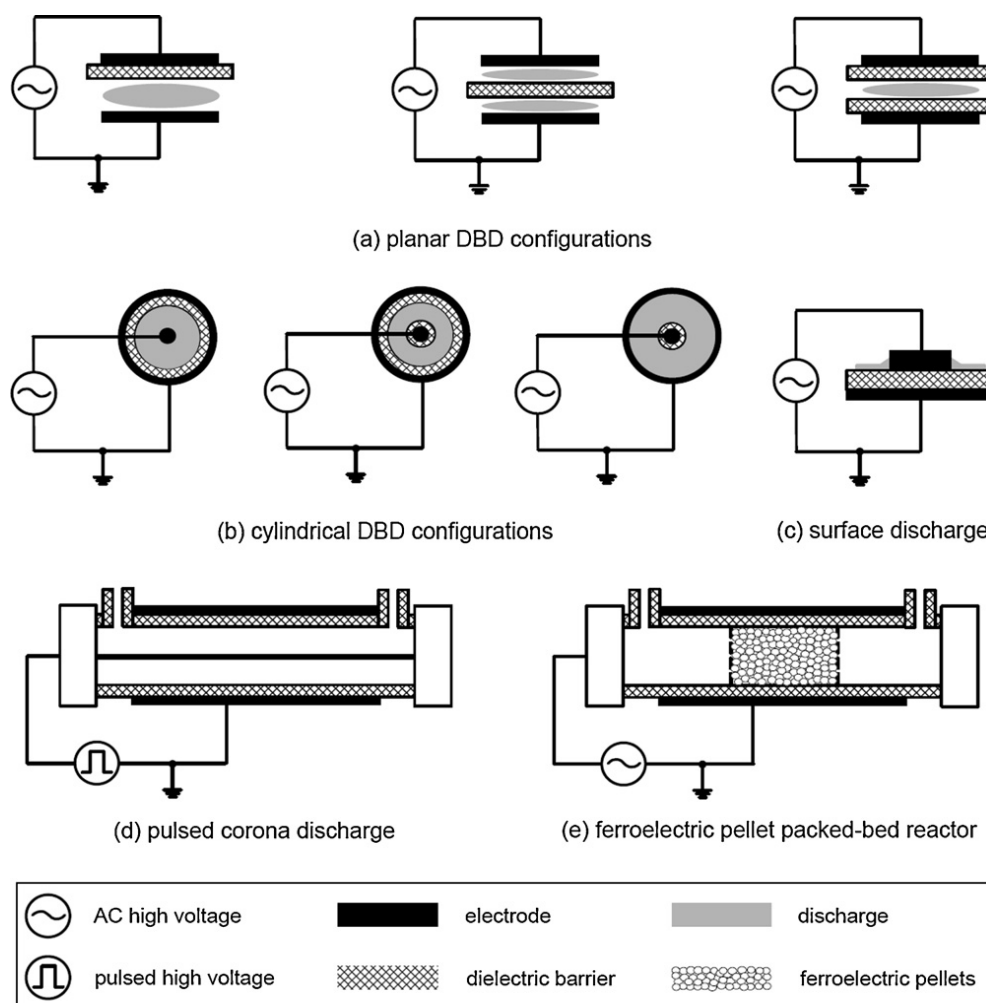


FIGURE 2.2 Dielectric discharge NTP reactors

(2) Dielectric barrier discharge reactor

A dielectric barrier discharge (DBD) or silent discharge, typically has at least one dielectric (e.g. glass, quartz or ceramic) material between the electrodes. DBDs are generally operated in either the planar (Fig.2.2(a)) or cylindrical (Fig.2.2(b))

configurations.[69] When the local electron density in the discharge gap reaches a critical value, a large number of separate and short-lived current filaments (microdischarges) are formed.[70] When a microdischarge reaches the dielectric layer, it spreads into a surface discharge and the accumulation of the transferred charge on the surface of the dielectric barrier making the electric field reduced. As the electric field further reduced, electron attachment prevails over ionization and the microdischarges are extinguished. When the polarity of the AC voltage changes, the formation of a microdischarge is repeated at the same location if the electron density again reaches a critical value necessary for electrical breakdown. Therefore, the dielectric in the discharge zone has two functions: (1) limiting the charge transferred by an individual microdischarge and (2) spreading the microdischarge over the electrode surface which increases the probability of electron collisions with bulk gas molecules.[70]

For lab-scale model, the cylindrical configuration is better because of its compact and easy to setup. Besides that, it is convenient to combine with a particulate filter for investigating NO_x treatment with diesel exhaust gas.

(3) Surface discharge reactor

Another type of DBD configuration is the surface discharge (Fig.2.2(c)).[69] In this reactor, a series of strip electrodes are attached to the surface of a high-purity alumina ceramic base. The remaining electrode is embedded in inner of the base and functions as an induction electrode. The ceramic base can be either planar or cylindrical. When an AC voltage is applied between electrodes, a surface discharge starts from the peripheral edges of each discharge electrode and stretches out along the ceramic surface. The surface discharges consist of many nanosecond surface streamers.[71]

This configuration is simple and easy to setup. However, the discharge is just on the surface of reactor so it is difficult to apply for a flow of gas which requires a volume discharge.

(4) Pulsed discharge reactor

A pulsed corona discharge (Fig.2.2(d)) reactor uses a pulsed power supply with a fast voltage rise time (tens of nanoseconds) to enable an increase in corona voltage and power without formation of sparks, which can damage the reactor and decrease the process efficiency.

The pulsed corona discharge usually consists of streamers, for which the ionization zone fills the entire electrode gap. The required voltage level to energize the discharge depends on the distance between the electrodes, the pulse duration and the gas composition.[72] The duration of a pulse voltage is typically in the order of 100–200ns to ensure that spark formation is prevented and that the energy dissipation by ions is minimal. The electrode configuration of a pulsed corona discharge reactor can be either wire-to-cylinder [36, 48, 73–75] or wire-to-plate [76–78].

This type of reactor requires a pulse generator for its operation. That makes system complicated and difficult to handle, especially in practical use.

(5) Ferroelectric pellet packed-bed reactor

A ferroelectric pellet packed-bed reactor (Fig.2.2(e)) is a packed-bed reactor filled with perovskite oxide pellets. The most widely used ferroelectric material is Barium titanate (BaTiO_3) due to its high dielectric constant ($2000 < \epsilon < 10000$). Other used ferroelectric materials are NaNbO_3 [79], MgTiO_4 , CaTiO_3 , SrTiO_3 , PbTiO_3 , [80] and $\text{PbZrO}_3\text{PbTiO}_3$ [81]. Application of an external electric field leads to polarization of the ferroelectric material and induces strong local electric fields at the contact points between the pellets and between the pellets and electrodes. This enables the production of partial discharges in the vicinity of each contact point between the pellets.

This configuration is suitable for gas treatment rather than gas with PM. Since PM may cover the surfaces of pellets and make them inactive, this system is not applicable for present purpose of this study.

2.1.2 Plasma reactor with DPF

(1) Application of plasma reactor to DPF system

The necessity of combination of deNO_x reactor and diesel particulate filter (DPF) to meet current diesel emissions legislation has been discussed in previous chapter. In the literature, some research works [25, 26, 36, 48, 62, 82] had been done on the NO_x removal phenomena with electric discharge or plasma condition. So far, however, there has been little discussion about the influence of PM on NO_x removal characteristics using plasma reactor.

(2) Selection of discharge reactor type

The most significant advantage of non-thermal plasma (NTP)(includes corona and dielectric barrier discharge (DBD)) for NO_x treatment is low temperature activity.

In other catalytic approaches, certain desired reaction paths can only be attained at high temperature and pressure. By using a NTP reactor, it can substantially lower the apparent activation energy and achieve activity already at much lower temperature. Another merit of NTP is that non-equilibrium plasma conditions can be provided at atmospheric pressure.

The main characteristic of the DBD is that a dielectric layer covers one of the electrodes, or sometimes both electrodes. The detailed theoretical description of DBD operation is summarized in Eliasson and Kogelschatz [27, 70]. When the voltage is applied between the electrodes, many micro-discharges, or plasma filaments are initiated, which are distributed in the discharge volume.

To meet the demand for deNO_x plasma reactor as mentioned above, the reactor should have a high endurance that leads a need of simple system. Furthermore, the discharge reactor should generate an stable discharge and high efficiency. Finally, the reactor needs to be compact and packed well. For all of those, a barrier discharge is a suitable solution.

(3) Selection of AC discharge

As choosing a barrier discharge reactor, the capacitive coupling of the dielectric material requires an alternative electric field to drive a displacement current. DBD reactor cannot be operated with DC voltages. For convenience, the normal AC power source of 100V and 50Hz is used. And voltage was elevated by a transformer to around 15kV.

(4) Dielectric material

The dielectric material is Pyrex glass which is made of borosilicate glass. Its composition is 80.6% SiO₂, 12.6% B₂O₃, 4.2% Na₂O, 2.2% Al₂O₃, 0.04% Fe₂O₃, 0.1% CaO, 0.05% MgO, and 0.1% Cl. It has density of 2.23g/cm³, mean excitation energy of 134eV, and volume resistivity of 1.2x10⁹ohm-cm. Another important parameter of dielectric material is dielectric constant, or relative permittivity, which is defined by the ratio of the amount of electrical energy stored in a material by an applied voltage, relative to that stored in a vacuum. Pyrex glass has a dielectric constant of 4.1.

(5) Concept of plasma reactor with DPF

Concept of plasma reactor with DPF relies on two ideas: concept of a needle-to-cylinder barrier discharge to form N radicals, and concept of barrier discharge in DPF to investigate mutual affect between NO_x removal process and PM. The

needle-to-cylinder (or wire-to-cylinder) type reactor was chosen since it showed the best performance among common reactor configurations in range of not very high applied voltage (under 20kV).[83, 84]

2.2 Apparatus and procedure

2.2.1 Experimental setup

(1) Barrier discharge deNO_x reactor with DPF

From the concept of a plasma reactor with DPF as talked before, a needle-to-cylinder type reactor and a wire-to-cylinder reactor combined with DPF were proposed. PM effects of NO_x removal such as absorption of NO_x and catalytic reduction of NO were experimentally investigated here as a feasibility study of new after-treatment system of diesel engine. A lab-scale reactor and simulated diesel exhaust gas of N₂, NO, NO₂, and O₂ mixture with PM were used to examine the effects of PM to NO_x removal characteristics.

Figure 2.3 shows the structure of reactor in details. The barrier discharge reactor consists of two sections in series. A pre-reactor section on the left side is a needle-to-cylinder type reactor. It consists of a steel needle with diameter 1.8mm working as high voltage electrode and a stainless steel foil of 105mm length working as ground electrode. The pyrex glass cylindrical tube with inner diameter 36mm, outer diameter 50mm, and 120mm length is used as dielectric material. On the

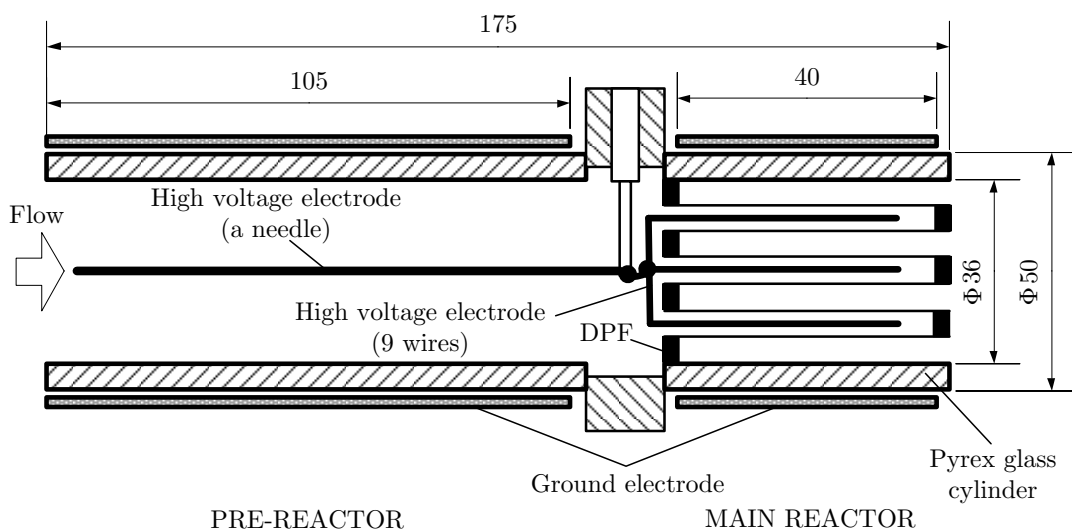


FIGURE 2.3 Dielectric barrier discharge reactor with DPF

right side is the main reactor section, that is wire-to-cylinder type reactor. It consisted of a DPF, a bunch of 9 wires (diameter 0.6mm) inside DPF working

as high voltage electrode and stainless steel foil with 40mm length working as a ground electrode. The cylinder of 60mm length with the same specifications as the pre-reactor's one covers DPF and high voltage electrode. DPF has two functions: as a PM loaded filter and as the dielectric barrier material. The needle and the 9-wire bunch are connected inside the cylinder to a high voltage power source. Also, two stainless steel foils are connected to a common ground point. The coupling points such as between cylinders, pipes in and out cylinders, electrodes into cylinders are sealed with rubber rings to prevent gas leakage. A picture of the real system is shown in Fig.2.4.

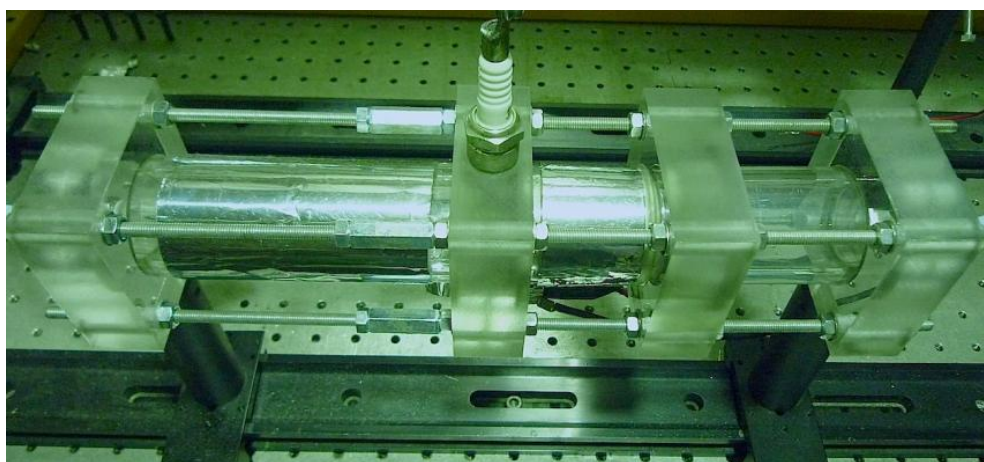


FIGURE 2.4 Picture of DBD reactor with DPF

(2) Diesel particulate filter (DPF)

The primary function of the DPF is to trap the soot particles. The DPF is often made of a porous material allowing the flowing of gases but trapping the soot particles contained in engine emissions. The exhaust gases must circulate through the porous medium because the input channels are closed at their end with a plug (see Fig.2.5). Consequently, the gases pass into the adjacent channels, or output channel, which are open at their end and closed at their entry.

The DPF used in our experiments was a cordierite wall-flow type, and downsized one for lab-scale experiment. Its dimensions are 35.5mm in outer diameter and 60mm in length. There are 117 channels (square holes) of 1.5mmx1.5mm. Total volume of the DPF was 31.6cm³. To load PM on the DPF, a diffusion flame PM formation system [85] was used. A photo of this DPF is in Fig.2.6.

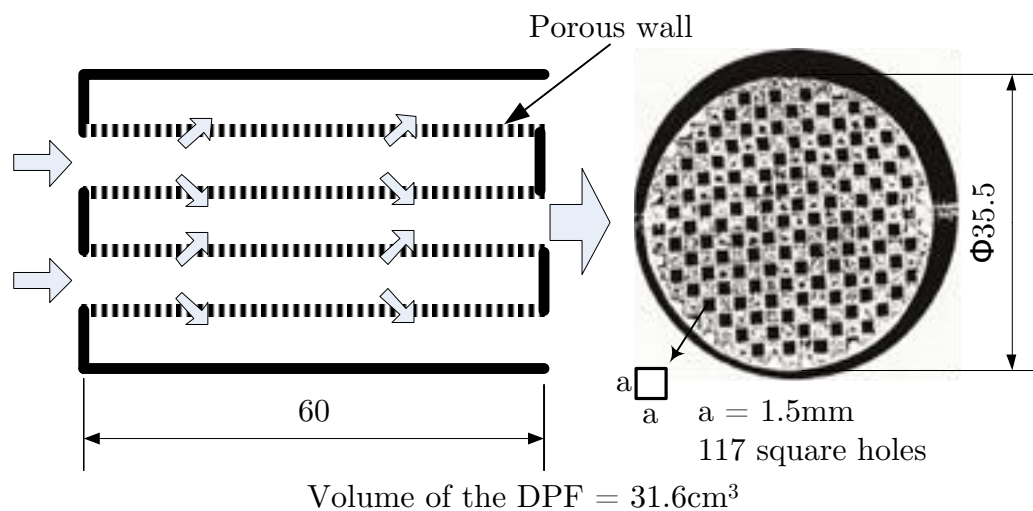


FIGURE 2.5 Structure of diesel particulate filter (DPF)

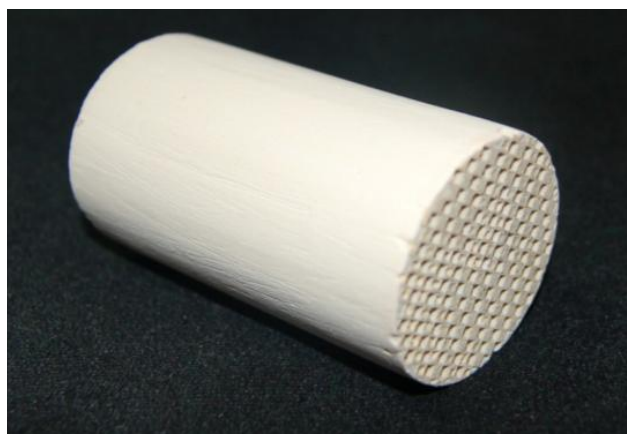


FIGURE 2.6 Photo of test DPF

(3) Experimental setup

A schematic of experimental setup is showed in Fig.2.7. A real look of the apparatus is on Fig.2.8. The test gas was a mixture of NO , NO_2 , O_2 and N_2 . NO_x concentration was kept constant at 112ppm while O_2 concentration was changed from zero to 20%. Simulated exhaust gas from cylinders passed through valves and pipeline system to reactors. The gas flow rates of 0.5, 1 and 2L/min were controlled by flowmeters (KOFLOC, RK 1250 series). After coming out from the reactor, the test gas was collected by a Tedlar bag and analyzed by an FTIR exhaust gas analyzer (Horiba Co., Ltd., MEXA-4000FT).

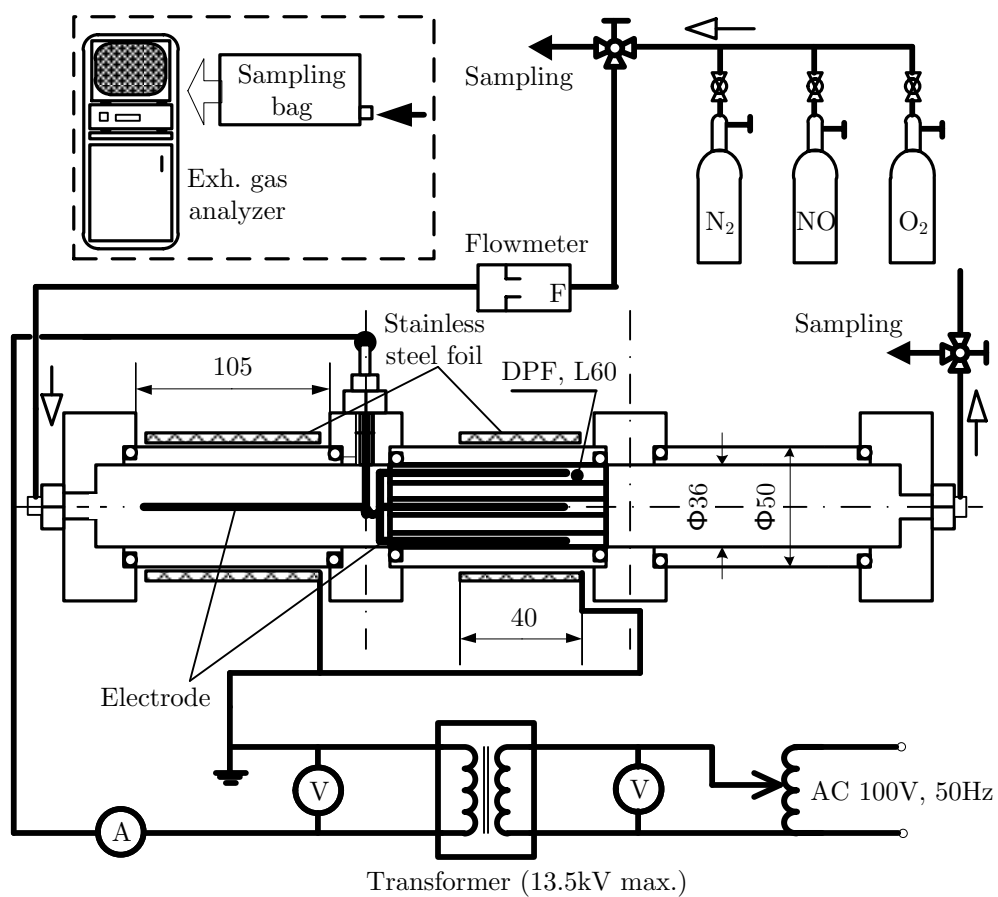


FIGURE 2.7 Schematic diagram of experimental apparatus

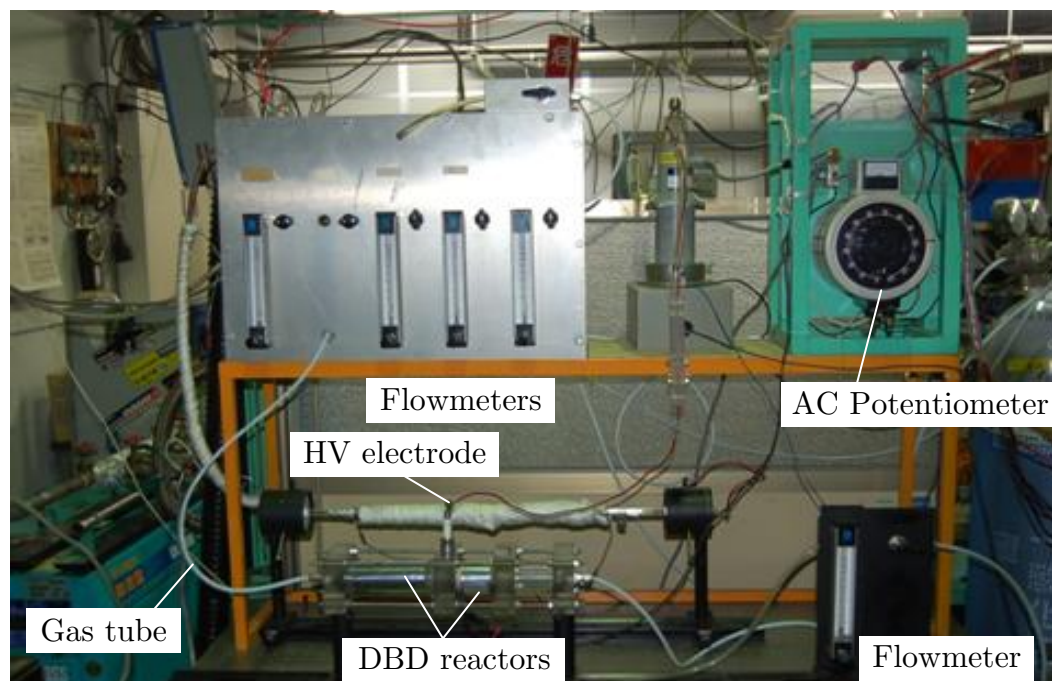


FIGURE 2.8 Picture of experimental apparatus

(4) High voltage AC power source

Figure 2.9 illustrated the high voltage circuit of the discharge reactor. The supply power source is a normal AC 100V, 50Hz which go through two transformers before reaching the reactor. The primary transformer, also a volt slider is used to adjust input applied voltage. The secondary transformer (neon transformer, ratio 1:150) converts the input voltage into high voltage in the range from 5kV to 15kV. A high voltage probe, Iwatsu HV-P30, with ratio 1000:1 is inserted into circuit to minimize load on the oscilloscope.

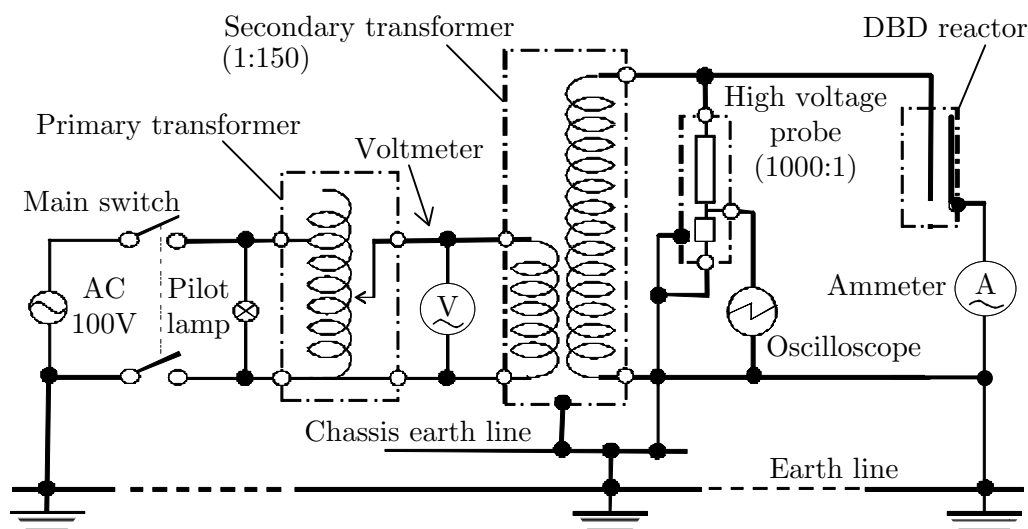


FIGURE 2.9 High voltage electric circuit of the discharge reactor

(5) Measurement of high voltage and electric current

The voltmeter is installed to measure induced voltage of the primary transformer (input value of the secondary transformer). The high voltage applied to DBD reactor is calculated by multiplying that value to 150 (conversion ratio of the secondary transformer). Due to highly difficulty in measurement of AC current in high voltage condition, the ammeter was installed on the earth side of the circuit (Fig.2.9).

(6) Gas and PM analysis

As mentioned above, gas concentrations (NO, NO₂, CO, CO₂, HC, etc.) were measured by the Fourier Transform Infrared (FTIR) analyzer, Horiba MEXA-4000FT. The principle of this FTIR analyzer is shown in Fig 2.10. Basically, infrared radiation from source (S) is passed through a sample in a cell. Some of the infrared

radiation is absorbed by the sample and some of it is transmitted to the optical detector (D). The resulting spectrum represents the molecular absorption and transmission, creating a molecular fingerprint of the sample. Since no two unique molecular structures produce the same infrared spectrum, so it can identify unknown materials and determine the amount of components in a sample mixture.

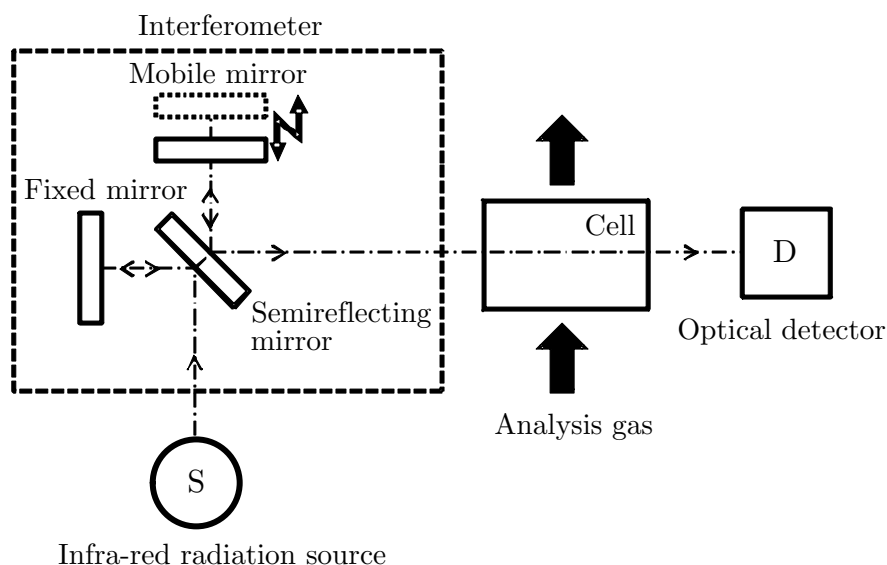


FIGURE 2.10 Principle of the FTIR analyzer

The interferometer is an optical measuring unit. It employs a semi-reflecting mirror (or beamsplitter) to take the incoming infrared beam and divide into two optical beams. One beam goes to the fixed flat mirror and the other goes to the movable one. Both two beams reflect off of their respective mirrors and are recombined at the beamsplitter. Because the path that one beam travels is a fixed length and the other is constantly changing as its mirror moves, the collected signal after the interferometer is interfering beam (or interferogram). The interferogram then is interpreted by a mathematical technique, Fourier transformation, to show the spectral information.

The detectable range of gas composition of the FTIR MEXA-4000FT is showed in Table 2.1. For PM composition, soot, SOF, and sulphate fractions were determined by the particle mass analyzer Horiba MEXA-1370PM. Its detection limit of soot is $0.2\mu\text{g}$, of SOF is $0.2\mu\text{g}$ and of sulphate is $8\mu\text{g}$. This analyzer uses quartz filter as PM trapping filter. It works under temperature condition from 5°C to 35°C . The analysis time is four minutes per sample.

TABLE 2.1 Working range of the FTIR analyzer MEXA-4000FT

Gas composition		Range	Gas composition		Range
Monoxide carbon	CO	0-200ppm	Formaldehyde	HCHO	0-500ppm
		0-1000ppm	Acetaldehyde	CH ₃ CHO	0-200ppm
		0-5000ppm	Methanol	CH ₃ OH	0-500ppm
		0-2%			0-2000ppm
		0-10%	Acetone	CH ₃ COCH ₃	0-100ppm
Dioxide carbon	CO ₂	0-1%	Methyl tertiary butyl ether	(CH ₃) ₃ COCH ₃	0-200ppm
		0-5%	Formic acid	HCOOH	0-100ppm
		0-20%	Methane	CH ₄	0-500ppm
Nitric oxide	NO	0-200ppm	Ethylene	C ₂ H ₄	0-500ppm
		0-1000ppm	Ethane	C ₂ H ₆	0-200ppm
		0-5000ppm	Propene	C ₃ H ₆	0-200ppm
Nitrogen dioxide	NO ₂	0-200ppm	1,3-butadiene	1,3-C ₄ H ₆	0-200ppm
Nitrous oxide	N ₂ O	0-200ppm	Isobutylene	iso-C ₄ H ₈	0-200ppm
Water	H ₂ O	0-24%	Benzene	C ₆ H ₆	0-500ppm
Ammonia	NH ₃	0-500ppm	Toluene	C ₇ H ₈	0-500ppm
Sulfur dioxide	SO ₂	0-200ppm		(NO+NO ₂)	

Figure 2.11 illustrates the operating principle of MEXA-1370PM. Firstly, the PM collected filter is placed in the analyzer's furnace and heated to 980°C in a N₂ gas flow. Then SOF and sulfate in trapped particles are vaporized by heat in N₂ atmosphere. Vaporized sulfate is deoxidized to SO₂ by heat and measured by SO₂ non-dispersive infra-red (NDIR) detector. Next, vaporized organic fraction is oxidized by constant flow of O₂ and measured as CO₂ by NDIR detector. Finally, output of CO₂ detector is integrated while N₂ is flowing to determine SOF mass and while O₂ is flowing to determine soot mass.

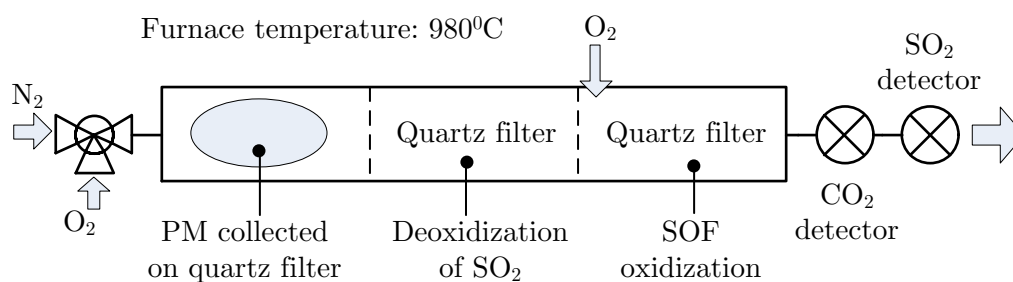


FIGURE 2.11 The operating principle of the PM composition analyzer Horiba MEXA-1370PM

To determine particle size distribution of PM, the Scanning Mobility Particle Sizer (TSI SMPS-3034) was used. The particle size range is from 10nm to 487nm. Total particle concentration is from 10² to 10⁷ particles per cubic centimeter (/cm³).

The schematic of operating principal of the TSI SMPS-3034 is expressed in Fig.2.12. The SMPS system measures the number size distribution of particles using an electrical mobility separation technique. This device has three main units: Bipolar Kr-85 charge neutralizer, DMA (differential mobility analyzer) for particle size separation, and CPC (condensation particle counter) for concentration measurement. Charged soot particles sample is passed through DMA, which con-

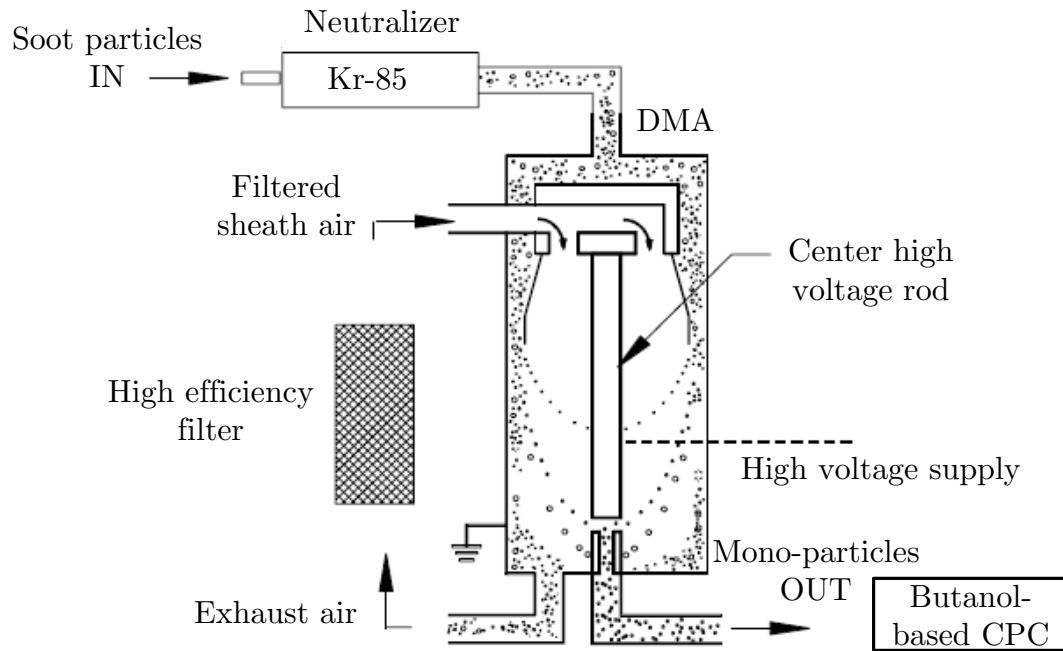


FIGURE 2.12 The operating principle of the PM particle size distribution analyzer TSI SMPS-3034

sists of two concentric metal cylinders. While the outer cylinder is grounded, a controlled negative voltage is applied to the inner cylinder. Two laminar flows, one containing a charged soot particles sample and the other containing particle-free sheath air, flow through an annular space between the two cylinders. At each specific voltage, only particles with a specific electrical mobility (inversely proportional to the particle diameter) are capable of passing through the DMA into a butanol-based CPC where the particles are counted. To obtain a full size distribution of a sample, the voltage applied to the inner cylinder of the DMA is exponentially scanned.

2.2.2 Test gas

Generally, average emission from diesel engine exhaust is at level of 50ppm-2500ppm of NO, 20ppm-400ppm of HC, 5ppm-600ppm of CO, and 8%-12.6% of O₂. To prevent from the complexity of using practical exhaust gas, the simulated gas mixture

of NO, NO₂, O₂ and N₂ was chosen. NO concentration was around 100ppm, O₂ fraction was varied from 5% to 20%. For almost cases in this study, the NO concentration of 100ppm, O₂ fraction of 10%, and N₂ left was used. For this gas composition, at gas flow rate of 1L/min, the partial flow rates of each gas were divided as follows: 0.1L/min for NO, 0.1L/min for O₂, and 0.8L/min for N₂. The typical experimental conditions in the literature including reactor type, concentrations of gas mixture, gas flow rate, and applied voltage range are shown in Table 2.2.

TABLE 2.2 Typical experimental conditions in the literature

Reference	Reactor type	NO ppm	NO _x ppm	O ₂ %	Flow L/min	Voltage kV
Penetrante et al. [86]	DBD	100			2	15–35
Obradovic et al. [12]	DBD	50–300		16	2.5	20
Arai et al. [34]	DC corona	100		0–20	1	0–15
Mok and Huh [26]	DBD-cat.		180	14.2	10	8–15
Mok [14]	Packed bed	275	300		5	12–17
Leipold et al. [37]	DBD	500		7–20	1–6	125–468W
Santillan et al. [48]	DBD	250–1000		10	1–13	9–20
Present work	DBD	100	112	0–20	0.5–2	0–15

Comparing to the practical diesel exhaust gas composition, O₂ fraction was in similar range. NO concentration of 100ppm was chosen because this concentration of NO is still meaningful at some certain operating conditions of the diesel engines. It has been used in some research works in the literatures [26, 34, 87] to study the NO_x removal characteristics. Additionally, the small lab-scaled size DBD reactor and the limited high voltage source in this study only has the capability of fulfilling experiments at this level of concentration. That is a reason why gas flow rates of 0, 1L/min, and 2L/min were used.

2.2.3 PM

(1) PM generator

To load PM on the DPF, a diffusion flame PM formation system [85] was used. The schematic layout of this system is illustrated in Fig.2.13. Liquid fuel from the tank was heated to 130°C by an electric heater. The combustion air was blown through a layer of mesh plate with alumina balls as a filter into combustion chamber. In

the combustion chamber of 60mmx60mmx240mm, as ignited, a diffusion flame of diesel fuel was formed and it generated PM. Then PM exhausted from the top of the chamber was loaded on the DPF by using the pump installed behind it.

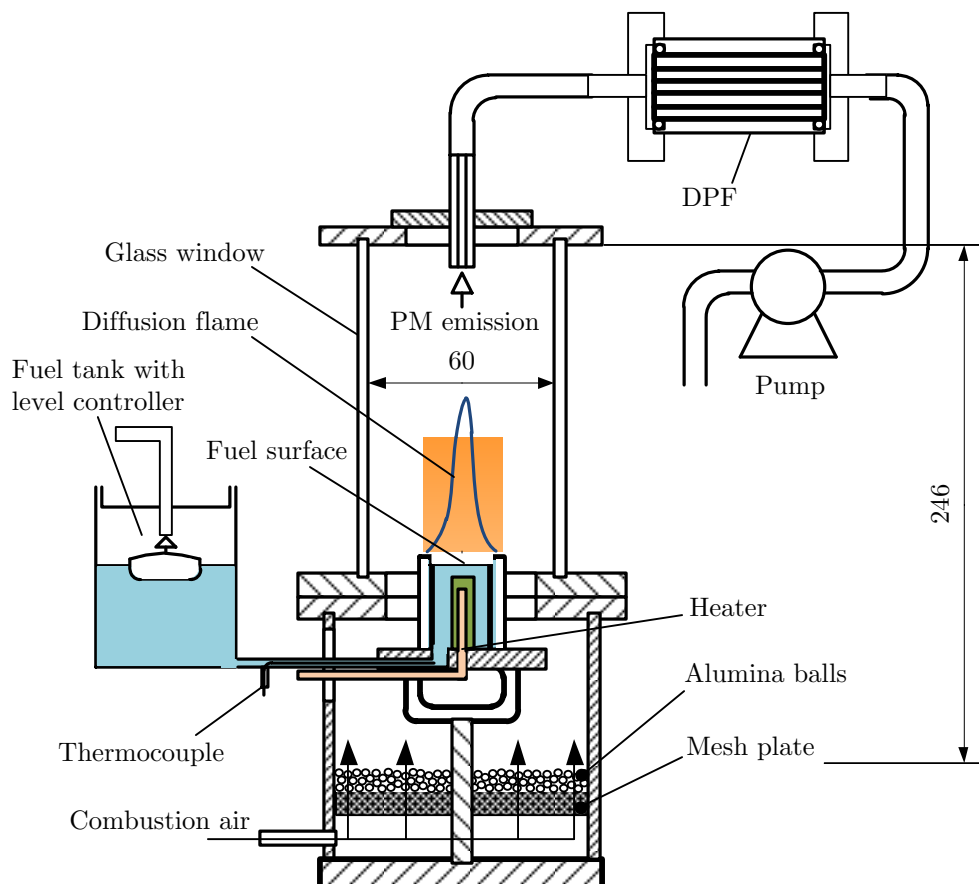
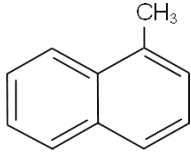
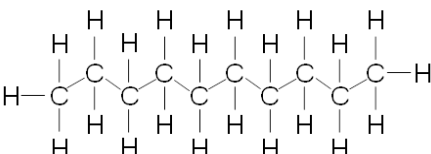



FIGURE 2.13 PM formation system with diffusion flame

(2) Fuel

Due to the chemical complexity of fossil diesel fuel, some representative compounds and mixtures are often used for research purpose. In this study, the mixture of α -methylnaphthalene and n-decane used as a surrogate diesel fuel to generate PM. When fuel with sulfur is required, thiophene will be added into the surrogate fuel. The formula and structure of α -methylnaphthalene, n-decane, and thiophene are shown in Table 2.3. The volumetric ratio to get surrogate fuel without sulfur and the one with 350ppm sulfur are also available. The mixture of 30% α -methylnaphthalene and 70% n-decane (cetane number of 58, [88]) was used as a standard fuel.

TABLE 2.3 Surrogate diesel fuel composition

	α -methyl-naphthalene	n-decane	Thiophene
Formula	$C_{10}H_7CH_3$	$CH_3(CH_2)_8CH_3$	C_4H_4S
Structure			
Volumetric ratio	30	70	
	Surrogate fuel without sulfur		
Volumetric ratio	30	70	0.7ml/1L
	Surrogate fuel with 350ppm sulfur		

(3) Characterization of test PM

The composition and particle size distribution of PM using in this study were showed in Figs.2.14 and 2.15. Figure 2.14 expresses the compositions of four different PM samples: PM01, PM02, PM_{SUL} and PM_{WET}. PM01 was sampled

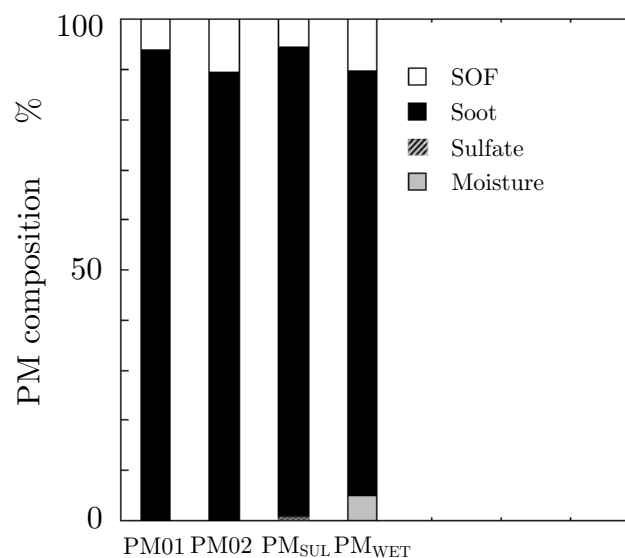


FIGURE 2.14 Composition of different PM samples

from above PM generator with the flame height $L_f=50$ mm whereas PM02 was the one with $L_f=30$ mm. PM_{WET} was similar to PM02 ($L_f=30$ mm) but the loaded DPF was not dried up with N_2 . And PM_{SUL} was taken with the fuel blended with 350ppm thiophene at the flame height of 50mm. The analysis results showed the SOF in cases of PM01 and PM02 were 6% and 11%, respectively. Sulfate fraction

in case of PM_{SUL} was 0.24%. For PM_{WET} , SOF was 10% and water (moisture) was 5%. In short, the flame height showed its effect on PM composition rather than fuel composition. For the same flame height ($L_f=30\text{mm}$ as PM_{02} , PM_{WET} ; $L_f=50\text{mm}$ as PM_{01} , PM_{SUL}), SOF was almost the same while soot fraction changed slightly according to fuel composition. In this study, to eliminate the effect of hydrocarbon and water on NO_x removal, most of taken PM samples with $L_f=30\text{mm}$ were dried up and had SOF about 10%.

Concerning particle size distribution, Fig.2.15 illustrated the experimental results using SMPS-3034 in cases of (1) fuel consumption rate $M_f=1.1\text{mg/s}$, flame height $L_f=30\text{mm}$ with or without sulfur addition and (2) $M_f=2.17\text{mg/s}$, $L_f=50\text{mm}$. At the flame height $L_f=30\text{mm}$, the number concentration got peak at particle diameter about 100nm. For $L_f=50\text{mm}$, the number got peak at particle diameter about 120nm. PM samples used in this study were taken from non sulfur fuel with $L_f=30\text{mm}$.

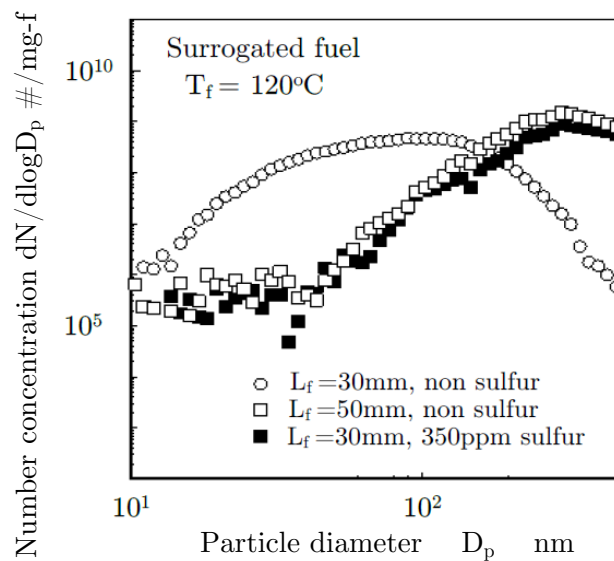


FIGURE 2.15 PM particle size distribution

(4) PM loading on DPF

Figure 2.16 shows the procedure of pre-treatment and PM loading on the DPF. It shows the steps to get the required PM mass for DPF. In this study, the PM mass of 100–200mg was chosen. The reason is that a PM loading of 1 to 5g/L was commonly reported in the literature as experimental data of the DPF. [48, 56, 82] The DPF used in this experiment was a kind of down-sized model with a volume of 0.0316L (Fig.2.5). Thus, 100mg PM loading means 3.2g/L. This was the general condition of PM loading.

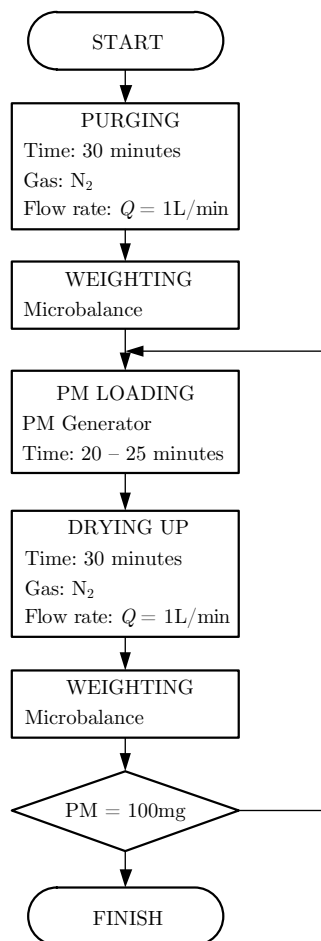


FIGURE 2.16 PM sampling chart

For loading PM, at first a new clean DPF is purged by N₂ in 30 minutes with a flow rate of 1L/min in order to make sure that there are no residues inside the DPF. Then it is put on the electric micro-balance to determine tare weight. After that, DPF was loaded with wet PM by the PM generator in 20–25 minutes. So in actual, PM, hydrocarbons and also water was loaded (see Fig.2.14). In order to determine PM mass and exclude the effect of hydrocarbon and water to NO_x removal characteristics, in the next step, the DPF with PM was dried up with N₂. Finally, the loaded DPF will be put on the micro-balance to check if the PM mass is 100mg or not. If the PM mass is still not enough, then the PM should be reloaded.

The state of a electrode inside a channel of DPF was sketched in Fig.2.17. The electrode is covered with a PM layer. An average thickness of PM layer was from 2–2.6 μ m. That was calculated with the mean PM density of 1mg/cm³ [89], and loaded PM mass of 100mg. It was assumed that PM was covered with the same thickness at every surface areas of the DPF.

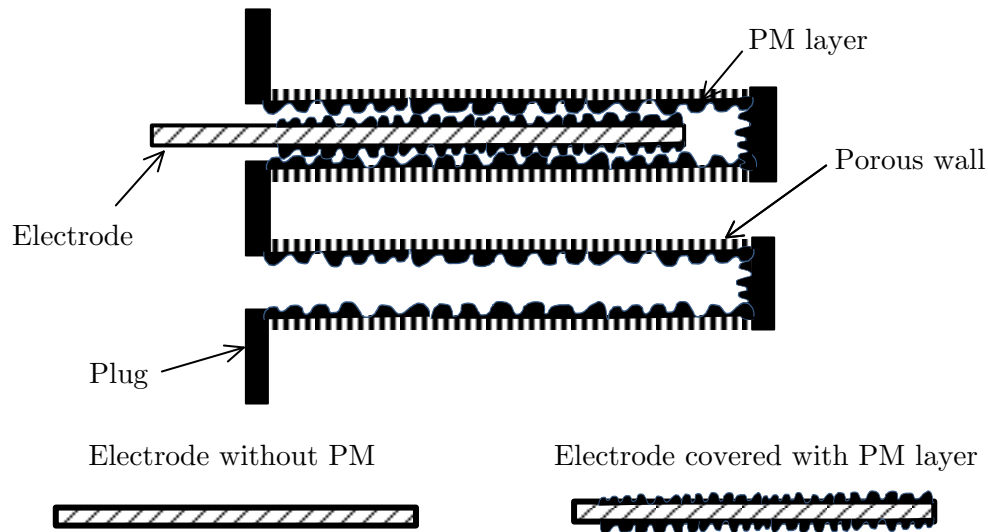


FIGURE 2.17 Model of electrode with PM inside DPF

2.2.4 Experimental parameter and data analysis

(1) Definition of NO_x

In this study, NO_x concentration in ppm was defined by sum of NO concentration in ppm and NO_2 concentration in ppm.

$$\text{NO}_x = \text{NO} + \text{NO}_2 \quad (2.1)$$

In some experiments, N_2O and N_2O_5 might be formed but they were not added into NO_x because they are out of emission legislations.

(2) Discharge energy density

Discharge energy density is defined as discharge power per unit of test gas volume, in J/L. It means the total discharge energy received in the reactor.

$$E = \frac{60 \cdot P}{Q} \quad (2.2)$$

where

P is the discharge power, in W (or J/s)

Q is the gas flow rate running through system, in litre per minute (L/min).

The calculation of discharge power P will be described in section 2.3.4.

(3) De NO_x efficiency

De NO_x efficiency in percent (%) was defined by the ratio between NO_x reduction from initial concentration in ppm and the input concentration in ppm.

2.2.5 Experimental condition and procedure

(1) Setup of experimental condition and gas sampling

All the experiments were carried out under room temperature conditions. The exhaust simulated gas comes from gas cylinders. There are three types of original gas to be used: N_2 , NO, and O_2 . Gases from cylinders were regulated by valves and flowmeters to ensure the dedicated composition. The sampling gas volume of 10L needs to be taken into the Tedlar bag so with the gas flow rates of 0.5, 1, 2L/min then sampling time should be 20, 10, and 5 minutes, respectively.

(2) Procedure

To investigate the NO_x removal characteristics following applied voltage or energy density, sampling gases were taken at every 1kV in the range of applied voltage (0–15kV). In addition, the by-pass sampling gas (no applied voltage and gas does not come into reactor) was also taken for evaluation.

In steady reaction and transient state tests, sampling gases were taken at every 1 hour running during experiment, i.e 0–6 hours maximum. The by-pass sampling gas was also taken as previous case.

In case of DPF loaded with PM, gas composition and sampling procedure was the same. PM sampling was already described in previous section 2.2.3.

In the next chapters, the experimental results of NO_2 removal in case of $N_2 + NO$ mixture comparing to those in case of $N_2 + NO + O_2$ mixture with O_2 fraction changed from 0–20% are showed. In details, five different O_2 fractions, namely 1%, 5%, 10%, 15% and 20% were reported.

Although it had been reported partly in previous research works [34, 38–40, 90, 91], the role of O_2 as an oxidation agent was extensively investigated in the present study. Additionally, from those results, the proposed reaction mechanism inside the reactor was confirmed.

2.3 Basic performance of the reactor

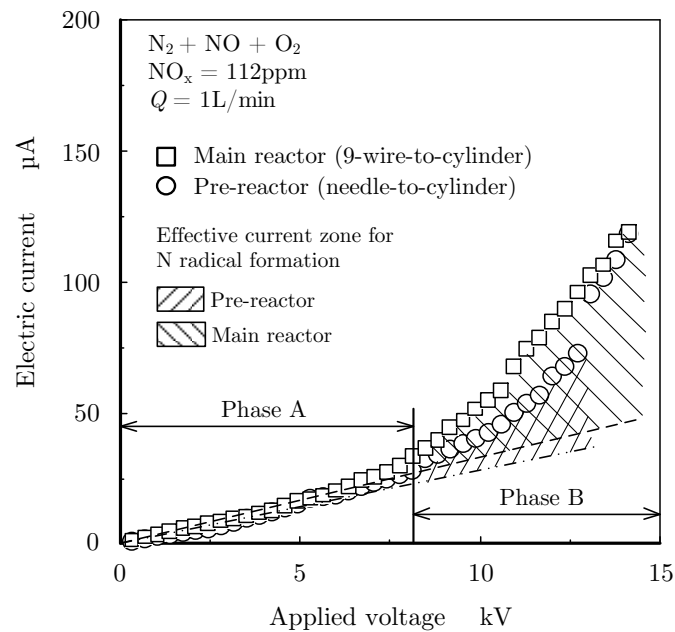
2.3.1 Spark discharge limit and maximum safety voltage

As the applied voltage increased from zero, the electric current of the reactors increased. The current started to increase rapidly from applied voltage of 8kV (equals to 54V at volt slider). When applied voltage beyond 14.3kV (equals to 95V at volt slider), spark discharge sometimes took place between outside of main reactor's cylinder and high voltage electrode. So the applied voltage of 14.3kV was

the maximum safety voltage of the reactor. For safety reason when experiments were taken place in a long time (up to six hours), the standard value of applied voltage was 12.75kV.

2.3.2 Electric currents of pre-reactor and main reactor

Electric currents of pre-reactor (needle-to-cylinder) and main reactor (9-wire-to-cylinder) are expressed in Fig.2.18. They were measured as each reactor stood alone, test conditions were the same in both cases. The maximum value of $118\mu\text{A}$ was reached at applied voltage of 14.3kV.



(a) Electric currents of pre-reactor and main reactor

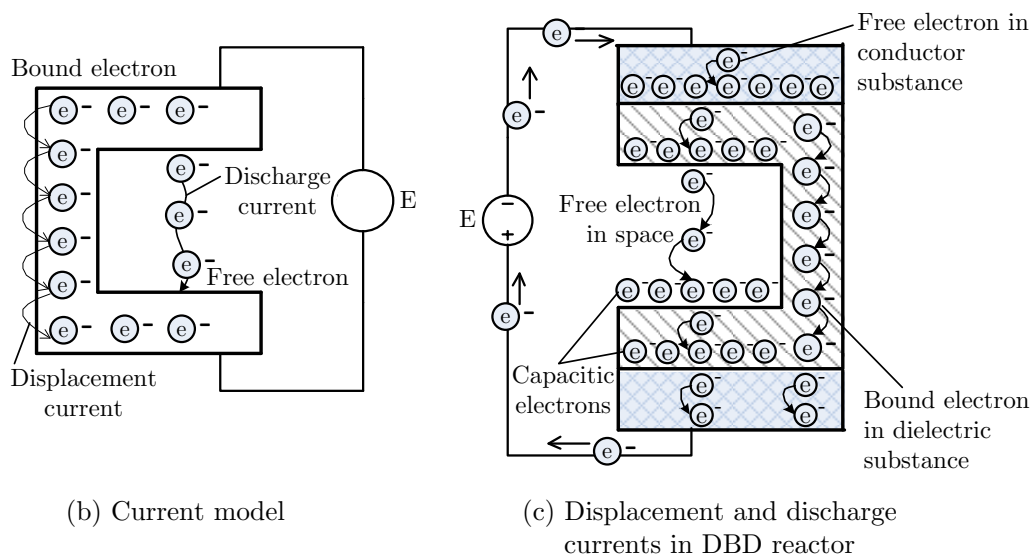


FIGURE 2.18 Discharge and displacement currents

From the experimental result in Fig.2.18(a), the current curves demonstrate two phases: phase A of displacement current and phase B of discharge current. These currents were illustrated by a current model in Fig.2.18(b). Discharge current was formed from the movement of free electrons in discharge volume whereas displacement current formed from bound electrons in dielectric substance. In other words, displacement current was created by electron displacement from atom to atom in a solid substance. Thus it is proportional to the applied voltage (dotted lines in Fig.2.18(a)). The description of displacement current in details can be seen as in Fig.2.18(c). At the initial stages of applied voltage in phase A, when the gas breakdown point was not reached, the circuit was closed by displacement current rather than charged particles transport.[6] When applied voltage was higher than the gas breakdown point (about 8kV in this case) in phase B, the current was a total of displacement current and discharge current. As a result, the current was increased considerably when applied voltage increased. Because it was very difficult to separate exactly the discharge current and displacement current (non-effective current for deNO_x) then overall current was used for energy index in this thesis.

2.3.3 Current-voltage characteristics

The current-voltage characteristics of the experimental system with gas mixture of NO_x, O₂, and N₂ at the flow rate of 1L/min is shown in Fig.2.19. NO_x concentration was kept constant at 112ppm; O₂ fractions of 0, 5%, 10%, and 15% whereas PM loaded in DPF were 0mg, 100mg, and 200mg.

Current-voltage characteristics shown here could be divided into two groups of curve: one with PM=0mg and the other with PM=100mg or 200mg. For each set of curves, as O₂ fraction increased, the electric current decreased. Due to the higher equilibrium constant of the decomposition reaction of molecular nitrogen comparing to that of molecular oxygen, so N₂ was more decomposed than O₂. As a result, with O₂=0%, the electric current was high. On the other hand, the electric current through the reactor with PM loaded on DPF was significantly higher than that without PM. It was considered that some ionized radicals formed from PM contributed the increase of electric current. This can be explained that the electrodes were covered with PM as showed in Fig.2.17, and it made the discharge surface area increased. Because the maximum safety voltage in case of NO + N₂ + O₂ is little lower than the one of NO + N₂ gas mixture (14.3kV) so the

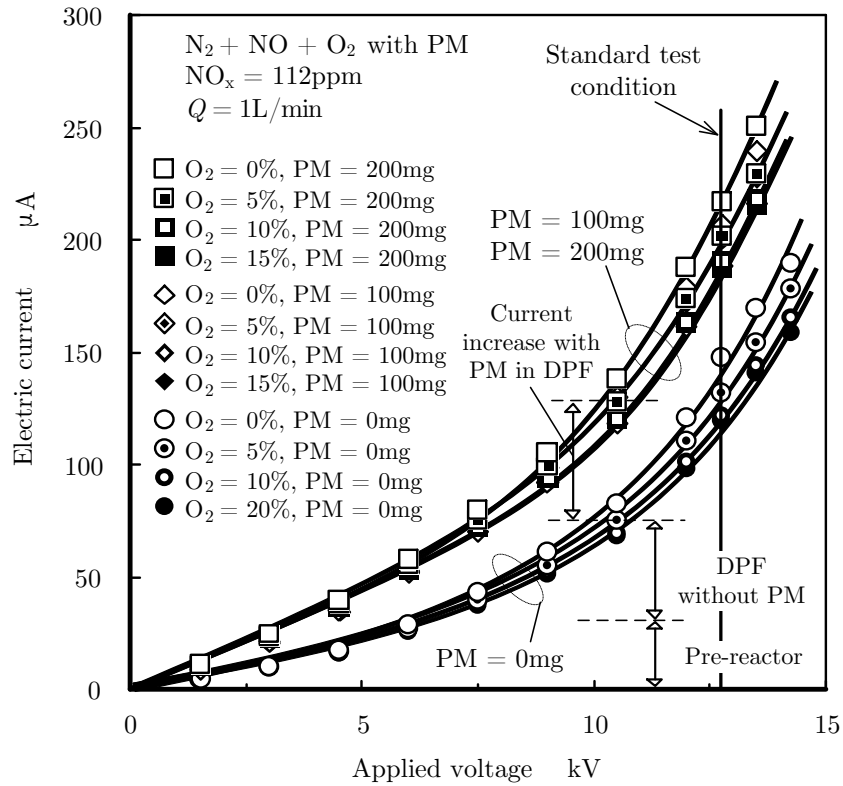


FIGURE 2.19 Current-voltage characteristics of the reactor

applied voltage of 12.75kV in Chapter 4 which was used as standard test condition for PM effect investigation. It is in the effective current zone (phase B in Fig.2.18).

2.3.4 Power factor and discharge power

To calculate the supplied power or energy density, the voltage and current (see Fig.2.9) were measured by the Sanwa digital multimeters CD772 which give the true root-mean-square (rms) values. Then the power equals to

$$P = V_{rms} \cdot I_{rms} \cdot \cos\varphi \quad (2.3)$$

whereas

P : Supplied power, in W or J/s

V_{rms} : The root-mean-square amplitude of voltage, in V

I_{rms} : The root-mean-square amplitude of current, in A

$\cos\varphi$: The power factor, with φ is the phase angle between the current and voltage.

In this case, $\varphi=18^\circ$, checked by the oscilloscope Kenwood OS-8010 as showed in Fig.2.20. Since $\cos(18^\circ)=0.951$ is almost unity, $\cos(18^\circ)=0.951 \cong 1$, then for experimental data analysis:

$$P = V_{rms} \cdot I_{rms} \cdot \cos(18^\circ) \cong V_{rms} \cdot I_{rms} \quad (2.4)$$

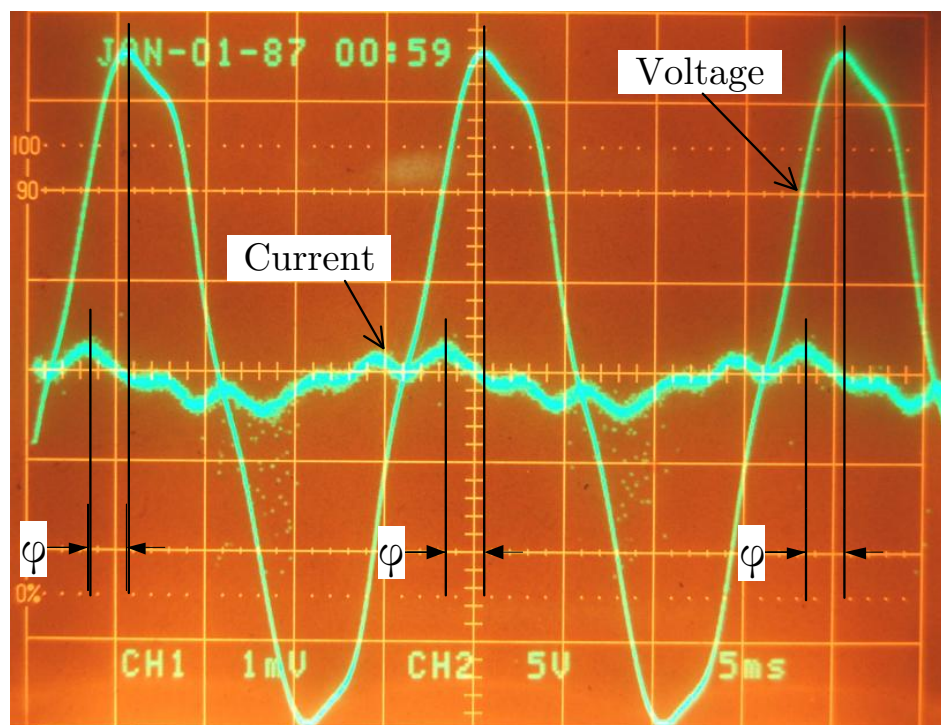


FIGURE 2.20 Phase angle of the reactor

2.4 Summary

In the literatures, there were various types of dielectric barrier discharge reactor configuration introduced to study NO_x removal characteristics. Some typical reactors were planar and cylindrical dielectric barrier discharge (DBD), surface discharge, pulsed corona discharge, and ferroelectric pellet packed-bed reactor configurations. The surface discharge configuration is quite simple but it is not suitable application for a volume discharge in this study. In contrary, pulsed corona discharge can create the volume discharge but its complexity make it difficult in practical use. The ferroelectric pellet packed-bed configuration can apply for gas treatment. However, this type of reactor does not meet purpose of this study regarding gas mixture with PM.

In this study, a cylindrical DBD reactor was chosen since its compact and simplicity for lab-scale experiments. It can combine well with a DPF to investigate NO_x treatment with diesel exhaust gas as objective of this study. In details, a needle-to-cylinder (or wire-to-cylinder) configuration was built because it showed the best performance among common reactor configurations with the not so high range of applied voltage. The cordierite wall-flow type DPF of lab-scaled size (outer diameter of 35.5mm and length of 60mm) was used.

Chapter 3

Effects of oxygen on NO_x removal characteristics

3.1 Fundamental NO removal reaction

Oxygen is the oxidization agent of molecule, and NO removal mechanism might be far different for the cases of with and without oxygen in gas mixture. Thus deNO_x process in the gas mixture without oxygen was first investigated for N radical effect where N radical was formed by dielectric barrier discharge in the N₂ + NO mixture. To investigate NO_x removal in NO + N₂ mixture, two types of test were carried out: steady reaction test (running under maximum safety voltage for 4 hours) and characteristics test (NO_x removal as a function of applied voltage or energy density).

Figure 3.1 shows the experimental results in case of steady reaction test, with clean DPF (PM=0mg), gas mixture of NO + N₂, and flow rate $Q=1\text{L}/\text{min}$. The vertical axis is gas concentration in ppm and the horizontal axis expresses running time in hours. Concentrations at point [0] indicate initial concentrations of source mixture. The point zero (0) is the real measured value at the reactor outlet before reactor is switched on (electric voltage equals to zero).

It can be seen that at point (0), there was a little amount of NO₂ detected. The reason is that there was a slight oxygen leaked into the pipeline and reactor due to the insufficient sealing. During sampling period, it mixed with gas mixture of N₂ + NO and there was enough time for some NO molecules to be oxidized into NO₂ according to below reaction scheme, so called the natural oxidation process.



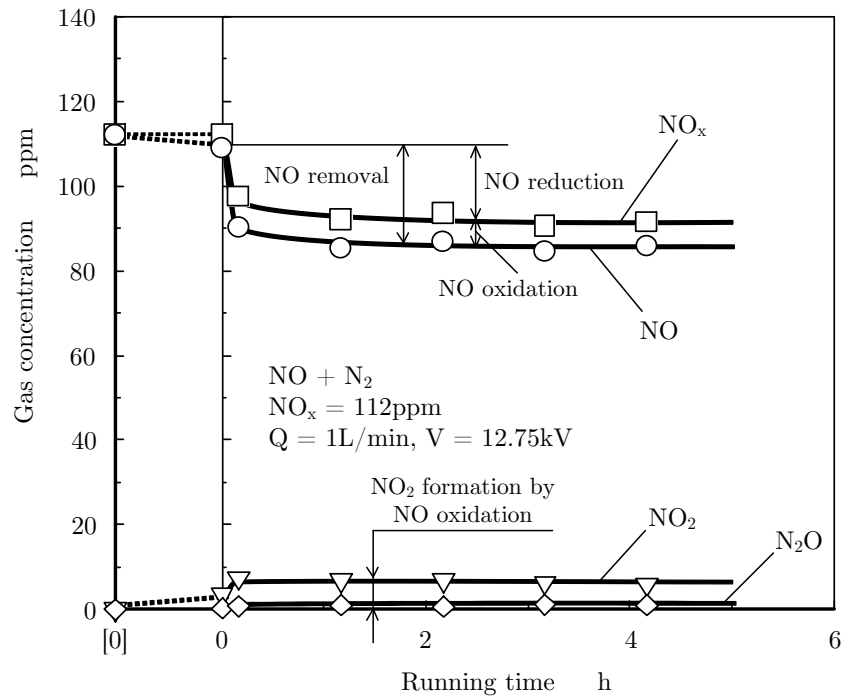
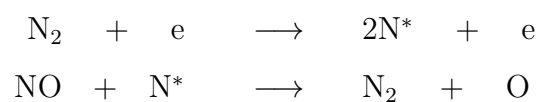


FIGURE 3.1 NO_x removal in N₂ + NO mixture ($Q=1\text{L}/\text{min}$)

According to Fig.3.1, NO₂ and N₂O concentrations were detected during experiment. Over four running hours, the N₂O concentration was almost zero, so it could be negligible. NO₂ formation was also NO oxidation. NO_x concentration (sum of NO and NO₂) decreased at first and then almost unchanged. It means that the reaction rate of NO_x removal, which was also the NO reduction rate, was independent of running time after applying electricity. However, there was some ppm of NO₂ detected although gas mixture did not contain O₂. In this chapter, experimental result of steady state (running time up to 4 hours) was only discussed, and the transient phenomenon will be discussed in chapter 4.

The reaction mechanism can be described as follows. When the NO reduction and NO₂ formation shown in the figure were taken into consideration, total NO change from initial value (NO removal) of 100ppm consists of NO reduction due to decomposition reaction (75%) and NO oxidation reaction (25%). It means that NO₂ formation is negative reaction for NO_x removal. The decomposition reaction of NO to return N₂, or NO reduction, was given by:



The O radical as a product from this reaction then oxidizes NO to form NO₂ (NO oxidation):



Besides that, there might have a small amount of NO was converted to NO₂ (NO oxidation) by following reaction scheme.



As for the formation of N₂O, it was considered that N₂O formation reaction was incomplete NO reduction of N radical with following reaction.



Then the existence of N₂O was one of the evidences of NO reduction process by N radical.

3.2 NO_x removal in NO + N₂ mixture

3.2.1 NO_x removal characteristics and less effective area

For NO_x removal characteristics test, results in case of gas mixture of 100ppm NO and N₂ left at flow rates of 2L/min, 1L/min and 0.5L/min are shown in Figs.3.2, 3.3, and 3.4. In order to clarify the main parameter of NO_x reduction, the gas flow rate was decreased to 1L/min to 0.5L/min, which are showed in Figs.3.3 and 3.4, respectively.

The experimental results at each value of gas flow rate were illustrated in both applied voltage (left figure) and energy density (right figure). The vertical axis is concentration of gas in ppm. The horizontal axis expresses the applied voltage in kV or the energy density in J/L. Energy density here is defined by supplied power per unit of gas flow rate. N₂O concentration is not concerned in this case because it was observed that N₂O was almost zero during experiments. In these figures, since the range of applied voltage was the same (0–13.5kV) for all values of gas flow rates (Figs.3.2, 3.3, and 3.4), it was expressed in the same scale on horizontal axis.

When the applied voltage is less than 12kV (Fig.3.2), the electric current was almost displacement current (phase A in Fig.2.18). This can be also observed in Fig.2.19. Displacement current did not produce any radical in the space because it did not mean the discharge. In this case, a weak discharge current with low voltage was generated with low energy radicals. Additionally, the intensity of electrical field depends on the space inside reactor and applied voltage. So the data expressed

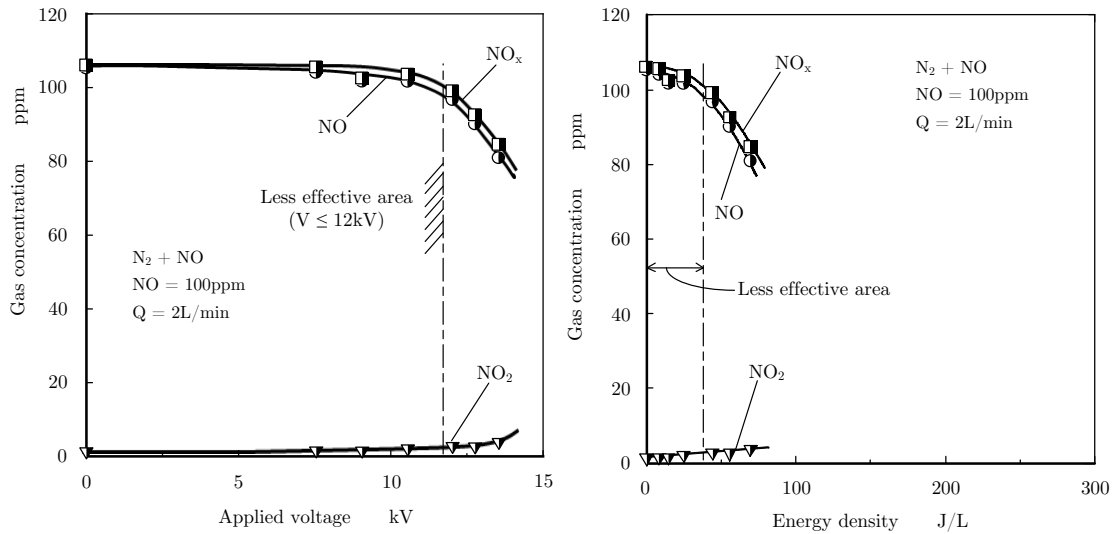
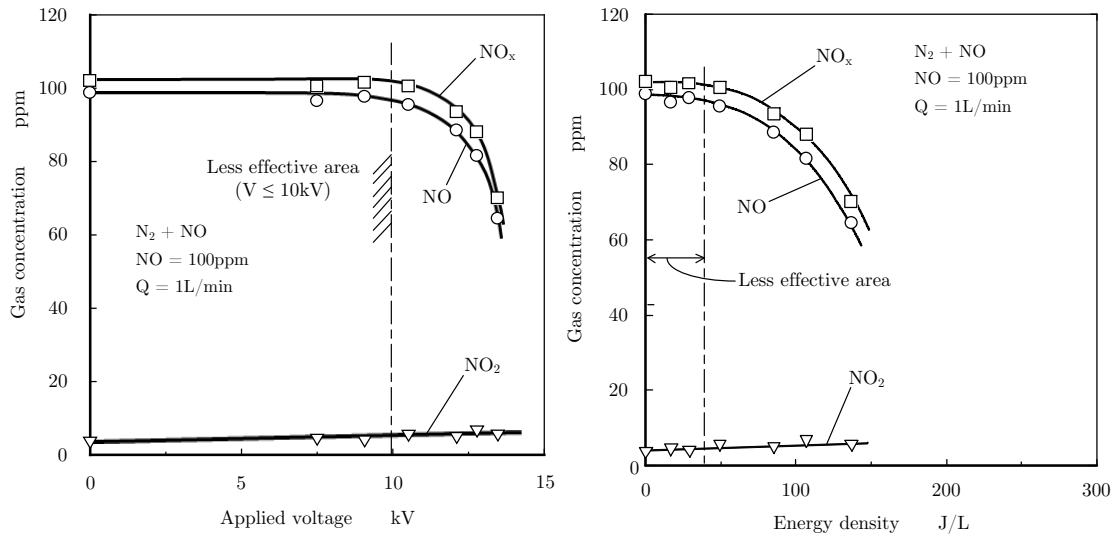


FIGURE 3.2 NO_x removal in $NO+N_2$ mixture (flow rate $Q=2L/min$)

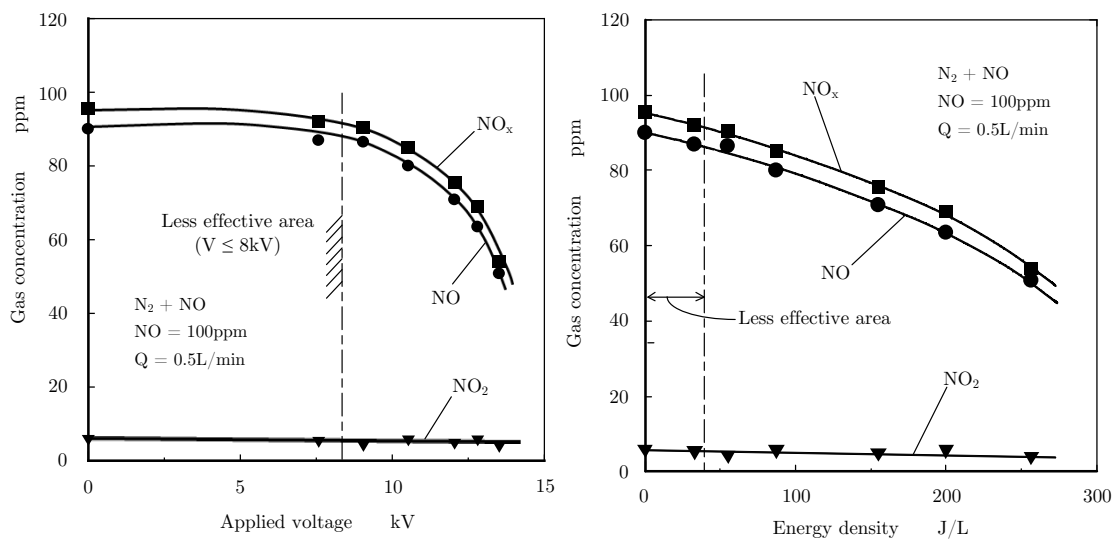
in applied voltage implies the NO_x removal characteristics of discharge space and intensity of electrical field. The data expressed in energy density, on the other hand, shows the NO_x removal characteristics for gas flowing through the reactor. It concerns both electrical field and the discharge energy to an unit volume of flowing gas.

Figure 3.3 shows the NO_x removal effect by barrier discharge reactor with mixture of 100ppm NO and N_2 left at flow rate of 1L/min. In this case, as NO reduction was 35ppm while NO_2 concentration increased up to 5ppm at $V=13.5kV$, the total NO_x concentration was decreased by 30ppm at this applied voltage. When energy density increased, the NO concentration decreased. At the flow rate of 2L/min (Fig.3.2), NO concentration was decreased from 106ppm to 80ppm and NO_2 concentration was decreased a few ppm. Then, the total NO_x removal at 12.75kV ($E=70J/L$) could be approximately 20ppm.

Then the above results are comparable to the previous work carried out by Zhu et al., 2005 [74], using a cylinder-to-cylinder DBD reactor to study the NO conversion with gas mixture of $NO + N_2$ at atmospheric temperature and pressure. At gas flow rate of 1L/min and the applied voltage of 12kV (similar to the maximum safety voltage in our experiments), the NO_x removal was 18% to initial value. In our experiments, the NO_x reduction was 30% from the initial value of 100ppm as showed in Fig.3.3. Comparing the results shown in Fig.3.2 and Fig.3.3, it was clear that under maximum safety voltage, 35ppm NO reduction and 5ppm NO_2 formation in Fig.3.3 is superior than 20ppm reduction in Fig.3.2.

FIGURE 3.3 NO_x removal in $NO + N_2$ mixture (flow rate $Q=1L/min$)

The experimental result in case the gas flow rate of $Q=0.5L/min$ is showed in Fig.3.4. NO_2 concentration was around 5ppm during experiment. When increasing the energy density to 256J/L, NO concentration was 40ppm lower than initial value at 0J/L. As a result, total NO_x concentration was also reduced 40ppm (equal to 44% from initial concentration). In terms of applied voltage, the less effective area was just limited at the applied voltage of 8kV.

FIGURE 3.4 NO_x removal in $NO+N_2$ mixture (flow rate $Q=0.5L/min$)

3.2.2 De NO_x efficiency and minimum energy density

The results shown in Figs.3.2, 3.3, and 3.4 pointed out that the less effective area in case of 2L/min was at the applied voltage less than 12kV ($E=40J/L$), in case

of 1L/min was at the applied voltage less than 10kV ($E=40\text{J/L}$), and in case of 0.5L/min was at the applied voltage less than 8kV ($E=40\text{J/L}$). This implies that the less effective area was controlled by energy density which was within the phase A in Fig.2.18 and Fig.2.19 (Chapter 2).

To summarize the experimental results of NO_x removal characteristics test in case of gas mixture of NO and N₂, Fig.3.5 expresses deNO_x efficiency depending on energy density at different gas flow rates. Because NO₂ concentration was insignificant, NO removal efficiency and NO_x removal efficiency were almost the same. The maximum NO_x removal efficiencies under the maximum applied voltage were 44%, 35%, and 23% at gas flow rate of 0.5L/min, 1L/min, and 2L/min, respectively. These results can be explained that as gas flow rate increasing, the reaction duration inside the reactor was shortened, so number of NO_x molecules which can take part in reactions with activated radicals, was accordingly decreased.

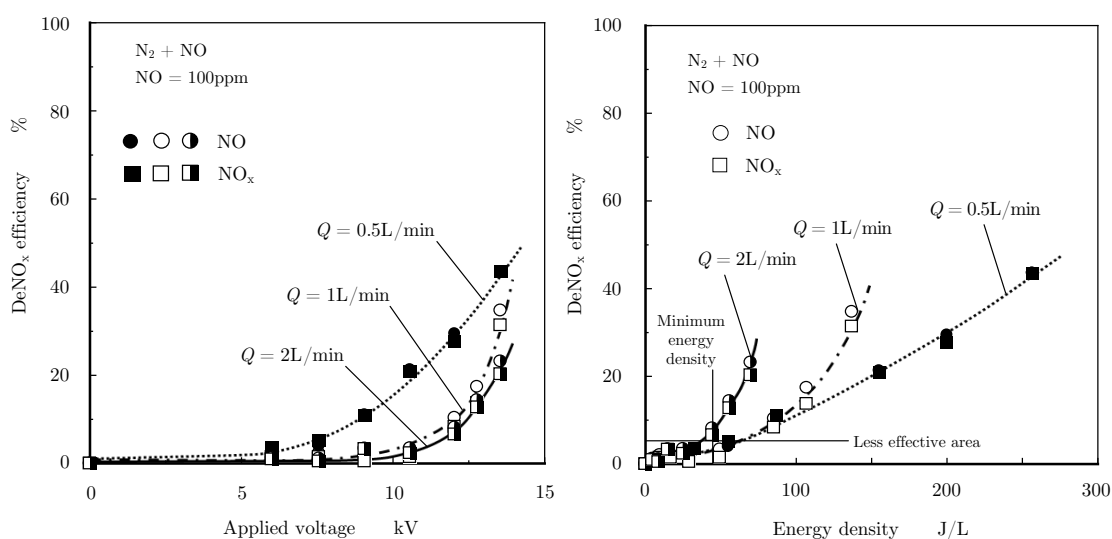


FIGURE 3.5 DeNO_x efficiency in N₂ + NO mixture

From the left figure of Fig.3.5, the deNO_x efficiency in case of gas flow rate of 0.5L/min increase started at lower voltage comparing to the cases of 1L/min and 2L/min. In addition, there was also a significant difference in deNO_x efficiency between them at the same applied voltage. At a low gas flow rate (0.5L/min), free activated radicals inside reactor might reach opposite electrode and take part in chemical reactions. Those conditions were not available at higher gas flow rates (1L/min and 2L/min).

As for the relation between deNO_x efficiency and energy density, deNO_x efficiency in the case of 2L/min showed different behavior with other cases. It means that both of energy density and applied voltage were the dominate parameters of NO_x removal reactions. Additionally, the relation between the less effective area in voltage and the minimum energy density in J/L can also be seen from Fig.3.5. The less effective area (deNO_x efficiency less than around 5%) changed at different gas flow rates but it seems that the minimum energy density was constant at about 40J/L. The minimum energy density was also the limit of displacement current, as shown in Fig.2.18. So another substantial parameter of NO_x removal is the minimum energy density.

3.3 NO_x removal in NO + N₂ + O₂ mixture

3.3.1 NO and NO₂ removal characteristics

NO_x removal characteristics with gas mixture of NO=100ppm, O₂=10%, and N₂ left at gas flow rate of 2L/min was investigated. The experimental result is illustrated in Fig.3.6. The left figures are expressed in applied voltage (kV), the right ones shows the data following energy density (J/L).

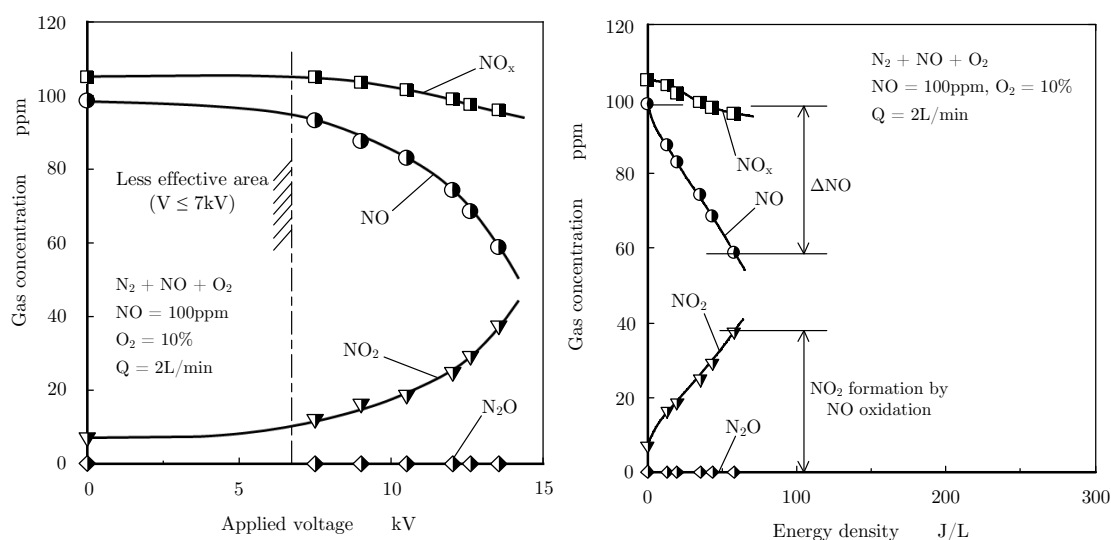


FIGURE 3.6 NO_x removal in N₂ + NO + O₂ mixture (O₂=10% and Q=2L/min)

At gas flow rate of 2L/min, as can be seen in left figure of Fig.3.6, the chemical reactions under discharge field started at lower applied voltage (about 7kV) than in case of gas mixture without oxygen (about 12kV, see Fig.3.2). Since O₂ decomposition was taken more easily than N₂ decomposition, O radical reaction might

be started at lower voltage discharge than N radical reaction. It was supposed that the NO oxidation reaction



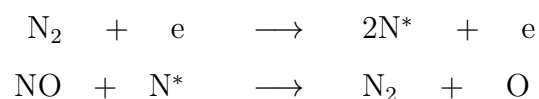
easily occur than the NO decomposition due to the higher activeness of O₃ or O radical comparing to N* radical



This can be used to explain the difference in the less effective area between the case of gas mixture without oxygen and the case of gas mixture with oxygen. In details, with gas mixture with oxygen and gas flow rate 2L/min, the less effective area was at the applied voltage less than 7kV. This value was smaller than the one in case of gas mixture without oxygen at the same gas flow rate ($V \leq 12\text{kV}$, Fig.3.2).

From the right side of Fig.3.6, as energy density increased, NO decreased ($\Delta\text{NO}=40\text{ppm}$) about 40% from initial concentration of 99ppm to 59ppm at the energy density of 58J/L and $V=13.5\text{kV}$. On the contrary, NO₂ increased from 7ppm to 37ppm ($\Delta\text{NO}_2=30\text{ppm}$) at same voltage. Therefore, the NO_x concentration decreased 10ppm (about 10%) from 106ppm to 96ppm. Moreover, in this condition the N₂O concentration can be negligible. It means that NO reduction process was not stronger than the cases of without oxygen mixture. The effect of oxygen made NO_x removal was far different from the case of gas mixture without oxygen showing in the previous section. In this case, the NO removal increased more drastically as the energy density increased. Conversely, the NO₂ formation concentration was also increased in inverse way. In total, there was only small amount of NO_x removal was observed.

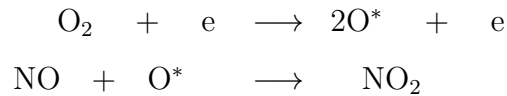
The reaction scheme in case of gas mixture with oxygen is described as follows. Since N₂O concentration was insignificant, NO removal from initial value (ΔNO) is a total of NO reduction and NO oxidation. Calculation from data in Fig.3.6 with ΔNO of 40ppm, NO₂ formation from NO oxidation of 38ppm under the maximum safety voltage. It means that the NO oxidation was 95% while the NO reduction was only 5%. The NO reduction scheme is similar to the case of gas mixture without oxygen:



The NO oxidation process in this case occurs with the existence from two sources: the O radical as a product of the latter reaction and oxygen from input gas mixture. By the first source, the oxidation reaction is:



The NO oxidation reaction scheme with oxygen from input gas mixture is as follows.



3.3.2 Effect of gas flow rate

In case that the gas flow rate was 1L/min, the NO_x removal characteristics are shown in Fig.3.7. NO concentration decreased rapidly as the energy density was increased. In total the NO removal of 60ppm was recorded at the maximum safety voltage. Inversely, NO₂ concentration increased from 10ppm to 54ppm. By that way, the NO_x concentration decreased only 16ppm. The starting point of effective discharge was about 8kV (see left figure) which was lower than that in case of gas mixture without oxygen ($V=10\text{kV}$).

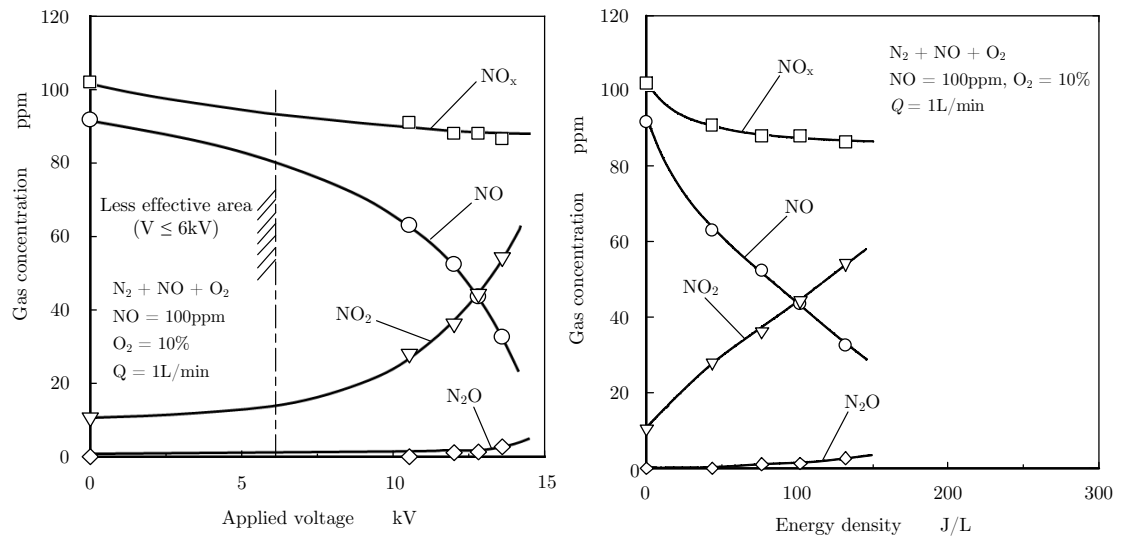


FIGURE 3.7 NO_x removal in N₂ + NO + O₂ mixture (O₂=10% and Q=1L/min)

Figure 3.8 shows the relation between NO_x removal by barrier discharge field with 100ppm NO, 10% O₂ and N₂ left mixture. The gas flow rate was 0.5L/min. The left figure showed that the discharge field started effective at about 7.5kV comparing to 8kV in case of gas mixture without oxygen. NO concentration

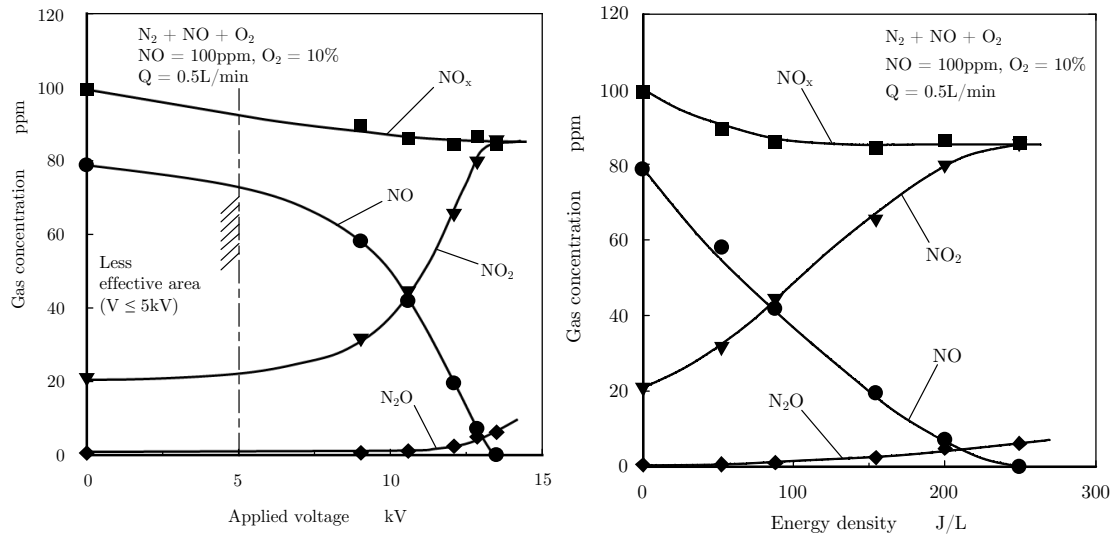


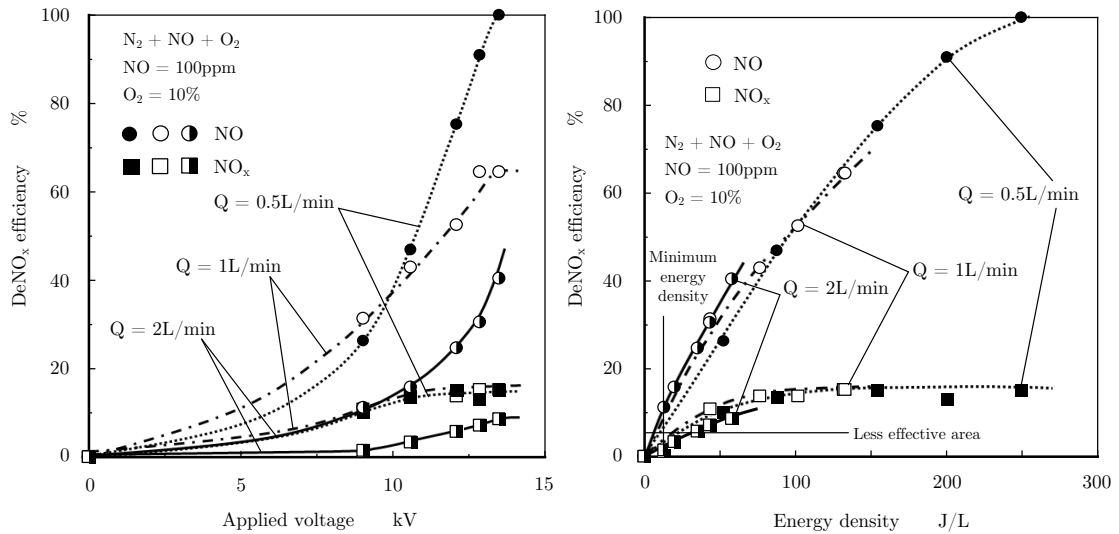
FIGURE 3.8 NO_x removal in $\text{N}_2 + \text{NO} + \text{O}_2$ mixture ($\text{O}_2=10\%$ and $Q=0.5\text{L}/\text{min}$)

decreased to 0ppm when the energy density reached 250J/L. On the other hand, NO_2 concentration increased from 21ppm to 85ppm. Consequently, NO_x removal was about 16ppm. In addition, though it slightly increased during experiment, N_2O concentration was only 6ppm at the maximum energy density for safety voltage.

3.3.3 De NO_x efficiency and minimum energy density

The summarized result in case of gas mixture of $\text{N}_2 + \text{NO} + \text{O}_2$ at gas flow rates of 0.5L/min, 1L/min, and 2L/min is illustrated in Fig.3.9. When the applied voltage was 13.5kV and constant, the NO removal from initial value of 100ppm were 40%, 65%, and 100% at gas flow rate of 2L/min, 1L/min, and 0.5L/min, respectively. However, at $V=13.5\text{kV}$ the maximum NO_x removal efficiency was only 15%. It caused by the existence of oxygen in gas mixture leading to dominated NO_2 formation process. Almost NO removal came from NO oxidation reaction scheme to form NO_2 . For this reason, at flow rate of 0.5L/min, even the NO concentration was decreased to zero but NO_x removal efficiency was about 15%. On the other hand, the existence of oxygen lowered the starting of effective applied voltage at which the chemical reactions by the activated radicals inside reactor really happened.

Comparing the data from Fig.3.5 and Fig.3.9, it can be seen that the minimum energy density was reduced from 40J/L ($\text{N}_2 + \text{NO}$ mixture, Fig.3.5) to around 10J/L ($\text{N}_2 + \text{NO} + \text{O}_2$ mixture, Fig.3.9). However, in $\text{N}_2 + \text{NO}$ mixture, de NO_x reaction was NO reduction while in $\text{N}_2 + \text{NO} + \text{O}_2$ mixture, de NO_x reaction was

FIGURE 3.9 DeNO_x efficiency in $\text{N}_2 + \text{NO} + \text{O}_2$ mixture

NO oxidation by O radical. The difference above can be explained that O_2 recombination ($\text{O}_2 \rightarrow 2\text{O}$) is easier to happen than N_2 ($\text{N}_2 \rightarrow 2\text{N}$).

The data on Fig.3.9 implies that for the gas flow rates of 1L/min and 2L/min, if the applied voltage continue to increase, the NO removal (by oxidation to NO_2) might increase. However, for all three cases, it seems that even if the applied voltage increases beyond 13.5kV, the deNO_x efficiency would not increase beyond 15%.

3.3.4 Effect of oxygen fraction

To investigate the effect of oxygen fraction on NO_x removal behavior under barrier discharge field, the gas flow rate $Q=0.5\text{L}/\text{min}$ was kept constant while oxygen fractions were changed in 0%, 10%, 15%, and 20%. Gas mixture consisted of 100ppm NO, O_2 , and N_2 remaining. The obtained results were previously shown in Fig.3.4 ($\text{O}_2=0\%$) and Fig.3.8 ($\text{O}_2=10\%$); and the new additional data are Fig.3.10 ($\text{O}_2=15\%$) and Fig.3.11 ($\text{O}_2=20\%$).

As mentioned before with oxygen and without oxygen mixtures, NO_x removal characteristics were far different. As for the mixtures with oxygen, when the energy density increased from 0 to 100J/L (applied voltage of 11kV), NO_x concentration decreased slowly and similarly in all three cases ($\text{O}_2=10\%$, 15%, and 20%). In this voltage condition, NO concentration decreased significantly but NO_2 concentration increased in the same order while N_2O was still negligible. Since NO_x was evaluated by total of NO and NO_2 , so from the point that NO completely oxidized to NO_2 ,

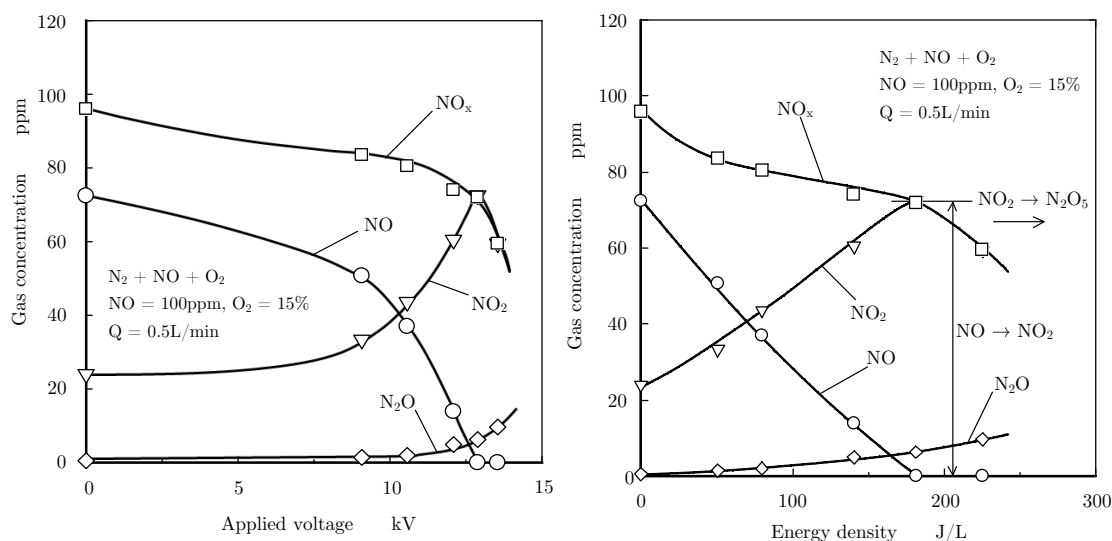


FIGURE 3.10 NO_x removal in $N_2 + NO + O_2$ mixture ($O_2=15\%$ and $Q=0.5L/min$)

NO_x concentration equals to NO_2 concentration which continued to be oxidized to N_2O_5 as energy density increased.

When the energy density increased beyond 100J/L, NO_x removal behavior is different for each gas mixture. With $O_2=10\%$ (Fig.3.8), NO concentration reduced to zero at energy density of 250J/L while NO_2 concentration increased up to 85ppm, thus NO_x removal in total was only 16ppm. In the case of $O_2=15\%$ (Fig.3.10), NO_2 concentration increased in the same way with gas mixture containing $O_2=10\%$ (Fig.3.8). On the other hand, NO concentration decreased and was zero at energy density of 180J/L. From that point, when energy density increased both NO_2 and NO_x concentrations went down. At energy density of 225J/L, NO_x concentration was 60ppm (equals to 37.5% removal from initial concentration).

For $O_2=20\%$ (Fig.3.11), NO concentration decreased faster than both of two cases mentioned above, while NO_2 concentration increased rapidly until the energy density reached 140J/L. At that point, NO concentration was zero and NO_2 concentration was 66ppm. After that, when energy density increased, both NO_2 as well as NO_x decreased very fast. At energy density of 224J/L, NO_x concentration was reduced to zero.

The phenomenon that NO concentration decreased to zero (at 12.8kV in case of 15% oxygen, 12kV in case of 20% oxygen) as seen in Figs.3.10 and 3.11 can be explained as follows. Since NO_x in this study is a total of NO and NO_2 , so from that point the NO_x concentration equals to NO_2 concentration. And with

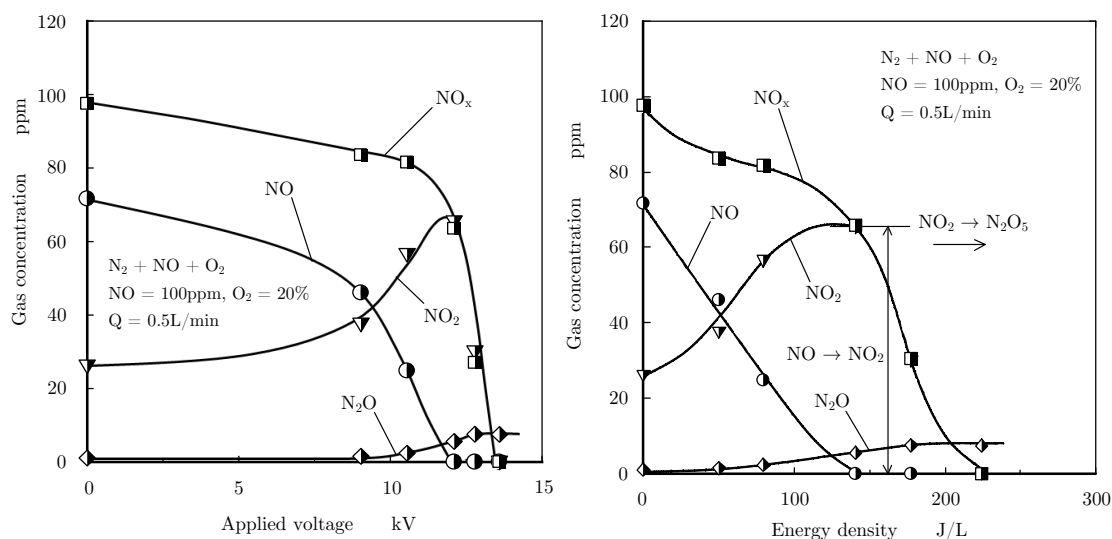
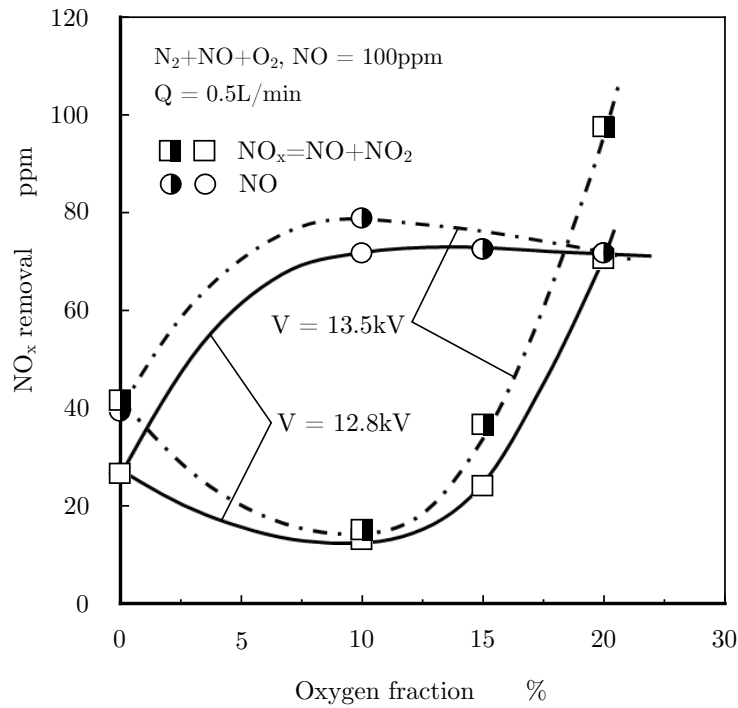


FIGURE 3.11 NO_x removal in $\text{N}_2 + \text{NO} + \text{O}_2$ mixture ($\text{O}_2=20\%$ and $Q=0.5\text{L/min}$)

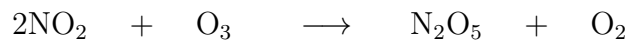
oxygen available in supplied gas mixture, NO_2 might continue to be oxidized to form N_2O_5 .

Consider the data reported by Saito et al., 2006 [38] using corona discharge reactor of a quartz glass tube (27mm inner diameter and 500mm in length) with the similar gas composition, the energy density needed to remove 100ppm of NO_x concentration was over 500J/L. In another work by Dors and Mizeraczyk, 2003 [44] using a corona discharge-catalyst hybrid system, the energy density to remove completely NO was over 400J/L. So in both cases, the energy density to remove NO_x is higher than in this study. It means that more effective removal of NO_x was performed in the present system.

The effect of oxygen on NO_x removal characteristics at $Q=0.5\text{L/min}$ is summarized in Fig.3.12. The vertical axis expressed the NO and NO_x removal in ppm which calculated as subtract the remaining concentration from the initial one. Data were collected with applied voltage of 12.8kV and 13.5kV. When oxygen fraction in gas mixture increased, the NO_x removal was also increased and removal efficiency was beyond 70%. However, NO_x removal was lower than in case of gas mixture without oxygen. The reason is that NO was oxidized with oxygen to form NO_2 . As oxygen of 15% and 20%, NO_x reduction in Fig.3.12 looks better than in case of oxygen fractions of 0 and 10%. Actually, after NO was completely converted to NO_2 , the formed NO_2 may continue to react with ozone to form N_2O_5 which was not measured in this study. Reaction scheme of this further oxidation

FIGURE 3.12 Effect of oxygen on NO_x removal at $Q=0.5L/min$

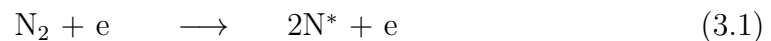
process is given as below.



3.4 Explanation using reaction scheme

The NO_x removal reaction mechanism in discharge field with gas mixture of N_2 , NO , and O_2 has been discussed in many papers.[25, 40, 43] Since in this study NO_x is total of NO and NO_2 , the NO_x removal mainly depends on NO reduction and NO oxidation processes. Moreover, N_2O concentration was determined very small and can be negligible, the NO_x removal can be calculated as a subtraction between the NO change from initial value and the NO_2 formation from NO oxidation process.

The NO reduction process occurs as following reaction scheme:

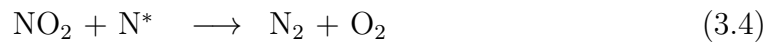


where e is electron.

Firstly, the N_2 molecules in the gas mixture were excited by discharge field to form N radicals (N^*). These radicals then react with NO to transform it into N_2 and O as in reaction (3.2). This process sometimes is called the primary mechanism

for NO destruction.[25] In case of gas mixture without oxygen, this was the main reaction of NO_x removal process. Calculation from data in Figs.3.2, 3.3, and 3.4 at critical value of applied voltage (13.5kV) showed that for gas mixture of NO + N₂, the NO removal was 85%, 82%, and 83.5% with gas flow rate of 0.5L/min, 1L/min, and 2L/min, respectively.

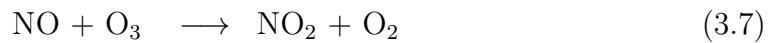
The decomposition reaction of NO₂ by N radicals may contribute to NO_x removal following below reactions:



On the contrary, in case of gas mixture with oxygen, the NO oxidation process to form NO₂ prevailed. The NO oxidation process with the existence of oxygen in gas mixture is described as below chemical reactions [25, 34, 90]. Initially, under discharge field, O radicals are formed and then they oxidizes O₂ to form ozone:

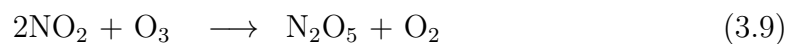


Then NO is oxidized by O radicals and ozone as follows:



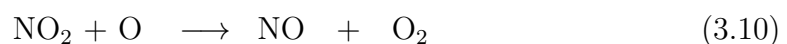
The calculation at the critical applied voltage of 13.5kV with the data in Figs.3.6, 3.7, and 3.8 showed that the NO removal efficiency by NO oxidation process was 88%, 92%, and 95% at gas flow rate of 0.5L/min, 1L/min, and 2L/min, respectively.

The experimental results with gas mixture of N₂ + NO + O₂ and O₂=15%, 20% pointed that at certain point where whole NO was oxidized to NO₂, if continue to increase energy density then formed NO₂ will be oxidized to N₂O₅. The reaction scheme for this further oxidation process is described as below reaction:



However, N₂O₅ could not be measured in this study.

Besides two main reaction schemes of NO reduction and NO oxidation as above, there are some auxiliary reactions might occur inside the reactor. The resulting balance between the formation and decomposition of NO and NO₂ is influenced by the reverse reaction:



Reaction (3.10) is also known as the secondary formation mechanism of NO.

3.5 Role of residence time

Residence time is an average amount of time that a gas spends in a reactor system.

It can be calculated from following equation.

$$\tau = \frac{60 \cdot V_s}{Q} \quad (3.11)$$

where

τ is residence time [sec]

V_s is the volume of the reactor system [litre]

Q is the gas flow rate running through system [litre/min].

A change in the gas flow rate varies directly the residence time in the reactor. Thus it is obviously that the gas flow rate affected to NO_x removal efficiency. When the gas flow rate is decreased the NO_x removal efficiency will increase. In other words, the longer the residence time is, the higher efficiency the NO_x removal can get. The reason is that with the same reactor and the same applied voltages so it can be assumed that the same amount of N radicals are formed. If the residence time, or the reaction time inside the reactor, is short then only some of N radicals can take part in NO destruction reaction (3.2). Accordingly, the NO_x removal efficiency is low.

The effect of residence time on NO_x efficiency can be seen in Fig. 3.13. The residence time was calculated according to equation (3.11). For gas flow rates of 0.5L/min, 1L/min, and 2L/min, the residence time was 16s, 8s, and 4s, respectively. Data were collected in case of gas mixture without oxygen and gas mixture with 10% of oxygen. In case of gas mixture without oxygen, as residence time increased from 4s to 16s, NO removal was increased from 17% to 44%. Since NO₂ was insignificant in this case as explained before, the NO_x removal was similar to NO removal efficiency.

Conversely, NO_x removal efficiency and NO removal efficiency are far different in case of gas mixture with oxygen. NO removal efficiency increased drastically as residence time increased and reached 100% at residence time of 16s. Nevertheless, NO_x removal efficiency was only about 15% and did not change even the residence time increased from 8s to 16s. This was explained by the NO oxidation process which is dominated when gas mixture contained oxygen. It means that the NO_x removal process seems saturated even if the residence time increased more.

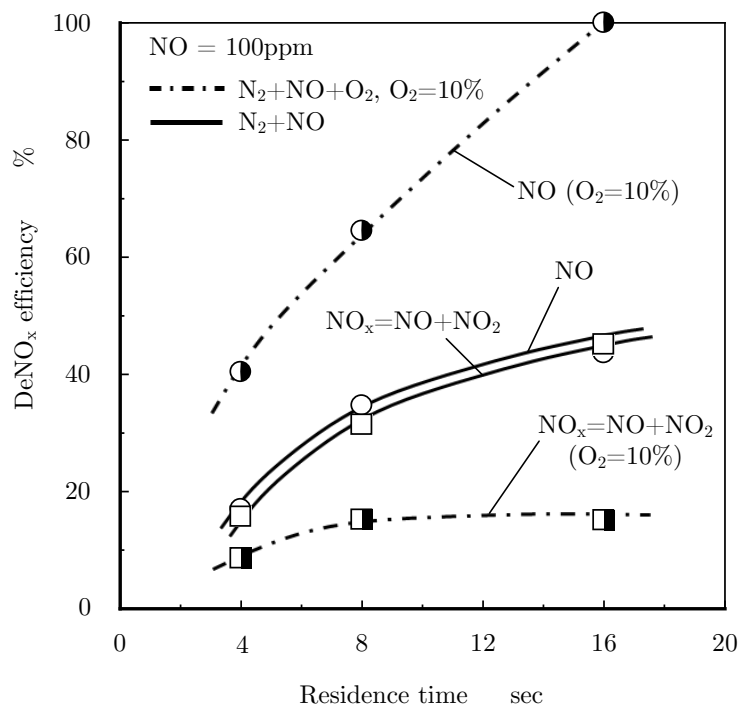


FIGURE 3.13 Effect of residence time on NO_x removal efficiency

3.6 Summary

NO_x removal behavior in dielectric barrier discharge with gas mixture of N₂, NO, and O₂; oxygen fraction from 0–20%, gas flow rates from 0.5L/min to 2L/min can be described as follows:

- (1) In case of gas mixture without oxygen, the NO removal was almost identical to NO_x removal.
- (2) Oxygen plays a major role in NO oxidation process to form NO₂ in case of gas mixture of N₂ + NO + O₂. As O₂ fraction increased, the NO oxidation process to form NO₂ ran faster. From the point that NO concentration was completely converted to NO₂, it may be that the further deNO_x process may occur to form N₂O₅ if the supplied energy density continue to increase.
- (3) With the existence of oxygen, NO concentration first goes down while NO₂ concentration increases; then from the point that NO concentration equals to zero, NO₂ decreased. It may be that formed NO₂ continues to further oxidation with ozone to form more oxidized nitrogen such as N₂O₅.
- (4) Residence time has an obviously effect on NO_x removal characteristics. The longer the residence time is, the higher NO_x removal can be received.

Chapter 4

Effects of particulate matter on NO_x removal characteristics

4.1 Purpose and experimental setup to investigate PM effect on NO_x removal

The objective of this chapter is to investigate the effects of particulate matter (PM) to NO_x removal characteristics under barrier discharge field. Moreover, the reaction mechanism is also discussed.

There are two kinds of PM to be used: “Fresh PM” (just loaded with PM generating system) and “Aged PM” (after hours running under applied voltage). These experimental results were compared to those in case of PDF without PM. Gas mixture in these experiments was NO + O₂ + N₂ with NO concentration of 112ppm, O₂ fractions of 1%, 5%, 10%, and N₂ remaining. Gas flow rate was kept constant at 1L/min. The running time tests were done in 4–6 hours applying the maximum safety voltage of the reactor. When the exhaust PM from PM generator was directly loaded, hydrocarbon and water in the exhaust gas were also loaded on DPF. The purpose of this study was to investigate the pure PM effect on NO_x removal, then, dry-up PM was used for experiments. The difference between wet PM and dry PM was explained in section 2.2.3 and procedure of dry-up is introduced in Fig.2.16.

Using “Fresh PM”, PM composition effect was investigated, test was started at high applied voltage condition, and then applied voltage was lowered. From that, Fig.4.1 and Fig.4.2 imply both effect of PM composition change and PM

aging. At the first step, the NO removal characteristics with different PM compositions (soluble organic fraction - SOF, and sulfate) were investigated to find out the standard test PM.

Figure 4.1 shows the relation between SOF fraction in PM with NO_x removal characteristics. The test condition was: initial NO concentration of 100ppm, oxy-

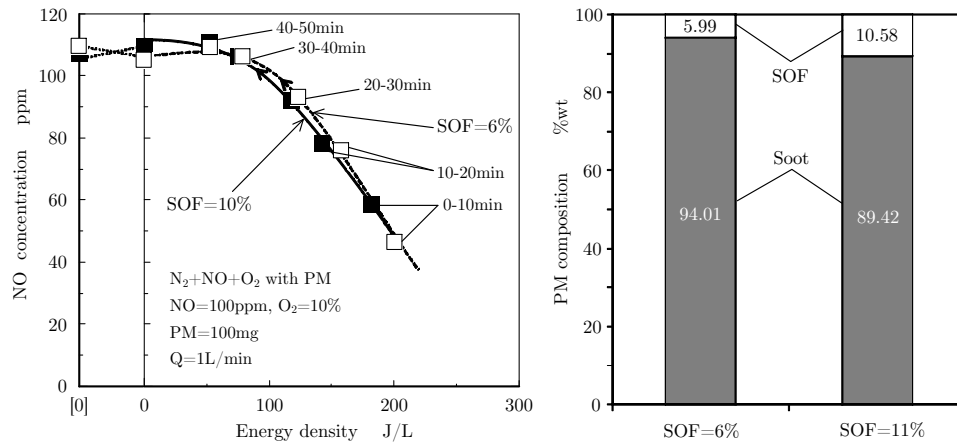


FIGURE 4.1 SOF fraction in PM and NO_x removal

gen fraction of 10%, DPF loaded with 100mg of PM, and gas flow rate of 1L/min. Two PM samples with SOF fraction of 6% and 10% were used. The SOF fraction was adjusted by changing the flame height and measured by the PM composition analyzer Horiba MEXA-1370PM. These PM samples properties were described in Chapter 2 (Fig. 2.14). From the experimental result, it can be said that SOF fraction change did not influence NO_x removal performance of the system.

Regarding the effect of sulfate fraction to NO_x removal characteristics, Fig.4.2 expresses the experimental data with zero sulfate and 0.24% sulfate. Sulfate frac-

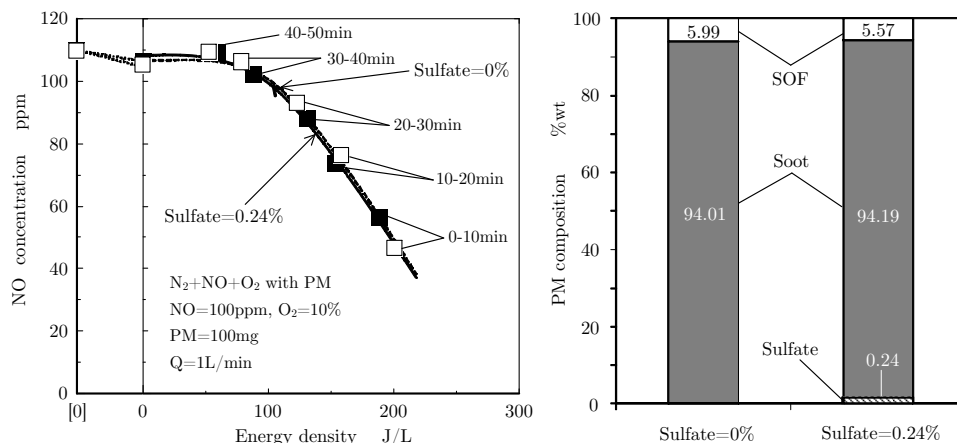


FIGURE 4.2 Sulfate fraction in PM and NO_x removal

tion was changed by fuel blended with thiophene. The results implied that sulfate fraction did not effect to NO_x removal characteristics.

So for simple, the PM with zero sulfate and SOF of 10% (the flame height of 30mm) was chosen as a standard test PM in this study.

4.2 Experimental results with PM loaded DPF

4.2.1 Simulated exhaust gas without oxygen

The effect of PM on NO_x removal characteristics by barrier discharge reactor with gas mixture without O₂ in two cases of a clean DPF and another one loaded with 100mg of PM were studied. Test gas conditions were: NO_x and N₂ mixture, NO_x=112ppm, gas flow rate of 1L/min. The constant applied voltage of 12.75kV was maintained under room temperature experiments.

Figure 4.3 shows the NO_x removal characteristics in case of PM loaded DPF. The test conditions were: NO_x + N₂ mixture, NO_x=112ppm, gas flow rate $Q=1\text{L}/\text{min}$, and PM=100mg. The energy density was 168J/L at the constant applied voltage of 12.75kV. The test results showed that NO₂ concentration was lower than that in case of DPF without PM (see Fig.3.1) and NO_x concentration was almost dominated with NO concentration. Then NO_x reduction ratio was higher than that

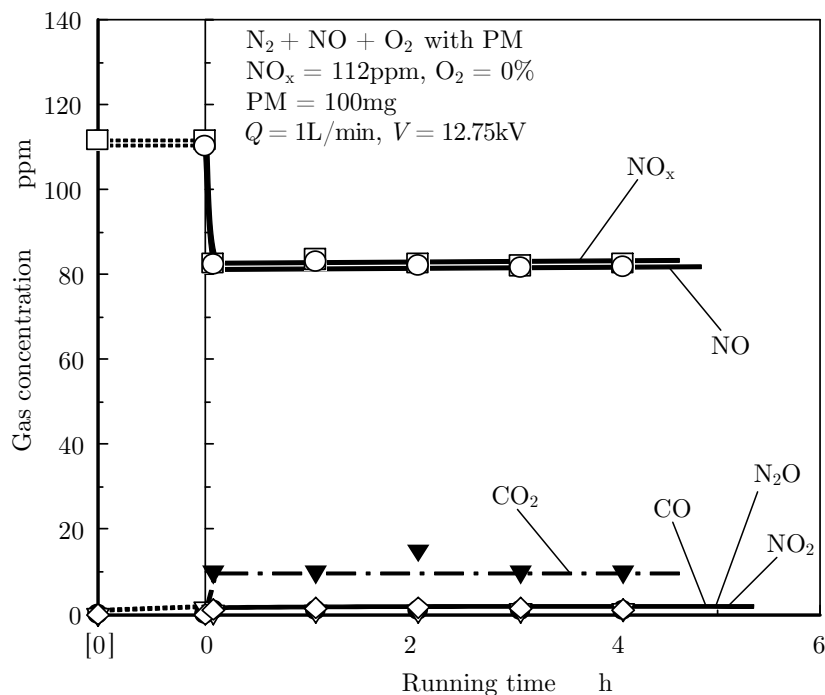
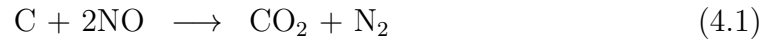


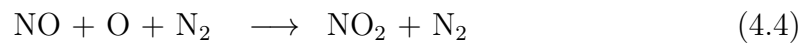
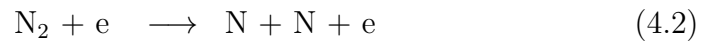
FIGURE 4.3 NO_x removal in N₂ + NO mixture (PM=100mg and $Q=1\text{L}/\text{min}$)

without PM. It meant that PM in DPF played some role in NO removal under oxygen absence condition.

The trace of CO₂ and CO revealed that C atoms from PM had taken part into NO_x reduction process. Firstly, NO concentration decreased by following reaction:



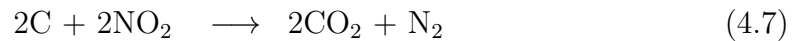
On the other hand, NO₂ is slightly formed from the oxidation of NO into NO₂ by O radical formed through NO reduction reaction.



At the next step, the mechanism, so called PM oxidation by NO₂, can be described as follows.



However, these two reactions (4.5) and (4.6) do not mean NO_x removal, they just make nitrogen dioxide NO₂ reduction into nitric oxide NO. Then the following reaction should be introduced to explain the NO₂ removal. This reaction is just effective with temperature in range of from 150°C to 300°C.



The data of NO_x removal characteristics in cases of DPF without PM (Fig.3.1) and DPF with PM=100mg (Fig.4.1) were summarized in Fig.4.4. More than 10ppm of NO_x was removed in the case of DPF with PM comparing to the case of DPF without PM. In addition, CO₂ concentration in Fig.4.3 was around 10ppm. It showed that reaction (4.7) was the main NO_x removal mechanism by PM. NO₂ formation of 10ppm in case of DPF without PM comparing to 1ppm in case of DPF with 100mg PM was the evidence of the reaction (4.7), but molecular balance between CO₂ and carbon atoms in PM was impossible because of small amount of PM mass reduction. In this study, the PM mass in order of mg (milligram) was checked before and after test but it was insignificantly changed. It might be that the PM mass reduced by NO_x should be checked in order of microgram. According to reaction 4.7, calculation with experimental result as mentioned above showed that 0.535μg/min oxidation of carbon results in 10ppm CO₂ and gas flow rate of 1L/min.

From current-voltage characteristics (see Fig.2.19), DPF with PM promoted the more electric current than DPF without PM. It caused another positive effect of NO_x removal. Finally, the experimental results represented in Fig.4.4 could lead to a conclusion that PM could be a reduction agent to remove NO_x .

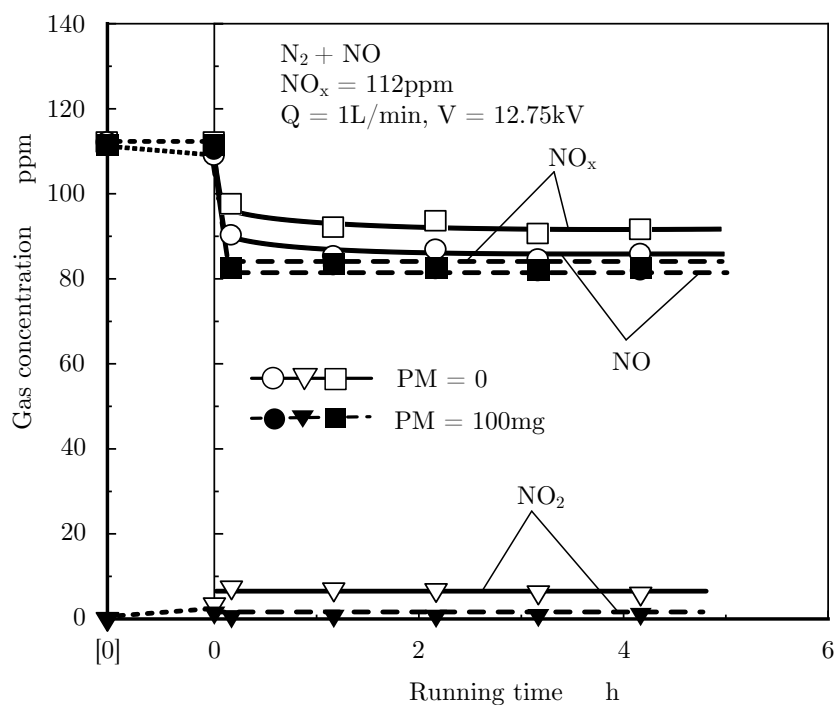


FIGURE 4.4 NO_x removal in $\text{N}_2 + \text{NO}$ mixture (with and without PM, $Q=1\text{L}/\text{min}$)

4.2.2 Simulated exhaust gas with oxygen

The role of O_2 as an oxidation agent in case of DPF without PM had been reported in previous chapter (see Chapter 3). In this section, the DPF loaded with 100mg of PM and four different O_2 fractions, namely 1%, 5%, 10%, and 15% were tested. Using “Fresh PM”, experiments were done in 4 hours applying voltage of 12.75kV.

The experimental results with $\text{O}_2=1\%$ and $\text{PM}=100\text{ mg}$ is shown in Fig.4.5. In this case, CO_2 and NO_2 concentrations showed time dependent characteristics with running time. Just after experiment was started, CO_2 formation was predominant but NO_2 formation increased gradually by running time. As the results, NO and NO_x concentrations were changed with running time. However, NO_x removal effect was less apparent than $\text{O}_2=0\%$ (Fig.4.3) when the running time was over two hours.

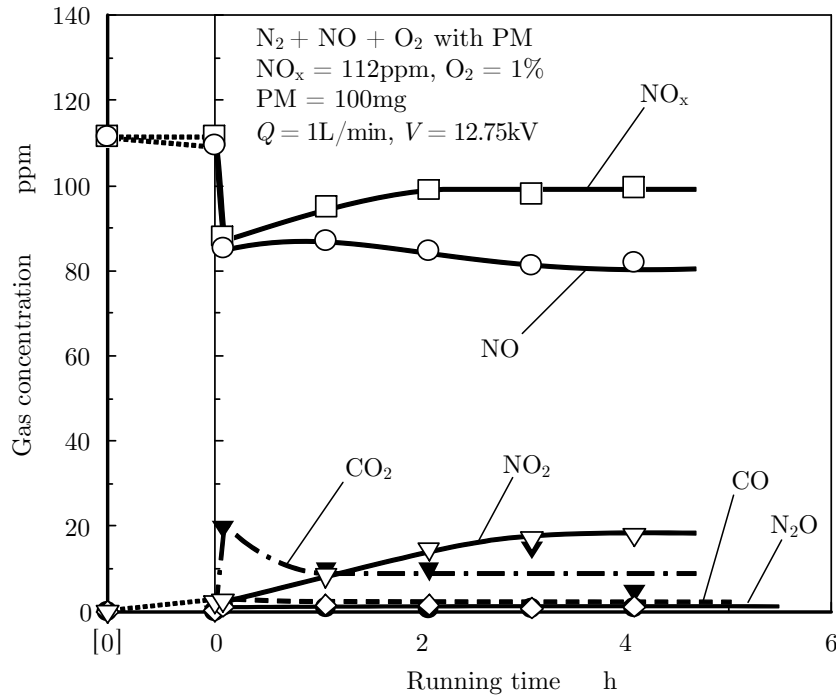
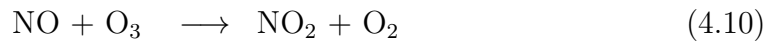
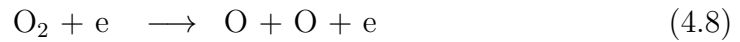
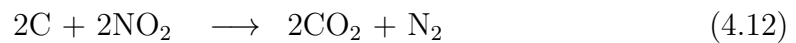
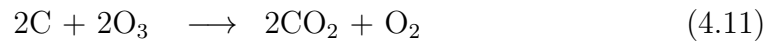


FIGURE 4.5 NO_x removal in N₂+NO+O₂ mixture (PM=100mg, O₂=1%, and Q=1L/min)

With the existence of O₂ under discharge field, ozone was formed. Thus, following reactions (4.8)–(4.10) should be considered as the NO oxidation mechanism.[34]



Under the presence of O₂, there was a possibility of direct PM oxidation with ozone. Its reaction scheme was as follows.



Then the CO₂ formation process was controlled by both reactions of (4.11) and (4.12). Reaction (4.11) was independent of NO_x removal process, and other experiments were needed to explain the whole behavior of CO₂ formation.

As shown in Fig.4.6, deterioration of NO_x removal performance was more apparent when O₂ concentration was 5%. It was obvious that when O₂ fraction increased, the NO₂ concentration increased correspondingly. After two hours running, NO₂ concentration reached 14ppm in case of O₂=1% (Fig.4.5) but it was

40ppm when O_2 was 5% (Fig.4.6). Then NO_x removal effect was only apparent during early one hour from start the experiment.

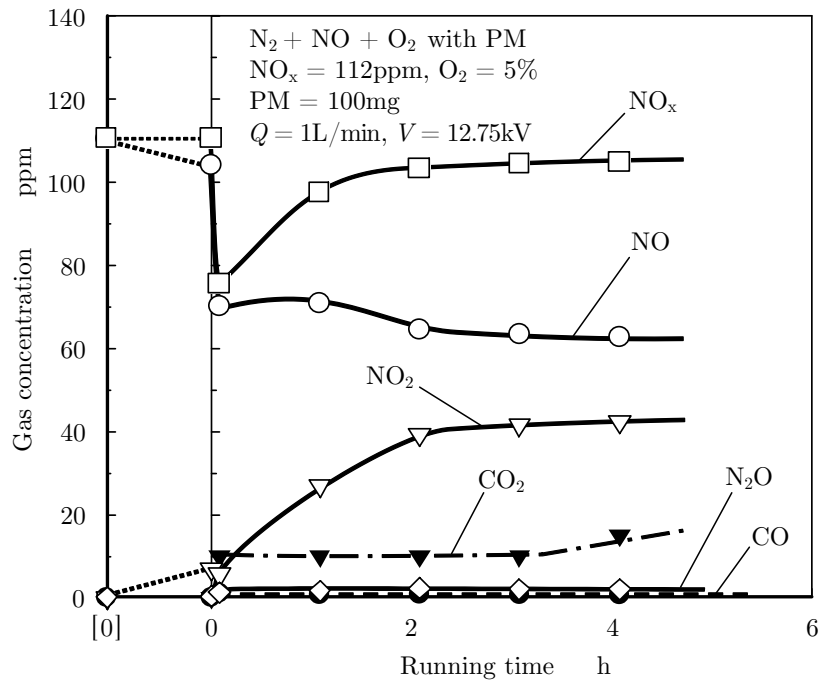


FIGURE 4.6 NO_x removal in $\text{N}_2 + \text{NO} + \text{O}_2$ mixture ($\text{PM} = 100\text{mg}$, $\text{O}_2 = 5\%$, and $Q = 1\text{L}/\text{min}$)

A similar behavior was also observed in cases of oxygen fraction of 10% and 15% as shown in Fig.4.7. NO_x removal effect was deeply at the first running hour (maximum NO_x removal was from 40ppm to 50ppm), then decreased following running time. And this effect halted just after 1.5h running in both cases of oxygen

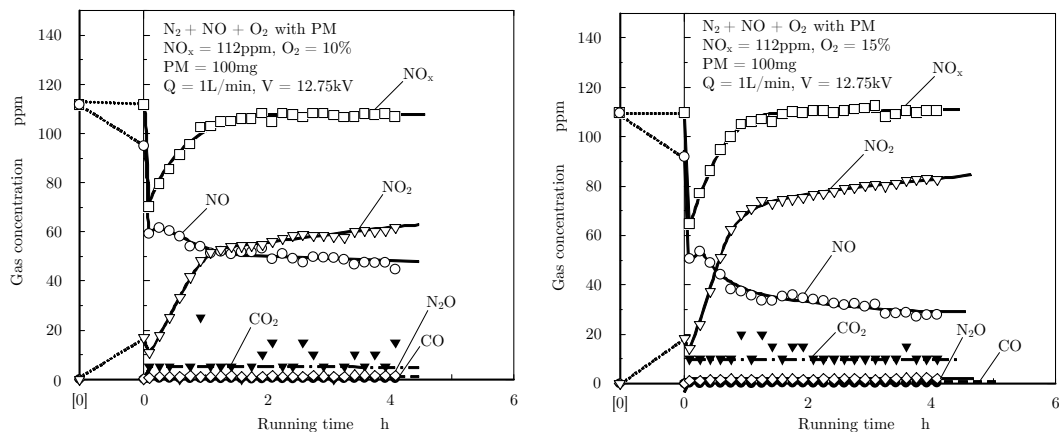


FIGURE 4.7 NO_x removal in $\text{N}_2 + \text{NO} + \text{O}_2$ mixture ($\text{PM} = 100\text{mg}$, $Q = 1\text{L}/\text{min}$, and $\text{O}_2 = 10\%$ and 15%)

fraction of 10% and 15%.

From experimental results above, it can be seen that CO_2 concentration did not increase with O_2 fraction. If the PM direct oxidation by O_2 was the main reaction scheme of CO_2 formation, it should increase as O_2 fraction increased. However, CO_2 behavior showed almost similar manner with the case shown in Fig.4.3 (gas mixture without oxygen). It means even though with the existence of O_2 , CO_2 might be formed by reaction scheme of reaction 4.7. And also it indicated that NO is oxidized by O radical more easily than PM. The details of O_2 concentration effect on NO_x removal is explained latter in section 4.3.2.

4.2.3 PM loading mass and NO_x removal characteristics

Figure 4.8 shows the NO_x removal characteristics at different mass of PM loaded on DPF. Gas mixture was 112ppm of NO_x , 10% of O_2 and N_2 left. Loaded PM were 0mg, 100mg, and 200mg. Applied voltage was kept constant at 12.75kV for all PM conditions. Then the electrical energy was changed from 101 μ A for

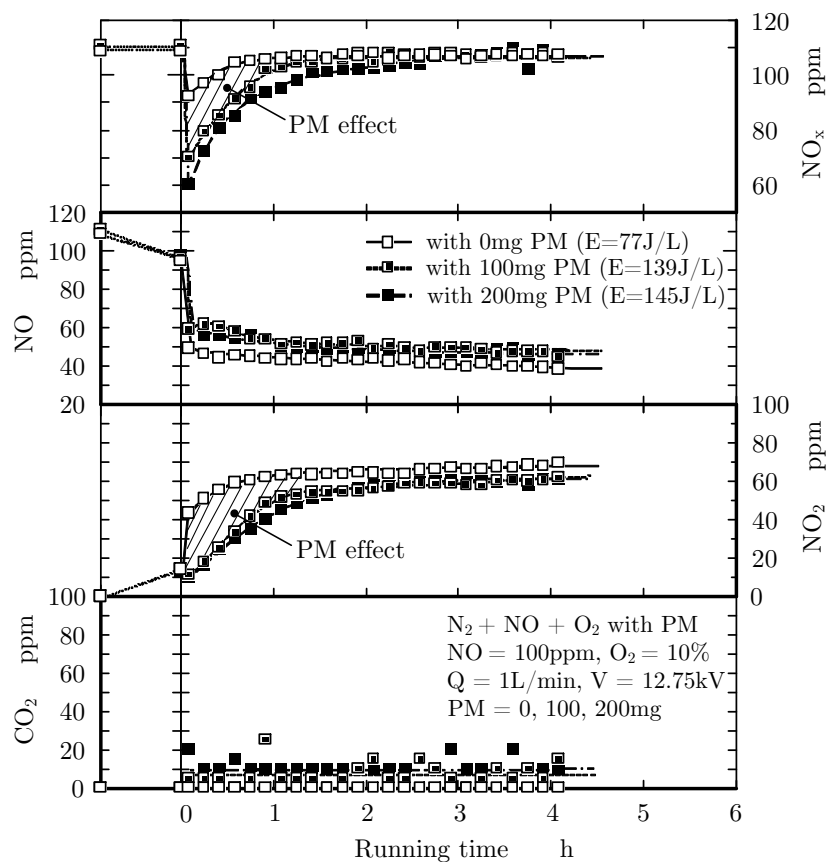


FIGURE 4.8 NO_x reduction at different PM mass loaded on DPF ($O_2=10\%$)

PM=0mg to 182 μ A for PM=100mg, and 190 μ A for PM=200mg. The test gas was sampled every ten minutes.

In this figure, PM effect on NO reaction was indicated by the hatching area. NO concentrations in all three cases of gas mixtures with oxygen were dropped at the first. After that, NO concentrations increased and was almost stable. Conversely, NO₂ concentration increased significantly from start to two running hours. NO₂ increase in cases of PM=100mg or 200mg was much slower than that in case of PM=0mg. As a result, NO_x concentrations with PM=100mg and 200mg were lower than that with PM=0mg. However, there was no significant difference in PM=100mg and PM=200mg. It means that NO₂ formation did not depend on PM loaded mass but seemed that it depended on oxygen or ozone formed by discharge.

The NO_x removal effect by PM was represented by the area which was surrounded by NO_x curve in case PM=0mg and those in cases of PM=100mg and 200mg. It suggested that NO_x removal promotion by PM appeared only in the beginning of the discharge but its promotion effect was vanished after two hours running.

4.3 PM aging

4.3.1 PM aging effect

To clarify the effect of PM aging on NO_x treatment under discharge field, another kind of test was conducted. Two simulated gas mixtures of NO, O₂, and N₂ with the same composition of were tested. One mixture was tested in order of increasing applied voltage from zero to the maximum safety voltage. This test run demonstrates the “Aged PM”. The other one, on the contrary, was started with the maximum safety voltage, then lowered to zero. Thus it expressed the test run of “Fresh PM”. The range of supplied energy density (or applied voltage) was the same in both cases. Both test results with NO + O₂ + N₂, NO=100ppm, O₂=10%, gas flow rate $Q=1\text{L}/\text{min}$ is illustrated in Fig.4.9 showing NO_x concentration in ppm following energy density in J/L.

The sample timing was marked at every testing point in the figure. It can be seen that if the maximum safety voltage of 12.75kV (equals to 180J/L) was applied as a started sampling point (in case of “Fresh PM” test), the NO_x reduction would be significant higher (about 50ppm) than the one in “Aged PM” test. However, as energy density decreased from peak value, NO_x concentration decreased quite fast. And both cases give the similar result at point 20-30 minutes of sampling.

In brief, the “Fresh PM” has a superior effect on NO_x treatment process under discharge field comparing to the “Aged PM”.

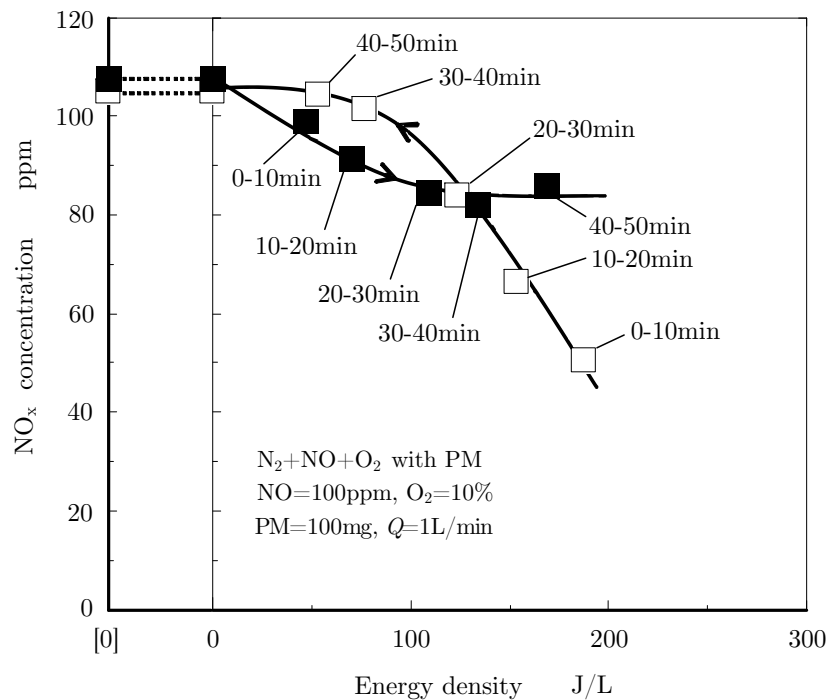


FIGURE 4.9 Effect of “Aged PM” on NO_x treatment

4.3.2 Experimental results in cases of DPF with “Fresh PM”

To assess the extensive impact of PM on NO_x removal, the experiments with “Fresh PM” was performed. “Fresh PM” means the PM just loaded with the diffusion flame PM formation system [85] during the reactor does not run yet. The data obtained with “Fresh PM” was expressed in Fig.4.10. For the next experiment, DPF was cleaned up and “Fresh PM” was loaded again on DPF for every experimental run. The data in the figure were taken during the first six minutes from the start of experiment. In the experiments, the DPF was loaded with 0mg, 100mg, and 200mg of PM. O₂ fractions of 0, 1%, 5%, 10%, and 15% were tested.

As observed, the NO concentration in this experiment was constantly decreased with increase O₂ fraction. However, there was not so much difference of NO reduction (about 50%) between 100mg and 200mg of PM mass. The NO₂ concentration increased up to 52ppm in case of PM=0mg and O₂=15% but increase of NO₂ was suppressed by PM. Even though high O₂ concentration such as O₂=15%,

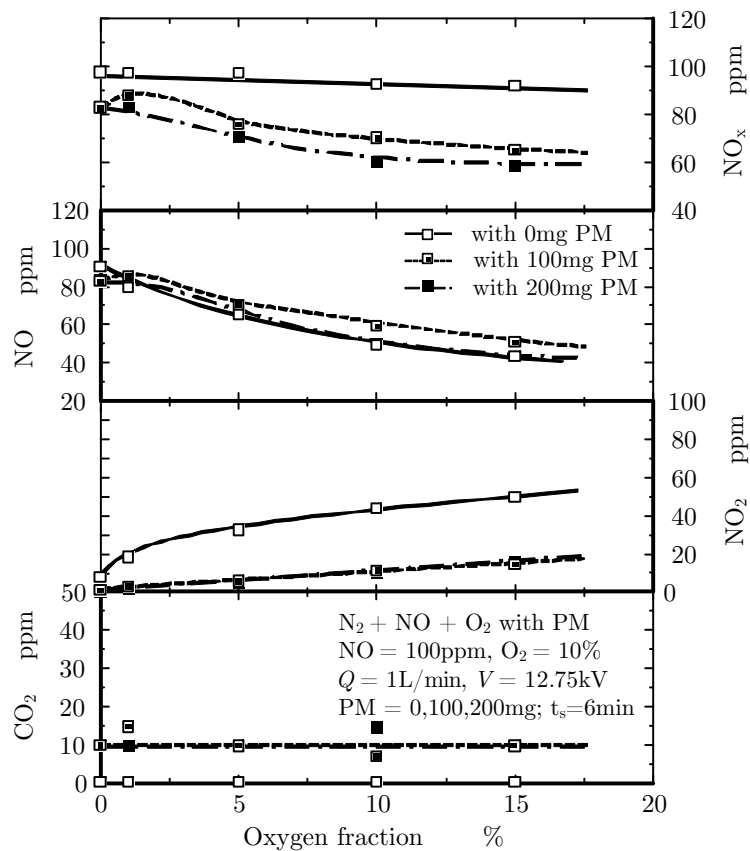


FIGURE 4.10 NO_x reduction at different O_2 fractions and “Fresh PM”

NO_2 concentrations of both $PM=100mg$ and $200mg$ were less than $20ppm$. Since CO_2 concentration did not increase with O_2 fraction, it was considered that both of catalytic reduction mechanism with PM and direct reduction mechanism with reaction (4.7) were coexisted.

With the presence of PM, NO_x removal was recorded at 22% and 30% with PM mass of $100mg$ and $200mg$ at $O_2=15\%$, respectively. These removal ratios were much higher than the case of $PM=0mg$ (3%). The removal of NO_x concentration as in Fig.4.10 implies that “Fresh PM” approved its role as NO_x reduction agent. The similar results obtained with $PM=100mg$ and $200mg$ could be explained by very closed levels of electrical currents showed in Fig.2.19.

4.3.3 Experimental results in cases of DPF with “Aged PM”

Figure 4.11 shows the effect of PM after a long running time on NO_x removal. In other words, “Aged PM” was used. Experimental conditions were same as the cases of Fig.4.10, but the test gas was sampled after four hours running.

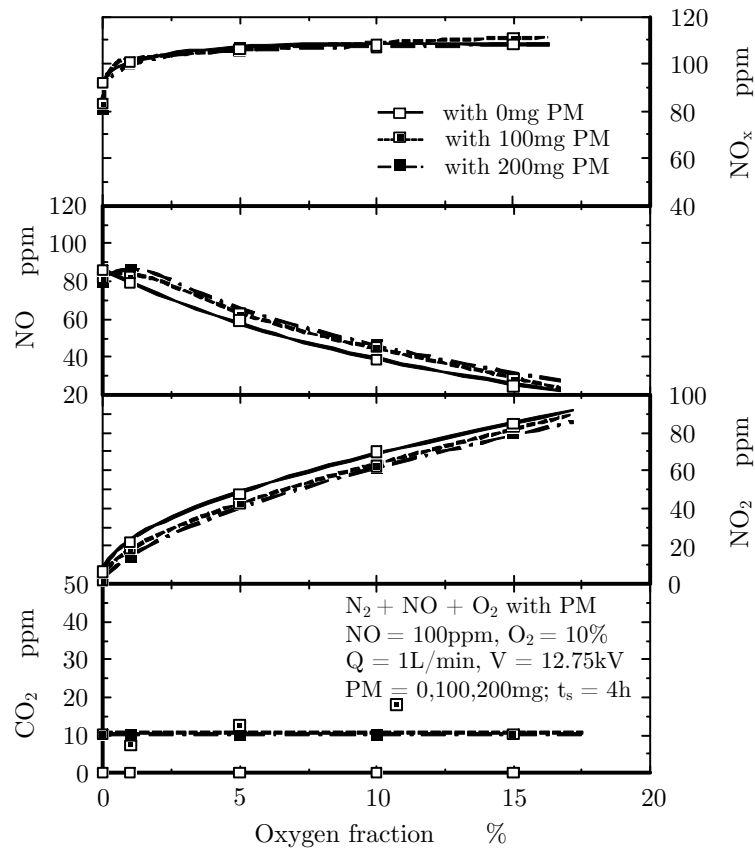


FIGURE 4.11 NO_x reduction at various PM mass and O_2 after 4 running hours

From the figure, NO decrease but NO_2 increase according to O_2 fraction were clearly observed. Nevertheless, there was almost no difference in gas concentrations (NO , NO_2 , and NO_x) for all three cases of PM mass. When $O_2=15\%$, NO concentration decreased to 25ppm, 30ppm, and 35ppm with PM mass of 0mg, 100mg, and 200mg, respectively. NO_2 increased in the same order and concentrations were 78ppm, 79ppm, and 82ppm. There was a slight PM effect on NO_x removal after a long period running under barrier discharge when O_2 fraction was below 5%. However, with higher O_2 concentration, no PM effect on NO_x removal was observed.

In actual DPF system, loaded PM was oxidized under forced regeneration process or continuous PM oxidation process during operation. It meant that loaded or deposited PM in DPF was partially oxidized PM, and it might show less effective role as indicated in Fig.4.11 (after long running PM). However new “Fresh PM” was always supplied from engine side and it deposited over on the old PM where its surface had already lost the effective role of NO_x removal. It meant that there are many possibilities of NO_x removal. In this report, a possibility of NO_x

removal with “Fresh PM” coupled with electric discharge could be pointed out experimentally.

4.4 NO_x adsorption effect by PM

It was clear that “Fresh PM” showed NO_x removal performance. However, its effect was not separated from NO_x adsorption effect on PM. Since the DPF and PM surface were activated with electrical barrier discharge, they might have some adsorption performance for molecules. Then, NO_x adsorption effect was checked with following experiment. To check the adsorption effect, the reactor was supplied with discharge energy in four hours then ran “idle” (no energy supplied) for next two hours. Test gas was sampled continuously for every ten minutes. Figs.4.12 and 4.13 shows the results of experiment.

Figure 4.12 was the experimental result of PM=0mg and energy density of 77J/L (V=12.75kV). NO_x concentration decreased in the first one hour running. Then it increased and was stable. After four hours running, the supplied energy was cut off. NO_x concentration showed 8ppm increase, then went down to the initial value.

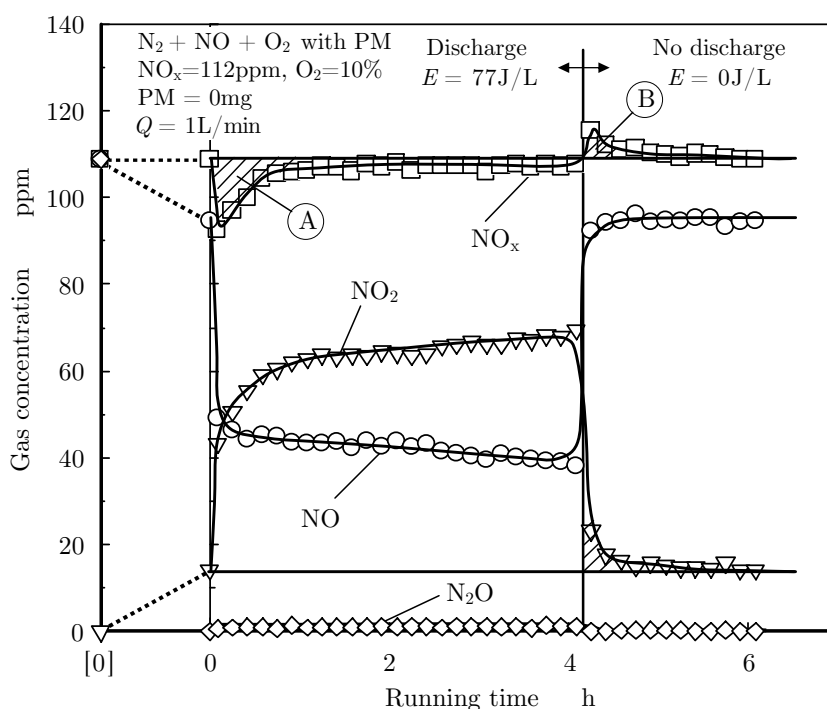


FIGURE 4.12 NO_x adsorption following barrier discharge energy at PM=0mg

Conversely, for PM=100mg and the supplied energy of 139J/L (V=12.75kV) (Fig.4.13), NO_x concentration decreased drastically at first then increased and kept

constant at some ppm lower than initial value of 112ppm. However, when energy was cut off, NO_x concentration raised up to 128ppm before decreasing slowly to the initial concentration.

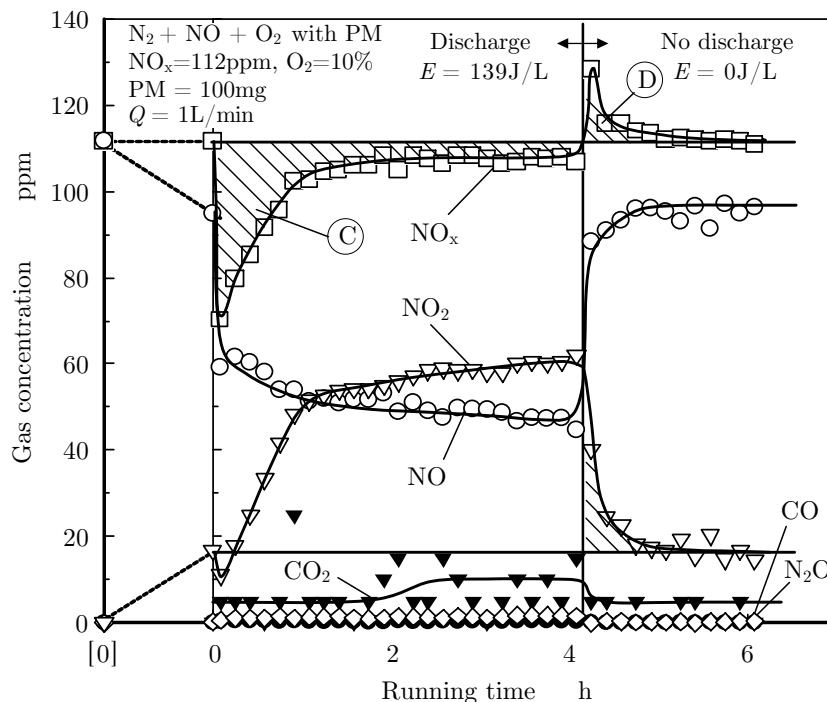


FIGURE 4.13 NO_x adsorption following barrier discharge energy at $\text{PM}=100\text{mg}$

As shown in Figs.4.12 and 4.13, area A represents the NO_x removal in case of $\text{PM}=0\text{mg}$ and area C represents the NO_x removal in case of $\text{PM}=100\text{mg}$. The difference between these areas indicates the combined effect of NO_x adsorption by PM, NO_x removal by PM as reduction agent and supplied energy increase by PM. NO_x adsorption and reduction agent effects of PM showed their maximum at early period of experiment (“Fresh PM”). In short:

A: NO_x removal at $\text{PM}=0\text{mg}$

C: NO_x removal at $\text{PM}=100\text{mg}$

C-A: Sum of effect of NO_x adsorption by PM, NO_x removal by PM as reduction agent and supplied energy increase by PM.

Most important result of this investigation was the effect of “Fresh PM” on NO_x removal. As shown in Figs.4.12 and 4.13, its effect could not be explained by the NO_x and ozone adsorption effect of PM. A realistic mechanism of NO_x reduction with “Fresh PM” is supposed that the active surface of “Fresh PM”

played a role of catalytic surface for NO_x removal and its effect was promoted by electric discharge. As for an “Aged PM” (after long running), surface of PM was oxidized and no catalytic effect might appear there.

On the other hand, when supplied voltage was cut off, area B demonstrates an overshoot of NO_x concentration. It was caused with released NO_x that was adsorbed in a clean DPF. In case of DPF with PM, area D demonstrates the same but clearer behavior than area B. However, released NO_x effect was not so large and was deteriorated during 20 minutes after cut-off the applied voltage. Then the NO_x removal effect appeared during first two hours could not be explained by the adsorption effect of “Fresh PM”.

Briefly, in Fig.4.12, the test was done with DPF without PM (bare DPF), area B represents the NO_x adsorption effect by DPF. The difference between areas A and B (or A-B) expresses the catalytic effect of bare DPF. In case of DPF with PM as showed in Fig.4.13, area D represents the NO_x adsorption effect by DPF and adsorption effect by “Fresh PM”. The value of (C-D) in this case expresses the catalytic effect of bare DPF and “Fresh PM”. From these results, it can be concluded that the value of (D-B) represents the net adsorption effect of “Fresh PM”. The net catalytic effect of “Fresh PM” is represented by the difference between (C-D) and (A-B). In other words:

B: NO_x adsorption by DPF

D: NO_x adsorption by DPF and “Fresh PM”

A-B: Catalytic effect of bare DPF

C-D: Catalytic effect of bare DPF and “Fresh PM”

D-B: Net adsorption effect of “Fresh PM”

(C-D)-(A-B): Net catalytic effect of “Fresh PM”.

Adsorption mass of molecules was generally proportional to adsorbent mass. However, “Fresh PM” effect shown in Fig.4.10 indicated that NO_x removal effect did not proportional with PM mass and it seemed to be proportional to electrical current. It also suggested that NO_x adsorption effect was not the main mechanism of NO_x removal with “Fresh PM”.

As for the cases of without O₂ conditions, no adsorption effect was observed in Fig.3.1 and Fig.2.19. It means that the overshoot shown in Figs.4.12 and 4.13 were related with O₂. When ozone was formed in the reactor, there were possibilities that NO_x and CO₂ accompanying with ozone was adsorbed and remained in the

reactor, and then they were released after cut-off the electrical current. However, this effect was not so much as mentioned above.

4.5 Summary

The effects of PM on NO_x removal efficiency was investigated by using a needle-to-cylinder dielectric barrier discharge reactor combined with a DPF. Gas mixture of NO, NO₂, N₂ and O₂ with the PM was used. The experimental results showed that

- (1) NO_x removal was promoted by PM under the dielectric barrier discharge in a NO_x and N₂ mixture without O₂.
- (2) PM also enhanced NO_x removal in the dielectric barrier discharge field with O₂ existence.
- (3) However, this effect deteriorated with running time. The most significant NO_x removal performance was observed when PM was “Fresh”.
- (4) Compared to “Fresh PM”, “Aged PM” showed an insignificant effect on NO_x treatment process under discharge field.

Chapter 5

NO_x removal performance in transient test

5.1 Purpose of various transient tests

Since the surface state of DPF and PM had great effect on deNO_x reaction, in the previous chapter, “Fresh PM” and “Aged PM” investigations were done. It means a kind of PM surface effect on deNO_x. Also some of adsorbed molecule on the surface had some effect on deNO_x reaction. Then pre-treatment of DPF with PM using DBD is considered some initial adsorption molecule effect on deNO_x mechanism.

This chapter introduces the NO_x removal behavior with PM in transient test in two modes: four running hours and six running hours. Test conditions in detail was shown in Table 5.1. Purposes of these tests are: (1) to check the adsorption

TABLE 5.1 Transient test conditions

Test	Test conditions with PM=100mg					
	1st hour	2nd hour	3rd hour	4th hour	5th hour	6th hour
4-(1)	N ₂ +O ₂ , E=0J/L	N ₂ +NO+O ₂ , NO=100ppm, E=138J/L		/		
4-(2)	N ₂ +O ₂ , E=78J/L	N ₂ +NO+O ₂ , NO=100ppm, E=140J/L				
4-(3)	N ₂ only, E=78J/L	N ₂ +NO+O ₂ , NO=100ppm, E=140J/L				
6-(1)	N ₂ +NO+O ₂ , NO=100ppm, E=138J/L			N ₂ +O ₂ , E=0J/L	N ₂ +NO+O ₂ , NO=100ppm, E=138J/L	
6-(2)	N ₂ +NO+O ₂ , NO=100ppm, E=117J/L			N ₂ +O ₂ , E=77J/L	N ₂ +NO+O ₂ , NO=100ppm, E=117J/L	
6-(3)	N ₂ +NO+O ₂ , NO=100ppm, E=134J/L			N ₂ only, E=76J/L	N ₂ +NO+O ₂ , NO=100ppm, E=134J/L	

and absorption effect of PM, (2) investigate the effect of one hour pre-treatment on adsorption and absorption processes, and (3) to clear up the difference between “Fresh PM” and “Aged PM”.

In four hours running mode, namely “Fresh PM” test, each test divided in two stages: the first stage of one hour and the second stage of three hours. By this experiments, NO_x removal characteristics with “Fresh PM” and different pre-treatments were investigated. In six hours running mode, namely “Aged PM” test, the tests divided in three stages: three hours, then one hour, and finally two hours. In this mode, the three hours running stage was added before different pre-treatments as in four hours mode. The pre-treatment stage with N₂ only and applied energy density in Tests 4-(3) and 6-(3) were done to investigate the N radical effect on NO_x removal process.

All the test was conducted with “Fresh PM” of 100mg at gas flow rate of 1L/min. The simulated gas through reactor was sampled continuously, i.e every ten minutes. Applied voltage was 12.75kV as same as Chapter 4, but energy density changed with conditions of PM.

5.2 “Fresh PM” pre-treatment effect on NO_x removal

5.2.1 NO_x removal characteristics in four hours running mode

In this mode, the first stage of one running hour was carried out with gas mixture of N₂ or N₂ + O₂, gas flow rate of 1L/min, and energy density of 78J/L. It means one hour pre-treatment before deNO_x experiment. The experimental results were showed in Figs.5.1, 5.2, and 5.3.

The experimental results showed that there was a difference in NO_x removal performance after first one running hour (pre-treatment stage). In all three cases, NO concentration changed in very similar way. However, NO₂ concentration was differed. As can be seen in Fig.5.1 (Test 4-(1)), there was no applied voltage at pre-treatment stage of “Fresh PM”, but NO₂ concentration was increased quickly as energy density started applying. It means that one hour treatment with non reactive N₂ + O₂ mixture did not affect PM aging. This can be explained by the oxygen adsorption effect by DPF at the pre-treatment stage and the effect of discharge field.

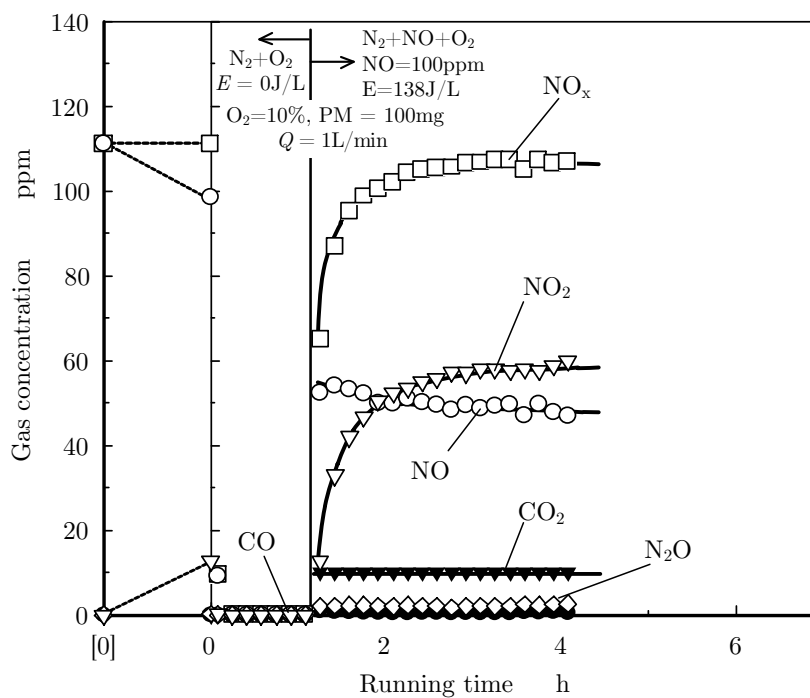


FIGURE 5.1 NO_x removal performance in 4 running hours mode (Test 4-(1): One hour pre-treatment in $N_2 + O_2$ atmosphere without DBD)

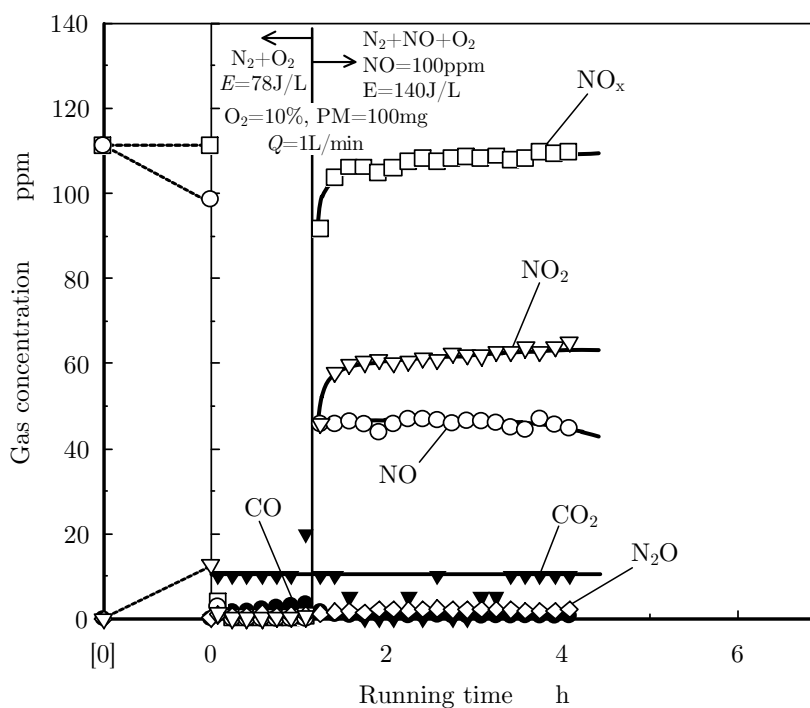


FIGURE 5.2 NO_x removal performance in 4 running hours mode (Test 4-(2): One hour pre-treatment with DBD in $N_2 + O_2$ atmosphere)

In Fig.5.2 (Test 4-(2)), the active oxygen and nitrogen under discharge field were already absorbed by DPF and “Fresh PM” at the pre-treatment stage, so there was no further adsorption of NO as described in Test 4-(1) above.

As the gas mixture at the first stage did not contained NO so the NO_x removal process just started at beginning point of the second stage. In case of gas mixture at the first stage consisted of $N_2 + O_2$ (Figs.5.1 and 5.2), there was a significant difference in NO_x removal performance between Test 4-(1) and Test 4-(2). In Fig.5.1 (Test 4-(1)), NO_x concentration dropped deeply at first then gradually increased following elapsed time. Conversely, NO_x concentration in Test 4-(2) just slightly reduced then increased to stable value. After two running hours, both cases showed a stable NO_x removal state until the end of test. The difference mentioned above can be explained by the existence of ozone at the beginning of the second stage in Test 4-(2). Although gas mixture of $N_2 + O_2$ was the same in both tests but there was no applied voltage ($E=0J/L$) so no ozone formed. Conversely, by applying a energy density $E=78J/L$ in the first stage of Test 4-(2), ozone was formed and available when the system shifted to the second stage. Ozone then at once oxidized NO to form NO_2 as gas mixture of $N_2 + NO + O_2$ entered the reactor. As a result, NO_x reduction was smaller.

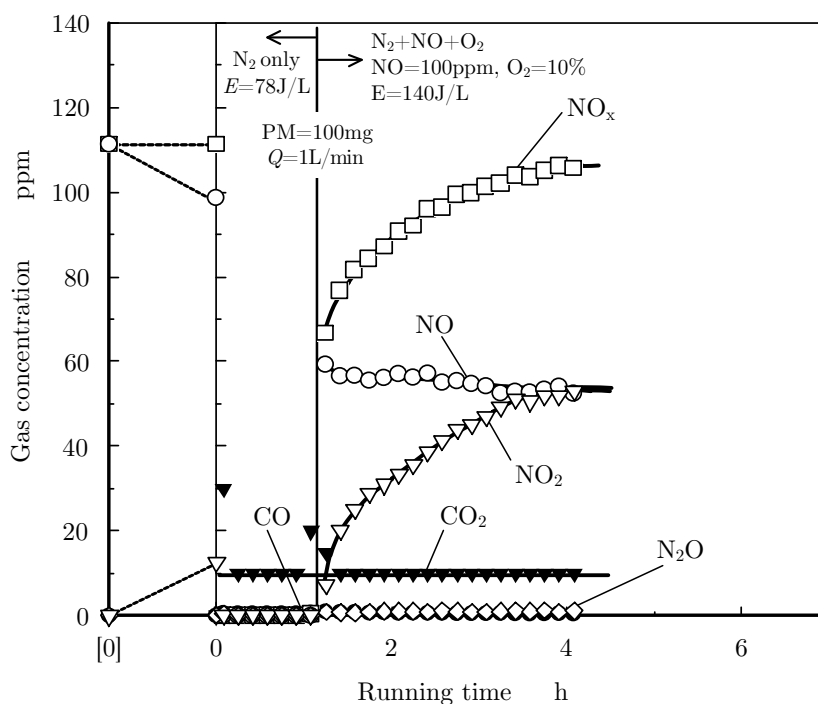


FIGURE 5.3 NO_x removal performance in 4 running hours mode (Test 4-(3): One hour pre-treatment with DBD in N_2 atmosphere)

In case of gas mixture at the first stage was nitrogen only and applying a energy density $E=78\text{J/L}$ (Fig.5.3, Test 4-(3)), the NO_x removal performance was similar with Test 4-(1) but the recovery speed of NO_x concentration was slower. Ozone did not concerned in this case since there was no oxygen in gas mixture even the energy density was applied. Instead of that, N radicals were created from N_2 during the first stage under discharge field. The N radicals then reacted to NO to return N_2 . In addition to no ozone available, this result led to NO_x reduction dropped at the beginning of the second stage as seen in Fig.5.3.

5.2.2 “Fresh PM” oxidation effect on NO_x removal

Although all three cases of Test 4-(1), Test 4-(2), and Test 4-(3) showed significant drops of NO_x reduction at the beginning of the second stage, the Test 4-(3) expressed the best NO_x removal performance as the summarized data pointed out in Fig.5.4. While NO concentrations was slightly changed during the tests, the NO_2

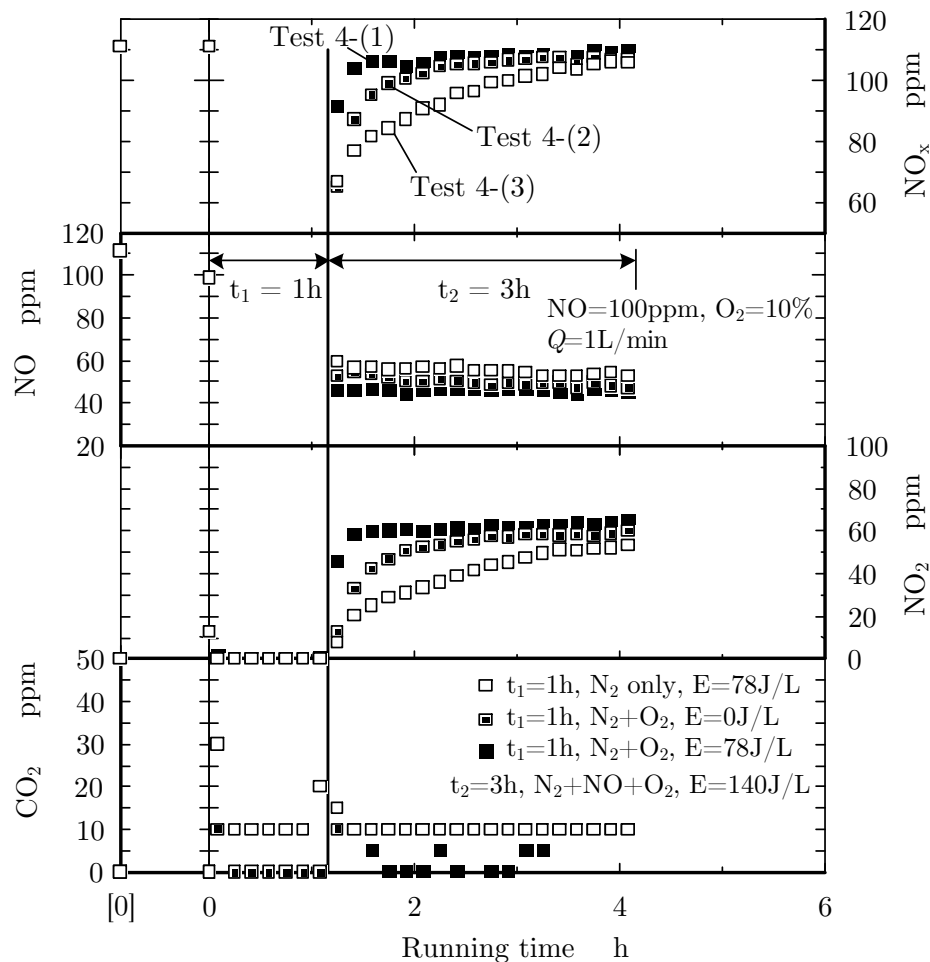


FIGURE 5.4 NO_x removal performance in 4 running hours mode in summary

concentrations varied substantially making the total NO_x concentration differed, especially in the first one hour of the second stage. This can be explained by the formation and availability of ozone or N radicals in previous paragraph.

Comparing the result from Test 4-(3) with N radical pre-treatment to previous results without pre-treatment in Fig.4.7 and Fig.4.13 (Chapter 4), it can be seen that the NO_x removal without pre-treatment was little higher than in case of with pre-treatment. In both cases of without pre-treatment, the maximum NO_x removal reached about 70ppm while in case of with pre-treatment, NO_x removal was 65ppm. However, the “Fresh PM” effect on NO_x removal in case of without pre-treatment was shorter, it disappeared after one running hour. When applying N radical pre-treatment as in Test 4-(3), the “Fresh PM” effect lasted for about three running hours (Fig.5.3).

On the other hand, as seen in Fig.5.4, NO_x removal by “Fresh PM” effect in case of Test 4-(3) showed the largest effect among three tests. It means that NO oxidation was suppressed by N radical adsorption on PM by pre-treatment process. By these results, it can be concluded that N radical pre-treatment is the most effective way of NO reduction.

5.3 “Aged PM” treatment effect on NO_x removal

5.3.1 NO_x removal characteristics in six hours running mode

In six hours running mode, the tests consisted of the first stage of three hours, the second stage of one hour, and the third stage of two hours. Gas mixture of $N_2 + NO + O_2$ employed in the first and third stages whereas either N_2 only or $N_2 + O_2$ was used in the second stage. The second and third stages in this mode had the same test procedure with the four hour mode, so it can be considered that this mode was a four hour mode with three hours “Aged PM”. The experimental results were illustrated in Figs.5.5, 5.6, and 5.7.

Figure 5.5 expressed the experimental result in case of pre-treatment with $N_2 + O_2$ mixture ($O_2=10\%$) and no power applied. The first stage of three hours and third stage of two hours were operated with $N_2 + NO + O_2$ gas mixture, $NO=100ppm$, and applied energy density of 138J/L. The gas flow rate of 1L/min was keep constant during the whole test. From the figure above, after pre-treatment stage, there was a small amount of NO_x removed (about 10ppm). In this case, the “Fresh PM” effect was not concerned because PM was under discharge field for four hours. Thus the NO_x removal as above should be explained

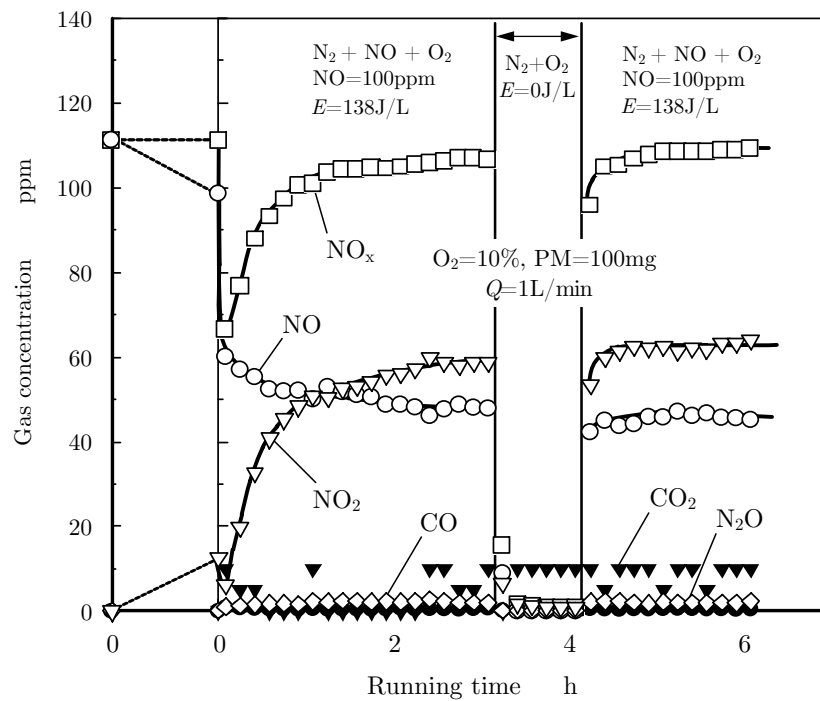


FIGURE 5.5 NO_x removal performance in 6 running hours mode (Test 6-(1): “Aged PM” and one hour treatment in $N_2 + O_2$ atmosphere without DBD)

by the absorption effect by PM, so-called the re-fresh effect. In Fig.5.6 was the NO_x removal performance in six hours mode with pre-treatment of $N_2 + O_2$ mixture and applied energy density of 77J/L. The first stage and third stage were run with gas mixture of $N_2 + NO + O_2$ ($NO=100ppm$, $O_2=10\%$), flow rate of 1L/min, and applied energy density of 117J/L. The result showed that there was no NO_x absorption effect by PM, or no re-fresh effect appeared. Because DPF and PM in this case already absorbed the active oxygen and nitrogen in the pre-treatment stage, so there was no NO_x absorption as in Fig.5.5 above. As shown in Fig.5.6, CO_2 concentration in pre-treatment stage was increased. It means PM inside DPF was oxidized under discharge field to form CO_2 . Since PM oxidation by O radical then there was no NO which should react with O radical at the beginning of the next stage.

Finally, Fig.5.7 illustrated the experimental result in six hours mode with pre-treatment stage of nitrogen only under applied energy density of 76J/L. The test conditions for the first three hours and two last hours stages were: $N_2 + NO + O_2$ gas mixture with $NO=100ppm$ and $O_2=10\%$, gas flow rate of 1L/min, and energy density of 134J/L. Comparing to the results shown in Figs.5.5 and 5.6, there was a small amount of NO_x removed (re-fresh effect). No evidence of PM oxidation

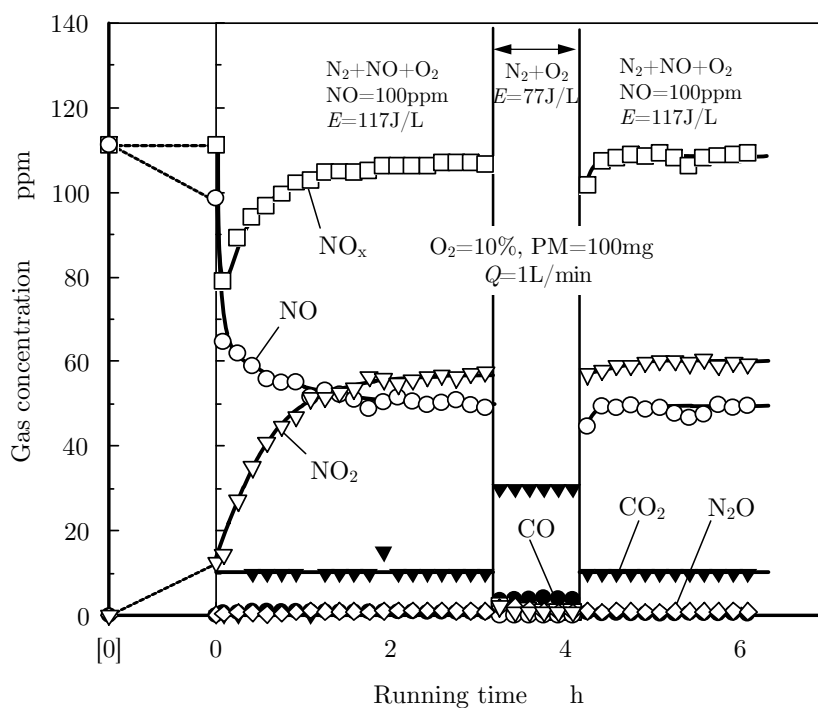


FIGURE 5.6 NO_x removal performance in 6 running hours mode (Test 6-(2): “Aged PM” and one hour treatment in $N_2 + O_2$ atmosphere with DBD)

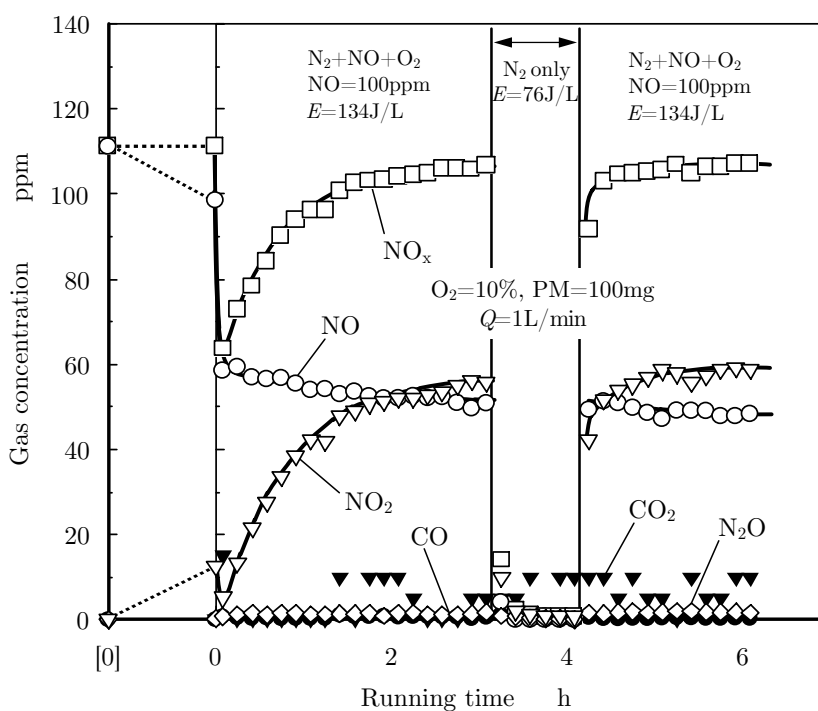


FIGURE 5.7 NO_x removal performance in 6 running hours mode (Test 6-(3): “Aged PM” and one hour treatment in N_2 atmosphere with DBD)

was found in this test.

5.3.2 Difference between “Fresh PM” and “Aged PM”

The NO_x treatment performance at the first stage of six hours mode in all three cases (Test 6-(1), Test 6-(2), and Test 6-(3)) were very similar except CO_2 at the refreshment time (Test 6-(2)). In that case, O radical was formed, but it did not consumed by NO oxidation then only the PM oxidation took place. The small difference might come from the variance of the energy density applying in these cases. The substantial reduction of NO_x concentration at the beginning of tests was explained by the effect of “Fresh PM” in previous chapter (see Chapter 4, Section 4.3).

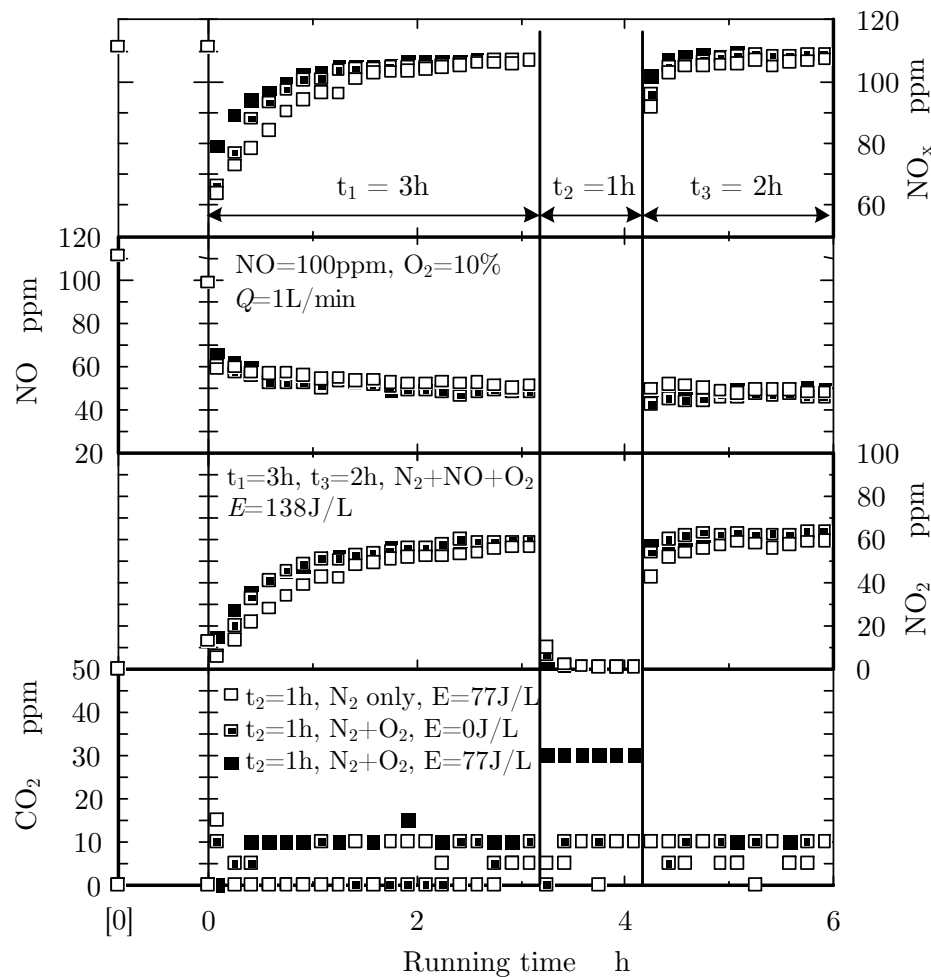


FIGURE 5.8 NO_x removal performance in 6 running hours mode in summary

A slightly difference in NO_x removal behavior could be found at the third stage of the tests. Although the test procedures for the second stage in six hour mode was the same with the one in four hour mode but the results were far

different. The similar formation mechanism of ozone and N radicals as explained above in four hours mode could apply here. However, the effect of “Aged PM” (after four running hours of the first and second stages) lowered NO_x concentration reduction. It can be concluded that even with “Aged PM”, the effect of N radical pre-treatment appeared.

5.4 N radical pre-treatment

The experimental results of NO_x removal performance in transient tests demonstrated the important role of N radical in pre-treatment stage. The test conditions of these tests were showed in Table 5.2. The experimental results of N radical pre-treatment tests had showed the most effective performance among conducted tests as discussed in previous section. It implies that N radical in pre-treatment stage played a key role in NO_x removal performance.

TABLE 5.2 N radical pre-treatment tests with PM

Test	N radical pre-treatment tests with PM=100mg					
	1st hour	2nd hour	3rd hour	4th hour	5th hour	6th hour
4-(3)	N_2 only, E=78J/L	N_2+NO+O_2 , NO=100ppm, E=140J/L				
6-(3)	N_2+NO+O_2 , NO=100ppm, E=134J/L			N_2 only, E=76J/L	N_2+NO+O_2 , NO=100ppm, E=134J/L	

Additionally, O radical was also formed in this stage and contributed to NO_x removal process. Thus the activities of O radical and N radical on PM was introduced in Fig.5.9.

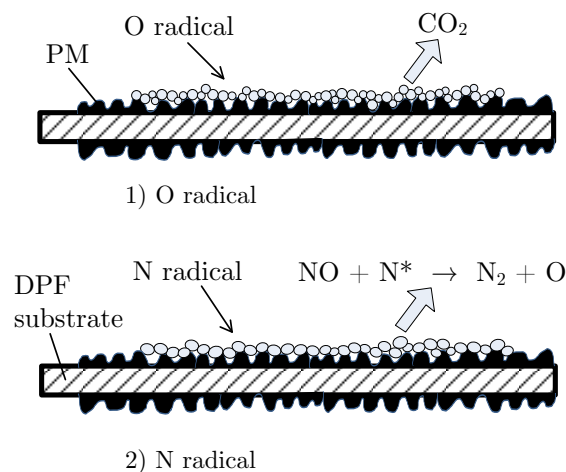


FIGURE 5.9 Illustration of adsorbed N radical and O radical on PM

On PM surface inside the DPF, the adsorbed O radicals might react to carbon (C) to form CO_2 . This PM oxidation effect was pointed out in Fig.5.6. Alternatively, the adsorbed N radicals tend to react with NO to return nitrogen ($N^* + NO \rightarrow N_2 + O$). This NO reduction effect was clearly observed with “Fresh PM” in Fig.5.3, and was also appeared with “Aged PM” in Fig.5.7.

5.5 Engine application

An application of dielectric barrier discharge (DBD) reactor to aftertreatment system of diesel exhaust was proposed and illustrated in Fig.5.10. At low load

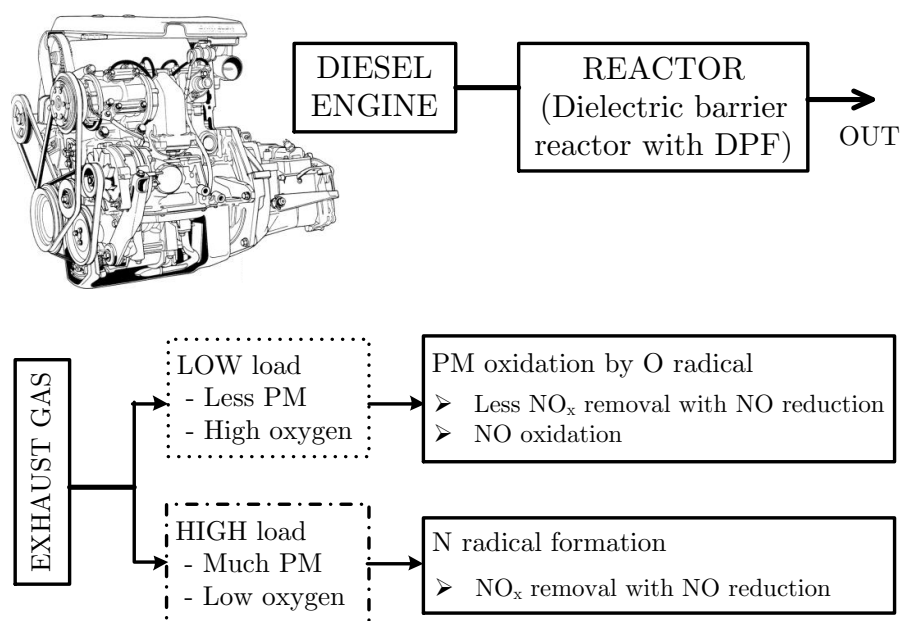


FIGURE 5.10 Application of DBD reactor to diesel exhaust aftertreatment system

condition of engine which is characterized by low PM mass and high oxygen concentration, the DBD reactor will promote the PM oxidation process by O radical. For NO_x removal, it supposed a less NO_x removal with NO reduction (return to nitrogen) and NO oxidation (to form NO_2). At certain times, the DBD reactor might not be operated to save power. Conversely, at high load condition which characterized by high PM mass and low oxygen concentration, it is suitable to operate the DBD reactor as an N radical generator. The NO_x removal with NO reduction will prevail in this operating condition.

5.6 Summary

The experimental results in both cases of four running hours in two stages and six running hours in three stages showed that the NO_x removal performance often started with significant drop of NO_x concentration then gradually reduced.

Through running the long time tests with different procedures of gas composition and applied energy density, it can be learned that the formation and availability of ozone and N radicals play major role in NO_x removal performance. Additionally, the effects of “Fresh PM” and “Aged PM” on NO_x removal process was confirmed.

Chapter 6

Conclusions

A combination of a dielectric barrier discharge reactor and a diesel particulate filter was developed to investigate experimentally the removal of nitrogen oxides. Simulated exhaust gas of NO, O₂, and N₂ at various concentrations was used. Gas flow rates through the reactor were 0.5L/min, 1L/min, and 2L/min. Additionally, PM generated from a diffusion flame system was loaded into DPF at different masses to study its influences on NO_x removal processes. From this work, some conclusions were made as follows.

- 1- Under barrier discharge field, PM improved the NO_x removal performance, however, its effects reduced following running time. The PM just loaded from PM generator and was not under applied voltage, so called “Fresh PM”, is supposed that the active surface of “Fresh PM” played a role of catalytic surface for NO_x removal and its effect was promoted by electric discharge. As for an “Aged PM” (after long running), surface of PM was oxidized and no catalytic effect occurs.
- 2- For a long running time, NO_x removal performance under barrier discharge field with the PM loaded DPF started with substantial drop of NO_x concentration, then gradually reduced and almost in stable state after about two hours. The formation and availability of ozone and N radicals at the beginning of NO_x removal process decide the efficiency of the system performance.
- 3- Oxygen promoted the NO oxidation process that was dominant in NO_x abatement behavior with a gas mixture of NO, O₂ and N₂. As O₂ fraction increases, the NO oxidation process to form NO₂ run to the point that NO concentration of zero. It means that the necessary energy density to

reduce NO to zero is lower and the required power to remove completely NO_x concentration is also lower.

- 4- N radical played major role in NO_x removal performance. It effectively reduced nitrogen oxide (NO) to return nitrogen that so-called NO reduction process. The N radical pre-treatment had shown a great effect on NO_x removal with “Fresh PM”. Additionally, this effect lasted for a longer time than in case of without pre-treatment process. The N radical pre-treatment effect was also observed in DPF with “Aged PM”.

In the real engine coupling with DPF system, loaded PM was oxidized under forced regeneration process or continuous PM oxidation process during operation. It meant that loaded or deposited PM in DPF was partially oxidized PM. However new “Fresh PM” was always supplied from engine side and it deposited over on the old PM where its surface had already lost the effective role of NO_x removal. It meant that there are many possibilities of NO_x removal. In this report, a possibility of NO_x removal with “Fresh PM” coupled with electric discharge could be pointed out experimentally.

However, this thesis still requires further study. The effect of temperature on NO_x removal performance should be added. In addition, the effect of other gas composition such as H₂O, CO, HC, etc. should also be considered.

Bibliography

- [1] P. Granger and V.I. Parvulescu, editors. *Past and present in DeNO_x catalysis*, volume 171 of *Studies in Surface Science and Catalysis*. Elsevier B.V., 2007.
- [2] Clean Air Technology Center. Nitrogen oxides, why and how they are controlled. Technical report, U.S. Environmental Protection Agency, 10 1999.
- [3] John B. Heywood. *Internal combustion engine fundamentals*. McGraw-Hill, 1988.
- [4] S. Elzey et al. FTIR study of the selective catalytic reduction of NO₂ with ammonia on nanocrystalline NaY and CuY. *Molecule Catalysis A-Chemical*, 285:48–57, 2008.
- [5] Fridell et al. Investigations of NO_x storage catalysts. *Catalysis and automotive pollution control IV, Studies in Surface Science and Catalysis*, 116: 537–547, 1998.
- [6] A. Fridman. *Plasma Chemistry*. Cambridge University Press, 2008.
- [7] B. M. Penetrante. Pollution control applications of pulsed power technology. In *Proceedings of the ninth IEEE international pulsed corona conference*, pages 1–5, 1993.
- [8] S. Masuda. Pulse corona induced plasma chemical process - a horizon of new plasma chemical technology. *Pure Applied Chemistry*, 60(5):727–731, 1988.
- [9] J. Zhang, Yanhui Wang, and Dezhen Wang. Nonlinear behaviors in a pulsed dielectric barrier discharge at atmospheric pressure. *Thin Solid Films*, 2010. doi: 10.1016/j.tsf.2010.11.062.
- [10] H.-E. Wagner et al. The barrier discharge: Basic properties and applications to surface treatment. *Vacuum*, 71:417–436, 2003.
- [11] I. Nagao et al. NO_x removal using nitrogen gas activated by dielectric barrier discharge at atmosphere pressure. *Vacuum*, 65:481–487, 2002.
- [12] B.M. Obradovic, G.B. Sretenovic, and M.M. Kuraica. A dual-use of BDB plasma for simultaneous NO_x and SO₂ removal from coal-combustion flue

- gas. *Hazardous Materials*, 185:1280–1286, 2011.
- [13] Hyun-Ha Kim. Nonthermal plasma processing for air-pollution control: A historical review, current issues, and future prospects. *Plasma Processes and Polymers*, 1:91–110, 2004.
- [14] Young Sun Mok. Oxidation of NO to NO₂ using the ozonization method for the improvement of selective catalytic reduction. *Chemical Engineering of Japan*, 37(11):1337–1344, 2004.
- [15] K. Hensel and M. Morvova. The conversion of NO_x in a corona discharge with an electrode material variation. *Plasma Physics*, 36(1):51–61, 1996.
- [16] G.R. Dey et al. Variable products in dielectric-barrier discharge assisted benzene oxidation. *Hazardous Materials*, 178:693–698, 2010.
- [17] C. W. Park et al. Simultaneous removal of odors, airborne particles, and bioaerosols in a municipal composting facility by dielectric barrier discharge. *Separation and Purification Technology*, 2010. doi: 10.1016/j.seppur.2010.11.024.
- [18] Ye et al. An investigation of the treatment of particulate matter from gasoline engine exhaust using non-thermal plasma. *Journal of Hazardous Materials*, B127:149–155, 2005.
- [19] Pisarello et al. Simultaneous removal of soot and nitrogen oxides from diesel engine exhausts. *Catalysis Today*, 75:465–470, 2002.
- [20] E. Sher. *Handbook of air pollution from internal combustion engines*. Boston: Academic Press, 1988.
- [21] Bensaid et al. Experimental investigation of soot deposition in diesel particulate filters. *Catalysis Today*, 147S:S295–S300, 2009.
- [22] K Yoshida et al. Diesel emission control system using combined process of nonthermal plasma and exhaust gas components' recirculation. *Thin Solid Films*, 518:987–992, 2009.
- [23] K. Skalska et al. Trends in NO_x abatement: A review. *Science of the Total Environment*, 408:3976–3989, 2010.
- [24] A. M. Vandenbroucke et al. Non-thermal plasmas for non-catalytic and catalytic VOC abatement. *Hazardous Materials*, 2011.
- [25] X. Hu et al. Transformations and destruction of nitrogen oxides - NO, NO₂ and N₂O - in a pulsed corona discharge reactor. *Fuel*, 82:1675–1684, 2003.
- [26] Y. S. Mok and Y. J. Huh. Simultaneous removal of nitrogen oxides and particulate matters from diesel engine exhaust using dielectric barrier discharge and catalysis hybrid system. *Plasma Chemistry and Plasma Processing*, 25

- (6):625–639, 2005.
- [27] U. Kogelschatz. Dielectric-barrier discharges: Their history, discharge physics, and industrial applications. *Plasma Chemistry and Plasma Processing*, 23(1), 2003.
- [28] S.-E. Yin et al. The effect of oxygen and water vapor on nitric oxide conversion with a dielectric barrier discharge reactor. *Plasma Chemistry and Plasma Processing*, 29:421–431, 2009.
- [29] Y. Kuroda et al. Effect of electrode shape on discharge current and performance with barrier discharge type electrostatic precipitator. *Electrostatics*, 57:407–415, 2003.
- [30] B. Dramane et al. Electrostatic precipitation in wire-to-cylinder configuration: Effect of the high-voltage power supply waveform. *Electrostatics*, pages 1–6, 2009.
- [31] H. Ohneda et al. Improvement of NO_x removal efficiency using atomization of fine droplets into corona discharge. *Electrostatics*, 55:321–332, 2002.
- [32] C. Fushimi et al. Influence of polarity and rise time of pulse voltage waveforms on diesel particulate matter removal using an uneven dielectric barrier discharge reactor. *Plasma Chemistry and Plasma Processing*, 28:511–522, 2008.
- [33] H. Lin et al. Removal of NO_x from wet flue gas by corona discharge. *Fuel*, 83:1251–1255, 2004.
- [34] M. Arai et al. Effect of oxygen on NO_x removal in corona discharge field: NO_x behavior without a reducing agent. *Combustion Science and Technology*, 176:1653–1665, 2004.
- [35] J. Vinogradov et al. NO_x reduction from compression ignition engines with DC corona discharge - An experimental study. *Energy*, 32:174–186, 2007.
- [36] M. Magureanu et al. Plasma-assisted catalysis for volatile organic compounds abatement. *Applied Catalysis B: Environmental*, 61:12–20, 2005.
- [37] F. Leipold et al. Reduction of NO in the exhaust gas by reaction with N radicals. *Fuel*, 85:1383–1388, 2006.
- [38] M. Saito et al. Effect of coexisting gases on NO removal using corona discharge. *JSME International Journal Series B*, 49(4):1282–1289, 2006.
- [39] M. Arai et al. NO reduction in a corona discharge field. *Transactions of the JSME Series B*, 68(676), 2002.
- [40] M. Arai et al. DeNO_x treatment in corona discharge field. In *19th International Colloquium on the Dynamics of Explosions and Reactive Systems*, 7

- 2003.
- [41] B.A. Kozlov and V.I. Solovyov. Limit current of a multipoint corona discharge. *Technical Physics*, 51(7):821–826, 2006.
- [42] T. Fujii et al. Removal of NO by DC corona reactor with water. *Electrostatics*, 51–52, 2001.
- [43] M. Dors et al. Removal of NO_x by DC and pulsed corona discharges in a wet electrostatic precipitator model. *Electrostatics*, 45:25–36, 1998.
- [44] M. Dors and J. Mizeraczyk. NO_x removal from a flue gas in a corona discharge-catalyst hybrid system. *Catalysis Today*, 89:127–133, 2004.
- [45] A. Fridman and L.A. Kennedy. *Plasma: Physics & Engineering*. Taylor & Francis Routledge, 2004.
- [46] J. Vinogradov et al. NO_x reduction from compression ignition engines with pulsed corona discharge. *Energy*, 33:480–491, 2008.
- [47] C. H. Huang et al. Removal of particulate matter from an air stream by a packed dielectric barrier discharge. *Korean Journal of Chemical Engineering*, 25, 2008.
- [48] M. Moscosa-Santillan et al. Design of DBD wire-cylinder reactor for NO_x emission control: Experimental and modeling approach. *Cleaner Production*, 16:198–207, 2008.
- [49] Rogemond et al. Characterization of model three-way catalysts. *Journal of Catalysis*, 186:414–422, 1999.
- [50] Birgersson et al. An investigation of a new regeneration method of commercial aged three-way catalysts. *Applied Catalysis B: Environmental*, 65: 93–100, 2006.
- [Matthey] Johnson Matthey. NO_x Adsorber Catalysts. URL <http://ect.jmcatalysts.com/>.
- [51] Clayton et al. Pt dispersion effects during NO_x storage and reduction on Pt/BaO/Al₂O₃ catalysts. *Applied Catalysis B: Environmental*, 90 : 662 – 676, 2009.
- [52] X. Li et al. Study of the relationship between microstructure and performance for NO_x storage catalysts. *Trans IChemE*, 80, Part A:190–194, 2002.
- [53] D. Bosteels and R.A. Searles. Exhaust emission catalyst technology. *Platinum Metals Review*, 46(1):27–36, 2002.
- [54] U.G. Alkemade and B. Schumann. Engines and exhaust after treatment systems for future automotive applications. *Solid State Ionics*, 177:2291–2296, 2006.

- [55] Forzatti et al. Effect of operating variable on the enhanced SCR reaction over a commercial $V_2O_5 - WO_3/TiO_2$ catalyst for stationary applications. *Catalysis Today*, 2011. doi: 10.1016/j.cattod.2011.11.006.
- [56] Boger et al. A next generation cordierite diesel particle filter with significantly reduced pressure drop. *SAE International*, 2011. doi: 10.4271/2011-01-0813.
- [57] T. Nishiyama and N. Emori. Commercialization of diesel particulate filter (DPF). Technical Report 48, Komatsu, 2002.
- [58] R. Burch, J.P. Breen, and F.C. Meunier. A review of the selective reduction of NO_x with hydrocarbons under lean-burn conditions with non-zeolitic oxide and platinum group metal catalysts. *Applied Catalysis B: Environmental*, 39:283–303, 2002.
- [59] B.R. Stanmore, J.F. Brillhac, and P. Gilot. The oxidation of soot: a review of experiments, mechanisms and models. *Carbon*, 39:2247–2268, 2001.
- [60] He Lin, Zhen Huang, and Wenfeng Shangguan. Characteristics of oxidation of diesel particulate matter over a spinel type $Cu_{0.95}K_{0.05}Fe_2O_4$ catalyst. *Chem. Eng. Technol.*, 31(10):1433–1427, 2008.
- [61] S. M. J. Grundmann and R.-J. Zahn. Treatment of soot by dielectric barrier discharges and ozone. *Plasma Chemistry and Plasma Processing*, 25(5):455–466, 10 2005.
- [62] S. Yao et al. Uneven dielectric barrier discharge reactors for diesel particulate matter removal. *Plasma Chemistry and Plasma Processing*, 26:481–493, 2006.
- [63] J. H. Byeon et al. Removal of gaseous toluene and submicron aerosol particles using a dielectric barrier discharge reactor. *Hazardous Materials*, 175:417–422, 2009.
- [64] J. Sentek et al. Plasma-catalytic methane conversion with carbon dioxide in dielectric barrier discharges. *Applied Catalysis B: Environmental*, 94:19–26, 2010.
- [65] C.-L. Song et al. Simultaneous removals of NO_x , HC and PM from diesel exhaust emissions by dielectric barrier discharges. *Hazardous Materials*, 166: 523–530, 2008.
- [66] R. Ravi et al. Temperature effect on hydrocarbon-enhanced nitric oxide conversion using a dielectric barrier discharge reactor. *Fuel Processing Technology*, 81:187–199, 2002.

- [Dieselnet] Dieselnet. Emission standards. URL <http://www.dieselnet.com/standards/>.
- [67] J.M. Trichard. Current tasks and challenges for exhaust after-treatment research: An industrial viewpoint. *Studies in surface science and catalysis*, 171:211–233, 2007.
- [68] Peng et al. Effect of catalysis on plasma assisted catalytic removal of nitrogen oxides and soot. *Chem. Eng. Technol.*, 29:1262–1266, 2006.
- [69] G. J. Pietsch. Peculiarities of dielectric barrier discharges. *Contributions to Plasma Physics*, 41:620–628, 2001.
- [70] B. Eliasson, M. Hirth, and U. Kogelschatz. Ozone synthesis from oxygen in dielectric barrier discharges. *Journal of Physics D: Applied Physics*, 20:1421–1437, 1987.
- [71] K. Urashima, J. S. Chang, and T. Ito. Reduction of NO_x from combustion flue gases by superimposed barrier discharge plasma reactors. *IEEE Transactions on Industry Applications*, 33:879–886, 1997.
- [72] R. McAdams. Prospects for non-thermal atmospheric plasmas for pollution abatement. *Journal of Physics D: Applied Physics*, 34:2810–2821, 2001.
- [73] Z. Fang et al. Experimental study on discharge characteristics and ozone generation of dielectric barrier discharge in a cylinder-cylinder reactor and a wire-to-cylinder reactor. *Electrostatics*, 66:421–426, 2008.
- [74] A. M. Zhu et al. Conversion of NO in NO/N_2 , $\text{NO}/\text{O}_2/\text{N}_2$, $\text{NO}/\text{C}_2\text{H}_4/\text{N}_2$ and $\text{NO}/\text{C}_2\text{H}_4/\text{O}_2/\text{N}_2$ systems by dielectric barrier discharge plasmas. *Plasma Chemistry and Plasma Processing*, 25(4):371–386, 2005.
- [75] E.H.W.M. Smulders, B.E.J.M. van Heesch, and S.S.V.B. van Paasen. Pulsed power corona discharges for air pollution control. *IEEE Transactions on Plasma Science*, 26:1476–1484, 1998.
- [76] K.-F. Shang et al. Reduction of NO_x/SO_2 by wire-plate type pulsed discharge reactor with pulsed corona radical shower. *Plasma Chemistry and Plasma Processing*, 26, 2006.
- [77] Y. Shi et al. Decomposition of mixed malodorants in a wire-plate type pulse corona reactor. *Environmental Science Technology*, 39:6786–6791, 2005.
- [78] K. Yamamoto et al. Simulation on soot deposition and combustion in diesel particulate filter. *Proceeding of the Combustion Institute*, 32:1965–1972, 2009.
- [79] W.J. Liang, J. Li, and Y.Q. Jin. Abatement of toluene from gas streams via ferroelectric packed bed dielectric barrier discharge plasma. *Hazardous*

- Materials*, 170:633–638, 2009.
- [80] A. Ogata et al. Decomposition of benzene using a nonthermal plasma reactor packed with ferroelectric pellets. *IEEE Transactions on Industry Applications*, 35:753–759, 1999.
- [81] U. Roland, F. Holzer, and F.D. Kopinke. Improved oxidation of air pollutants in a non-thermal plasma. *Catalysis Today*, 73:315–323, 2002.
- [82] J.-O. Chae. Non-thermal plasma for diesel exhaust treatment. *Electrostatics*, 57:251–262, 2003.
- [83] C. Wang, G. Zhang, and X. Wang. Comparisons of discharge characteristics of a dielectric barrier discharge with different electrode structures. *Vacuum*, pages 1–5, 2011.
- [84] K. Takaki et al. Influence of electrode configuration on ozone synthesis and microdischarge property in dielectric barrier discharge reactor. *Vacuum*, 83:128–192, 2009.
- [85] Y. Kobayashi et al. Soot precursor measurement in benzene and hexane diffusion flames. *Combustion and Flame*, 154:346–355, 2008.
- [86] Penetrante et al. Basic energy efficiency of plasma production in electrical discharge and electron beam reactors. In *Symposium on non-thermal plasma technology for air contaminant control*, 1996.
- [87] M.A. Jani et al. An experimental comparison between electrode shapes for NO_x treatment using a dielectric barrier discharge. *Phys. D: Applied Physics*, 33:3078–3082, 2000.
- [88] Wang et al. An experimental and kinetic modeling study of the autoignition of α -methyl-naphthalene/n-decane/air mixtures at elevated pressures. *Combustion and Flame*, 157:1976–1988, 2010.
- [89] J.S. Olfert, J.P.R. Symonds, and N. Collings. The effective density and fractal dimension of particles emitted from a light-duty diesel vehicle with diesel oxidation catalyst. *Aerosol Science*, 38:69–82, 2007.
- [90] M. Arai et al. NO removal from exhaust gas in a corona discharge field. *Review of Automotive Engineering*, 27(1):61–67, 2006.
- [91] Q. V. Tran et al. NO_x removal behavior in a dielectric barrier discharge field. In *Proceedings of the 15th Asia Pacific Automotive Engineering Conference*, October 2009.
- [92] Yperen et al. Novel Pd-based three-way catalysts. *Catalysis and automotive pollution control IV, Studies in Surface Science and Catalysis*, 116:51–60, 1998.

- [93] Lin et al. Temperature-programmed oxidation of diesel particulate matter in a hybrid catalysis-plasma reactor. *Proceeding of the Combustion Institute*, 31:3335–3342, 2007.
- [94] Lu et al. Plasma oxidation of benzene using DBD corona discharges. *Materials Engineering and Performance*, 17(3):428–431, 2008.
- [95] A. Caron and L. Dascalescu. Numerical modeling of combined corona-electrostatic fields. *Electrostatics*, 61:43–55, 2004.
- [96] J. Zhang, K. Adamiak, and G.S.P. Castle. Numerical modeling of negative-corona discharge in oxygen under different pressures. *Electrostatics*, 65:174–181, 2007.
- [97] Li et al. Non-thermal plasma-assisted catalytic NO_x storage over Pt/Ba/Al₂O₃ at low temperature. *Applied Catalysis B: Environmental*, 90:360–367, 2009.
- [98] M. Derakhshesh, J. Abedi, and M. Omidyeganeh. Modeling of hazardous air pollutant removal in the pulsed corona discharge. *Physics Letters A*, 373:1051–1057, 2009.
- [99] Mennad et al. Theoretical investigation of ozone production in negative corona discharge. *Current Applied Physics*, 10:1391–1401, 2010.
- [100] Ciambelli et al. The role of NO in the regeneration of catalytic ceramic filters for soot removal from exhaust gases. *Catalysis Today*, 60:43–49, 2000.
- [101] Saiyasitpanich et al. Removal of diesel particulate matter in a tubular wet electrostatic precipitator. *Electrostatics*, 65:618–624, 2007.
- [102] M. A. Tas, R. van Hardeveld, and E.M. van Veldhuizen. Reactions of NO in a positive streamer corona plasma. *Plasma Chemistry and Plasma Processing*, 17(4):371–391, 1997.
- [103] S.-J. Lee, S.-J. Jeong, and W.-S. Kim. Numerical design of the diesel particulate filter for optimum thermal performance during regeneration. *Applied Energy*, 86:1124–1135, 2009.
- [104] D.-H. Kim, Y. S. Mok, and S.B. Lee. Effect of temperature on the decomposition of trifluoromethane in a dielectric barrier discharge reactor. *Thin Solid Films*, 2010. doi: 10.1016/j.tsf.2010.11.060.
- [105] M.P. Cal and M. Schluep. Destruction of benzene with non-thermal plasma in dielectric barrier discharge reactor. *Environmental Progress*, 20(3):151–156, 2001.
- [106] Y.S. Mok and S.W. Ham. Conversion of NO to NO₂ in air by a pulsed corona discharge process. *Chemical Engineering Science*, 53(9):1667–1678, 1998.

- [107] Zhang et al. Comparison of experiment and simulation on dielectric barrier discharge driven by 50 Hz AC power in atmospheric air. *Electrostatics*, 68: 445–452, 2010.
- [108] Lee et al. Characteristics of plasma-assisted hydrocarbon SCR system. *International Journal of Hydrogen Energy*, 36:11718–11726, 2011.
- [109] W.S. Kang, H.S. Kim, and S.H. Hong. Atomic oxygen generation by in-situ plasma and post-plasma in dielectric barrier discharges for surface treatment. *Thin Solid Films*, 2010. doi: 10.1016/j.tsf.2010.04.045.
- [110] Okubo et al. Total diesel emission control technology using ozone injection and plasma desorption. *Plasma Chemistry and Plasma Processing*, 28:173–187, 2008.
- [111] Tighe et al. The kinetics of oxidation of diesel soot by NO₂. *Combustion and Flame*, In press, 2011.
- [112] Yan et al. Oxidation and reduction processes during NO_x removal with corona-induced nonthermal plasma. *Plasma Chemistry and Plasma Processing*, 19(3):421–443, 1999.
- [113] Miessner et al. NO_x removal in excess oxygen by plasma-enhanced selective catalytic reduction. *Catalysis Today*, 75:325–330, 2002.
- [114] Lee et al. NO_x removal characteristics in plasma plus catalyst hybrid process. *Plasma Chemistry and Plasma Processing*, 24(2):137–154, 2004.
- [115] J. Chen and J.H. Davidson. Model of the negative DC corona plasma: Comparison to the positive DC corona plasma. *Plasma Chemistry and Plasma Processing*, 23(1):83–102, 2003.
- [116] Vander Wal et al. HRTEM study of diesel soot collected from diesel particulate filters. *Carbon*, 45:70–77, 2007.
- [117] S.S. Gill, G.S. Chatha, and A. Tsokakis. Analysis of reformed EGR on the performance of a diesel particulate filter. *International Journal of Hydrogen Energy*, 36:10089–10099, 2011.
- [118] Yamamoto et al. Simulation on catalytic reaction in diesel particulate filter. *Catalysis Today*, 153:118–124, 2010.
- [119] J. S. Chang, P. A. Lawless, and T. Yamamoto. Corona discharge process. *IEEE Transactions on Plasma Science*, 19:1152–1166, 1991.
- [120] Y. S. Mok and I.-S. Nam. Removal of nitric oxide in a pulsed corona discharge reactor. *Chem. Eng. Technol.*, 22:527–532, 1999.
- [121] J. L. Hueso et al. Plasma chemistry of NO in complex gas mixtures excited with a surfatron launcher. *Phys. Chem. A*, 109:4930–4938, 2005.

- [122] S. Muller and R.-J. Zahn. On various kinds of dielectric barrier discharges. *Contrib. Plasma Phys.*, 36:697–709, 1996.
- [123] S. Collura et al. On the composition of the soluble organic fraction and its influence during the combustion of exhaust diesel soot. Technical report, 2002.
- [124] M. Schejbal et al. Modelling of soot oxidation by NO_2 in various types of diesel particulate filters. *Fuel*, 89:2365–2375, 2010.
- [125] S. Yao et al. Methane conversion using a high-frequency pulsed plasma: Discharge features. *AIChE*, 47(2):419–426, February 2001.
- [126] A. Schaefer-Sindlinger et al. Efficient material design for diesel particulate filters. *Topics in Catalysis*, 42–43:307–317, May 2007.
- [127] G.-B. Zhao et al. Effect of CO_2 on nonthermal-plasma reactions of nitrogen oxides in $\text{N}_2 \cdot 2\cdot$ percent-level concentrations. *Ind. Eng. Chem. Res.*, 44: 3935–3946, 2005.
- [128] W. Kim et al. Development of a novel simulated diesel particulate matter generator system. *Fuel*, 89:2047–2053, 2010.
- [129] Timothy V. Johnson. Review of diesel emissions and control. *SAE International*, 2010.
- [130] Timothy V. Johnson. Diesel emissions control in review. *SAE International*, 2009.
- [131] S. Y. Chang. NO/NO_x removal with C_2H_2 as additive via dielectric barrier discharges. *AIChE*, 47(5), 2001.
- [132] I. Jogi et al. NO conversion by dielectric barrier discharge and TiO_2 catalyst: Effect of oxygen. *Plasma Chemistry and Plasma Processing*, 29:205–215, 2009.
- [133] S. Collura et al. Influence of the soluble organic fraction on the thermal behaviour, texture and surface chemistry of diesel exhaust soot. *Carbon*, 43: 605–613, 2004.
- [134] W-S. Shin. Hydrocarbon effects on the promotion of non-thermal plasma $\text{NO} - \text{NO}_2$ conversion. *Plasma Chemistry and Plasma Processing*, 23(4), 2003.
- [135] J. Oi-Uchisawa et al. Effect of feed gas composition on the rate of carbon oxidation with Pt/SiO_2 and the oxidation mechanism. *Applied Catalysis B: Environmental*, 21:9–17, 1999.
- [136] M. Matti Maricq et al. Chemical characterization of particulate emissions from diesel engines: A review. *Aerosol Science*, 38:1079–1118, 2007.

-
- [137] K. S. Martirosyan et al. Behavior features of soot combustion in diesel particulate filter. *Chemical Engineering Science*, 2009.
- [138] T. Hammer. Application of plasma technology in environmental techniques. *Plasma Physics*, 39(5):441–462, 1999.